AN ABSTRACT OF THE DISSERTATION OF

Anders E. Carlson for the degree of Doctor of Philosophy in Geology presented on January 12, 2006.

Title: Dynamics of the Laurentide Ice Sheet

Abstract approved:_____

Peter U. Clark

This dissertation concentrates on the controlling factors on the instability of the Laurentide Ice Sheet (LIS) and their effects on abrupt climate change. Northern Hemisphere climate fluctuated abruptly during the last deglaciation possibly related to variability in Atlantic meridional overturning circulation (AMOC) and reduced aerial extent of the LIS. Reductions in AMOC can be induced by changes in the hydrologic cycle which in turn may be controlled by instabilities in the LIS due to subglacial hydrology, sliding and till deformation.

Sedimentological observations of the Tiskilwa Till, Illinois, and Sky Pilot Till, Manitoba determined that the LIS deposited these tills in a ≤1 m thick deforming layer as strain migrated upwards due to till accretion. These tills experienced high strain in a deforming layer thick enough contribute to ice sheet motion.

Simulations of the subglacial hydrology of the James Lobe (JL) of the LIS suggest that the JL had little affect on regional groundwater flow and that subglacial aquifers were incapable of draining meltwater from the ice-till interface. However, a canal basal drainage system with canals up to 70 cm wide spaced 40 to 70 m apart could drain the ice-till interface keeping the JL coupled to its bed.

To resolve the effects of LIS retreat on the hydrologic cycle, a suite of new freshwater routing proxies indicate that western Canadian Plains freshwater was routed to the St. Lawrence at the start of the Younger Dryas with an increase in base flow discharge sufficient to reduce AMOC. These proxies identified a previously unrecognized intra-Younger Dryas routing event at ~12 ka, the impact of which indicates the tight coupling of AMOC, climate and the hydrologic cycle.

To determine the role of the LIS in Holocene climate change, ^{10}Be ages from western Quebec were used to date the final disappearance of the LIS at ~6.8 ka following a period of rapid retreat and thinning that contributed to a rapid rise in sea level. The disappearance of the LIS initiated the Holocene Thermal Maximum, while the attendant reduction in freshwater runoff induced the formation of Labrador deep sea water.

Dynamics of the Laurentide Ice Sheet

by
Anders E. Carlson

A DISSERTATION

submitted to

Oregon State University

in partial fulfillment of
the requirements for the
degree of

Doctor of Philosophy

Presented January 12, 2006
Commencement June, 2006

Doctor of Philosophy dissertation of Anders E. Carlson presented on January 12, 2006

APPROVED:

Major Professor representing Geology

Chair of the Department of Geosciences

Dean of the Graduate School

I understand that my dissertation will become part of the permanent collection of Oregon State University libraries. My signature below authorizes release of my dissertation to any reader upon request.

Anders E. Carlson, Author

ACKNOWLEDGMENTS

I would first and foremost like to thank Peter Clark for serving as my mentor and advisor for my years at Oregon State University. I have benefited greatly from his breadth in the fields of glacial geology and paleoclimatology. I am grateful for his sharing of his ideas with me as well as encouraging me to pursue my own interests. He has provided the financial support for this dissertation and encouraged my attendance at many conferences around the Northern Hemisphere. Thank you.

I would like to thank my committee members for their interest, support and constructive criticism: Roy Haggerty, Andrew Meigs, Alan Mix, and Herbert Huddleston. Alan Mix also provided stimulating conversations on river and ocean chemistry and turned me on to the use of stable carbon isotopes in planktonic foraminifera.

As for collaborators, I am indebted to Ed Brook for instructing and coaching me through the many steps of ^{10}Be processing. I thank John Jenson for several great field seasons in Illinois and Manitoba and for our ongoing discussions on till dynamics and basal drainage. Ardith Hansel showed John and I several excellent sites for us to examine and sample Tiskilwa Till. Chandrakant Desai, Dinshaw Contractor and Shantanu Sane contributed to enlightening discussions of till rheology and behavior. Dorthe Wildenschild and Justin LaNier explained groundwater modeling and specifically MODFLOW to me. Steven Hostetler, Garry Clarke and Don Barber provided essential feedback on freshwater routing and river chemistry. Anne deVernal and Claude Hillaire-Marcel contributed data and funded my attendance to the 8.2 ka cold event meeting. June Padman, Maziet Cheseby, Heather Benway and Molly Phipps instructed me in the art of foraminifera picking and made the days in the lab fly by. Thanks to Brian Haley, Gary Klinkhammer and Andy Unger for the help with the ICP-MS. Katrin Meissner provided initial climate model simulations. I thank Grant Raisbeck for an enlightening visit to Orsay and discussions around the Accelerator Mass Spectrometer. I also thank my field assistants for making sampling an enjoyable endeavor; Aubri Jenson, Ra Camacho, and Allan Carlson.

Martin Roy, Vincent Rinterknecht, Faron Anslow, Lica Ersek and Brent Goehring all made for fun times in the lab and provided me with someone to bounce not-so-well thought out ideas off of. I especially thank Vincent for demonstrating the ^{10}Be processing technique and Faron for being the go-to math guy.

I would like to thank the Department of Geosciences and College of Oceanic and Atmospheric Sciences for their support. Bedford Institute of Oceanography, Saskatchewan Watershed Authority, GEOTOP and Centre de Spectrométrie Nucléaire et de Spectrométrie de Masse, Orsay, France also provided support in various ways.

Furthermore, I thank all my friends and family for their encouragement over the years and for listening to me drone on over a bar or dinner table about glaciers, climate change and various theories. I especially thank Justin Azhocar, Cara Fritz and Dave Bolling for making Corvallis interesting. And lastly, I thank my wife, distraction and muse, Kelley Lake, for her ongoing support and comfort through it all. And to everyone, take it easy.

CONTRIBUTION OF AUTHORS

The four manuscripts in this dissertation are the result of collaborative research from multiple institutions. Peter Clark is a co-author on chapters 2, 3, 4 and 5. Peter provided the overall direction that saw these manuscripts through to completion. He also contributed extensively to the organization, editing and revision of these manuscripts. Furthermore, many of his hypotheses were the starting ground for this research. As a co-author on chapters 2 and 3, John Jenson co-led field work in Illinois and Manitoba and provided constructive discussions on subglacial till behavior. In addition, he suggested the use of a karst analogue for subglacial drainage systems and significantly improved these manuscripts. In chapters 4 and 5, Edward Brook provided constructive criticism of geochemical modeling, demonstrated the processing of ^{10}Be targets and discussed cosmogenic data analysis. Roy Haggerty contributed critical comments and reviews to chapter 3. Brian Haley contributed to chapter 4 by running the foraminifera samples on the ICP-MS. Gary Klinkhammer contributed to chapter 4 through discussions of U chemistry and ICP-MS. Katrin Meissner helped with chapter 4 by running initial climate model simulations of freshwater routing events. Grant Raisbeck acted as a co-author on chapter 5 by demonstrating ^{10}Be target preparation and loading and running the targets on the Accelerator Mass Spectrometer.

TABLE OF CONTENTS

TABLE OF CONTENTS (Continued)

LIST OF FIGURES

LIST OF TABLES

Dynamics of the Laurentide Ice Sheet

CHAPTER 1

INTRODUCTION

1.1. Forward

Northern Hemisphere climate experienced several large and abrupt changes during the last deglaciation that have been recorded worldwide by a variety of paleoclimate proxies (see reviews in Alley and Clark, 1999; Clark et al., 2002). These fluctuations, manifested as rapid temperature changes of glacial to interglacial magnitude, are associated with, and were likely caused by, changes in Atlantic meridional overturning circulation (AMOC) (Fig. 1.1) (Broecker, 1994; Bond et al., 1997; 1999; Alley and Clark, 1999; Hughen et al., 2000; McManus et al., 2004). Changes in AMOC formation have been linked to the Laurentide Ice Sheet (LIS) and its effects on the hydrologic cycle suggesting possible forcing mechanisms arising from the LIS (Fig. 1.1) (e.g. Broecker et al., 1989; MacAyeal, 1993; Broecker, 1994; Clark, 1994; Alley and Clark, 1999; Clark et al., 1999; 2001; Hostetler and Bartlein, 1999; Hostetler et al., 1999).

Although the timing of millennial-scale climate change is reasonably well constrained, the potential forcing mechanisms require further investigation. Over the past twenty five years, two fields of thought have arisen to the cause of millennial-scale variability; one with a Northern Hemisphere, ice sheet-AMOC related forcing as suggested above, the other involving changes in tropical heat budget and temperature gradient, such as long-term El Niño-Southern Oscillation (ENSO) variability, with the signal propagated to the extra-tropics and poles via atmospheric and oceanic feedbacks (Cane, 1998; Clement and Cane, 1999). Some paleoclimate records from the tropical

Pacific suggest El Niño like conditions during cold, stadial periods in the Northern Hemisphere (e.g., Stott et al., 2002; Koutavas et al., 2002), whereas other records suggest that El Niño like conditions existed during warm, interstadial conditions in the Northern Hemisphere (e.g., Turney et al., 2004). Furthermore, additional records of ENSO activity suggest reduced variability during the cold, highly variable periods in the Northern Hemisphere (e.g., Tudhope et al., 2001). Thus, the tropics may play a role in millennial-scale climate change, but the impact and what there role exactly is has yet to be determined.

The Northern Hemisphere trigger for millennial-scale climate change relates changes in the freshwater budget of the North Atlantic and AMOC to variability in Northern Hemisphere Ice Sheets. A leading mechanism to change the freshwater budget involves increased iceberg discharge from mainly the LIS with iceberg contributions also sourced from the other circum-North Atlantic Ice Sheets (Fig. 1.1) (MacAyeal, 1993; Broecker, 1994; Andrews, 1998; Bond et al., 1997; 1999). Another mechanism involves the rapid advance and retreat of the southern margin of the LIS and its effects on freshwater routing to the North Atlantic (Fig. 1.1) (Broecker et al., 1989; Teller, 1990; Clark, 1994; Licciardi et al., 1999; Clark et al., 2001). Specifically, advance of the LIS blocks eastward drainage of North American freshwater, routing water to the Gulf of Mexico whereas retreat of the LIS allows drainage to resume to the east into the North Atlantic with attendant freshening and reduced AMOC. Both increased iceberg flux and freshwater routing may be working in concert to force millennial-scale climate change (e.g., Fig. 1.1) with atmospheric and oceanic teleconnections transmitting the signal to the tropics and beyond. A third mechanism operating during deglaciation that may cause abrupt climate change is the rapid reduction in the aerial extent of the LIS, which may induce abrupt warming and cause step-like climate change (Felzer et al., 1996; Renssen et al., 2005; Shuman et al., 2005).

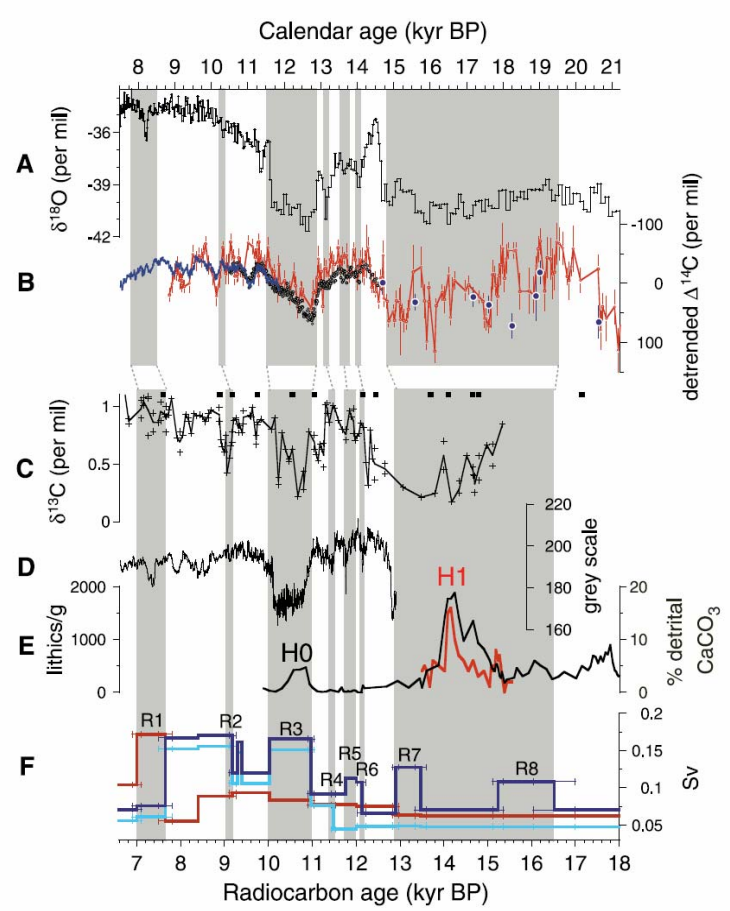

Figure 1.1. Deglacial time series for the North Atlantic region. Grey bars denote timing of freshwater routing events. (**A**) GISP2 $\delta^{18}O$ record; (**B**) detrended $\Delta^{14}C$ (a proxy of AMOC); (**C**) benthic $\delta^{13}C$ (a proxy of nutrients and AMOC); (**D**) Cariaco Basin grey scale (a proxy of productivity and wind strength); (**E**) ice rafted debris record (a proxy of iceberg discharge); (**F**) North American freshwater discharge (dark blue is Hudson and St. Lawrence Rivers, light blue is St. Lawrence, and red is Hudson Strait. (From Clark et al., 2001 and references therein.)

Both of the Northern Hemisphere mechanisms to cause millennial-scale variability involve the substrate of the LIS. Increased iceberg flux from the LIS, specifically from the Hudson Bay/Strait sector, has been attributed to thermodynamic switching from a frozen to wet-bed state at the base of the ice sheet (MacAyeal, 1993). A wet-bedded ice sheet can accelerate through attendant basal sliding and deformation of the underlying soft sediment leading to increased iceberg discharge. Similarly, the rapid advance and retreat of the southern margin of the LIS likely resulted from high basal pore water pressure developed in the subglacial sediment which enhanced some combination of basal sliding at the ice-till interface and sediment deformation (Clark, 1994; Clark et al., 2001). The main problem with these mechanisms for enhanced ice sheet motion is that basal sliding requires some unknown process to stabilize the ice sheet whereas the role of subglacial sediment deformation in controlling and

contributing to ice sheet motion is poorly understood and contentiously debated (e.g., Clarke, 1987; Kamb, 1991; Humphrey et al., 1993; Fischer and Clarke, 1994; Jenson et al., 1995; Hindmarsh, 1997; Iverson et al., 1998; Piotrowski and Tulaczyk, 1999; Boulton et al., 2001; Piotrowski et al., 2001; 2004; Moore and Iverson, 2002).

These controls on ice sheet motion and attendant relationship to AMOC and abrupt climate change need to be better constrained to improve predictions of the cryospheric/climatic response to future global warming. The response of ice sheets, specifically the West Antarctic Ice Sheet, to sea level rise may be underestimated if subglacial sediment and hydrology plays an important role in enhancing the flux of ice to the ocean thus leading to collapse of the ice sheet (MacAyeal, 1992; Bentley, 1997; De Angelis and Skvarca, 2003). Investigating the role of sediment deformation in contributing to fast ice flow and ice sheet stability as preserved in the geologic record of the LIS will provide insight into the behavior of present day ice sheets resting on soft sediment. Furthermore, the sensitivity of ice sheets to global warming can, at present, only be assessed with coupled ice sheet-climate models (e.g., Ridley et al., 2005) which may underestimate the rate of ice sheet retreat (e.g., Alley et al., 2005). Determining the retreat rate of the last Northern Hemisphere Ice Sheet to disappear under a climate warmer than present, the LIS, will help in testing the skill of these model predictions. In addition, the increased freshwater flux to the North Atlantic due to an enhanced Arctic hydrologic cycle (Peterson et al., 2002) or retreat of the Greenland Ice Sheet (Fichefet et al., 2003; Ridley et al., 2005) may impact AMOC with attendant climatic effects. Understanding how previous changes in the hydrologic cycle of the North Atlantic affected AMOC and climate will aid in predicting the sensitivity of AMOC to future changes in the hydrologic budget.

This dissertation addresses these issues by determining the contributions of subglacial sediment deformation and subglacial hydrology to ice sheet motion and stability. It also resolves the role of the LIS and freshwater routing in forcing the canonical abrupt climate event, the Younger Dryas cold event (12.9 to 11.7 ka), and the timing and rate of Holocene deglaciation of the LIS and the effect that deglaciation had Holocene climate.

1.2. Summary of Chapters

This dissertation contains four research components revolving around the dynamics of the LIS and the role of the LIS in abrupt climate change. Chapter 2 is a sedimentological study of the Tiskilwa Till of the Lake Michigan Lobe in central Illinois and the Sky Pilot Till of the Hudson Bay lowlands in northeastern Manitoba. This chapter addresses the depositional environments of these tills and discusses the relative contributions of sliding and sediment deformation to ice sheet motion.

Chapter 3 investigates the subglacial hydrology of the James Lobe (JL) of the LIS using a 3-D groundwater flow model that determines the effects of the JL on regional groundwater flow. In addition, a canal-type basal drainage system is simulated for the first time at the ice lobe scale (1000's of km), which quantitatively delineates a mechanism that allows the JL to remain coupled to its bed rather than experience wide spread decoupling and collapse.

Chapter 4 presents new proxies (U/Ca, Mg/Ca, Sr-isotopes) of freshwater routing that identify the forcing mechanism behind the Younger Dryas cold event. These proxies also identify a previously unrecognized intra-Younger Dryas routing event that perturbed and extended the Younger Dryas by several hundred years. The impact of this short-lived event demonstrates the tight coupling between AMOC, climate and the hydrologic cycle.

Chapter 5 determines the timing of retreat and final disappearance of the LIS in the Holocene using cosmogenic ^{10}Be ages from western Quebec. By dating the disappearance of the LIS, its role in initiating the Holocene Thermal Maximum and Labrador deep sea water formation is established. Furthermore, these ages determined the contribution of the LIS to an abrupt rise in sea level that occurred just prior to deglaciation and allow a comparison against model predictions of the future response of the Greenland Ice Sheet to global warming.

These four chapters have evolved into stand-alone papers that are currently in review or in preparation for submission. Chapter 2 is titled *Sedimentological observations from the Tiskilwa Till, Illinois, and Sky Pilot Till, Manitoba* and is in press at Géographie physique et Quaternaire. Chapter 3 is titled *Subglacial hydrology*

of the James Lobe of the Laurentide Ice Sheet and is intended for submission to Quaternary Science Reviews. Chapter 4 is titled *Freshwater forcing of ocean and climate variability during the Younger Dryas cold interval* and is currently in review at Nature. Chapter 5 is titled *Rapid Holocene Deglaciation of the Labrador Sector of the Laurentide Ice Sheet* and is intended for submission to Science.

1.3. References

Alley, R.B., and Clark, P.U., 1999, The deglaciation of the Northern Hemisphere: Annual Review of Earth and Planetary Science, v. 27, p. 149-182.

Alley, R.B., Clark, P.U., Huybrechts, P., and Joughin, I., 2005, Ice-Sheet and Sea-Level Changes: Science, v. 310, p. 456-460.

Andrews, J.T., 1998, Abrupt changes (Heinrich events) in late Quaternary North Atlantic marine environments: a history and review of data and concepts: Journal of Quaternary Science, v. 13, p. 3-16.

Bentley, C.R., 1997, Rapid sea-level rise soon from West Antarctic Ice Sheet collapse?: Science, v. 275, p. 1077-1078.

Bond, G., Showers, W., Cheseby, M., Lotti, R., Almasi, P., deMenocal, P., Priore, P., Cullen, H., Hajdas, I., and Bonani, G., 1997, A pervasive millennial-scale cycle in North Atlantic Holocene and glacial climates: Science, v. 278, p. 1257-1266.

Bond, G., Showers, W., Elliot, M., Evans, M., Lotti, R., Hajdas, I., Bonani, G., and Johnson, S., 1999, The North Atlantic's 1-2 kyr climate rhythm: relation to Heinrich events, Dansgaard/Oeschger cycles and the Little Ice Age, *in* Clark, P.U., Webb, R.S., and Keigwin, L.D., eds., Mechanisms of Global Climate Change at Millennial Time Scales: Geophysical Monograph 112, p. 35-58.

Boulton, G.S., Dobbie, K.E., and Zatsepin, S., 2001, Sediment deformation beneath glaciers and its coupling to the subglacial hydraulic system:. Quaternary International, v. 86, p. 3-28.

Broecker, W.S., 1994, Massive iceberg discharges as triggers for global climate change: Nature, v. 372, p. 421-424.

Broecker, W.S., Kennett, J.P., Flower, B.P., Teller, J.T., Trumbore, S., Bonani, G., and Wolfli, W., 1989, Routing of meltwater from the Laurentide Ice Sheet during the Younger Dryas cold episode: Nature, v. 341, p. 318-321.

Cane, M. A., 1998, A role for the Tropical Pacific: Science, v. 282, p. 59-61.

Clement, A.C., and Cane, M., 1999, A role for the tropical Pacific coupled ocean-atmosphere system on Milankovitch and Millennial time scales. Part I: a modeling study of tropical Pacific variability, *in* Clark, P.U., Webb, R.S., and Keigwin, L.D. eds., Mechanisms of Global Climate Change at Millennial Time Scales: Geophysical Monograph 112, p. 363-371.

Clark, P.U., 1994, Unstable behavior of the Laurentide Ice Sheet over deforming sediment and its implication for climate change, Quaternary Research: v. 41, p. 19-25.

Clark, P.U., Alley, R.B., and Pollard, D., 1999, Northern Hemisphere ice-sheet influences on global climate change: Science, v. 286, p. 1104-1111.

Clark, P.U., Marshall, S.J., Clarke, G.K.C., Hostetler, S.W., Licciardi, J.M., and Teller, J.T., 2001, Freshwater forcing of abrupt climate change during the last glaciation: Science, v. 293, p. 283-287.

Clark, P.U., Pisias, N.G., Stocker, T.F., and Weaver, A.J., 2002, The role of the thermohaline circulation in abrupt climate change: Nature, v. 415, p. 863-869.

Clarke, G.K.C., 1987, Subglacial till: a physical framework for its properties and processes: Journal of Geophysical Research, v. 92, p. 9023-9036.

De Angelis, H., and Skvarca, P., 2003, Glacier surge after ice shelf collapse: Science, v. 299, p. 1560-1562.

Felzer, B., Oglesby, R.J., Webb III, T., and Hyman, D.E., 1996, Sensitivity of a general circulation model to changes in northern hemisphere ice sheets: Journal of Geophyscial Research, v. 101, p. 19,077-19,092.

Fichefet, T., Poncin, C., Goosse, H., Huybrechts, P., Janssens, I., and LeTreut, H., 2003, Implications of changes in freshwater flux from the Greenland ice sheet for the climate of the 21st century: Geophysical Research Letters, v. 30, doi: 10.1029/2003GL017826.

Fischer, U.H., and Clarke, G.K.C., 1994, Ploughing of subglacial sediment: Journal of Glaciology, v. 40, p. 97-106.

Hindmarsh, R., 1997, Deforming beds: viscous and plastic scales of deformation: Quaternary Science Reviews, v. 16, p. 1039-1056.

Hostetler, S.W., and Bartlein, P.J., 1999, Simulation of the potential responses of regional climate and surface processes in Western North America to a canonical Heinrich event, *in* Clark, P.U., Webb, R.S., and Keigwin, L.S., eds., Mechanisms of Global Climate Change at Millennial Time Scales: Geophysical Monograph 112, p. 313-327.

Hostetler, S.W., Clark, P.U., Bartlein, P.J., Mix, A.C., and Pisias, N.J., 1999, Atmospheric transmission of North Atlantic Heinrich events: Journal of Geophysical Research, v. 104, p. 3947-3952.

Hughen, K.A., Southon, J.R., Lehman, S.J., and Overpeck, J.T., 2000, Synchronous radiocarbon and climate shifts during the last deglaciation: Science, v. 290, p. 1951-1954.

Humphrey, N., Kamb, B., Fahnestock, M., and Engelhardt, H., 1993, Characteristics of the bed of the lower Columbia Glacier, Alaska: Journal of Geophysical Research, v. 98, p. 837-846.

Iverson, N.R., Hooyer, T.S., and Baker, R.W., 1998, Ring-shear studies of till deformation: Coulomb-plastic behavior and distributed strain in glacier beds: Journal of Glaciology, v. 44, p. 634-642.

Jenson, J.W., Clark, P.U., MacAyeal, D.R., Ho, C., and Vela, J.C., 1995, Numerical modeling of advective transport of saturated deforming sediment beneath the Lake Michigan Lobe, Laurentide Ice Sheet: Geomorphology, v. 14, p. 157-166.

Kamb, B., 1991, Rheological nonlinearity and flow instability in the deforming bed mechanism of ice stream motion: Journal of Geophysical Research, v. 96, p. 16,585-16,595.

Koutavas, A., Lynch-Stieglitz, J., Marchitto, T.M., and Sachs, J.P., 2002, El Niño-like pattern in ice age Tropical Pacific sea surface temperature: Science, v. 297, p. 226-230.

Licciardi, J.M., Teller, J.T., and Clark, P.U., 1999, Freshwater routing by the Laurentide Ice Sheet during the last deglaciation, *in* Clark, P.U., Webb, R.S., and Keigwin, L.D. eds., Mechanisms of Global Climate Change at Millennial Time Scales: Geophysical Monograph 112, p. 177-201.

MacAyeal, D.R., 1992, Irregular oscillations of the West Antarctic ice sheet: Nature, v. 359, p. 29-32.
MacAyeal, D.R., 1993, Binge/purge oscillations of the Laurentide Ice Sheet as a cause of the North Atlantic's Heinrich events: Paleoceanography, v. 8, p. 775-784.
McManus, J.F., Francois, R., Gherardi, J.-M., Keigwin, L.D., and Brown-Leger, S., 2004, Collapse and rapid resumption of Atlantic meridional circulation linked to deglacial climate changes: Nature, v. 428, p. 834-837.
Moore, P.L., and Iverson, N.R., 2002, Slow episodic shear of granular material regulated by dilatant strengthening: Geology, v. 30, p. 843-846.
Peterson, B.J., Holmes, R.M., McClelland, J.W., Vörösmarty, C.J., Lammers, R.B., Shiklomanov, A.I., Shiklomanov, I.A., and Rahmstorf, S., 2002, Increasing river discharge to the Arctic Ocean: Science, v. 298, p. 2171-2173.
Piotrowski, J.A., Larsen, N.K., and Junge, F.W., 2004, Reflections on soft subglacial beds as a mosaic of deforming and stable spots: Quaternary Science Reviews, v. 23, p. 993-1000.
Piotrowski, J.A., Mickelson, D.M., Tulaczyk, S., Krzyszkowski, D., and Junge, F.W., 2001, Were deforming subglacial beds beneath past ice sheets really widespread?: Quaternary International, v. 86, p. 139-150.
Piotrowski, J.A., and Tulaczyk, S., 1999, Subglacial conditions under the last ice sheet in northwest Germany: ice-bed separation and enhanced basal sliding?: Quaternary Science Reviews, v. 18, p. 737-751.
Renssen, H., Goosse, H., Fichefet, T., Brovkin, V., Driesschaert, E., and Wolk, F., 2005, Simulating the Holocene climate evolution at northern high latitudes using a coupled atmosphere-sea ice-ocean-vegetation model: Climate Dynamics, v. 24, p. 23-43.
Ridley, J.K., Huybrechts, P., Gregory, J.M., and Lowe, J.A., 2005, Elimination of the Greenland Ice Sheet in a high CO_2 climate: Journal of Climate: v. 18, p. 3409-3427.
Shuman, B., Bartlein, P.J., and Webb, T., 2005, The magnitudes of millennial- and orbital-scale climatic change in eastern North American during the Late Quaternary: Quaternary Science Reviews, v. 24, p. 2194-2206.
Stott, L., Poulsen, C., Lund, S., and Thunell, R., 2002, Super ENSO and global climate oscillations at millennial time scales: Science, v. 297, p. 222-226.
Teller, J.T., 1990, Volume and routing of late-glacial runoff from the Southern Laurentide Ice Sheet: Quaternary Research, v. 34, p. 12-23.
Tudhope, A.W., Chilcott, C.P., McCulloh, M.T., Cook, E.R., Chappell, J., Ellam, R.M., Lea, D.W., Lough, J.M., and Shimmield, G.B., 2001, Variability in the El Niño-Southern Oscillation through a glacial-interglacial cycle: Science, v. 291, p. 1511-1517.
Turney, C.S.M., Kershaw, A.P., Clemens, S.C., Branch, N.B., Moss, P.T., and Fifield, L.K., 2004, Millennial and orbital variations in El Niño/Southern Oscillation and high-latitude climate in the last glacial period: Nature, v. 428, p. 306-310.

CHAPTER 2

SEDIMENTOLOGICAL OBSERVATIONS FROM THE TISKILWA TILL, ILLINOIS, AND SKY PILOT TILL, MANITOBA

Anders E. Carlson (1), John W. Jenson (2), Peter U. Clark (1)

(1) Department of Geosciences, Oregon State University, Corvallis, OR 97331, USA

(2) WERI, University of Guam, Mangilao, GU 96923, USA

Carlson, A.E., Jenson, J.W., and Clark P.U., in press, Field observations from the Tiskilwa Till, IL and Sky Pilot Till, MB of the Laurentide Ice Sheet: Géographie physique et Quaternaire.

2.1. Abstract

We present sedimentological observations from the Tiskilwa Till in northern Illinois, and the Sky Pilot Till in northern Manitoba, that indicate deposition of these tills by subglacial deformation. These generally homogenous tills grade downward into more heterogeneous tills that incorporate underlying sediment into their matrix, indicating entrainment of older sediments by sediment deformation. Deformed sand inclusions within these tills imply deformation of the tills and inclusions prior to deposition. The Tiskilwa Till has relatively high fabric strength throughout its thickness, whereas fabric strength in the Sky Pilot Till generally increases up-section in 2- to 3-m thick increments. Fabric orientations in both tills rotate up-section, possibly due to changes in ice-flow direction associated with the thickening and thinning of ice, and changes in ice-flow divide location. In both the Tiskilwa and Sky Pilot Tills, the change in fabric orientation occurs over intervals of ~1 m, suggesting that the maximum depth of deformation was ≤1 m insofar as any greater depth of deformation would have reoriented till fabric during maximum ice extent and retreat. In the case of the Sky Pilot Till, the up-section increase in macrofabric strength indicates that strain increased up-section. These data suggest that these tills were deposited in a time transgressive manner as strain migrated upwards with the delivery of new till either released from the ice base or advected from up-ice.

2.2. Introduction

Warm-based ice sheets resting on beds of unconsolidated sediment (soft beds) are thought to play important roles in global climate and sea level change (Clark *et al*., 1999). In modern polar ice sheets, warm-based ice streams will likely modulate ice sheet responses to global warming (MacAyeal, 1992; Bentley, 1997). Similarly, warm-based Pleistocene ice sheets may have influenced the responses and contributions of the ice sheets to global climate change (MacAyeal, 1993; Clark, 1994; Marshall and Clark, 2002). Accordingly, over the past two decades, considerable

research has been directed toward identifying and understanding the mechanisms governing the movement of warm-based ice over soft beds.

Although it is generally agreed that such movement involves some combination of sliding and deformation of underlying sediment, determining the relative contribution of each, and the details of the mechanical processes by which they act or interact, has remained elusive. Initial studies using seismic reflectivity to evaluate basal conditions beneath Ice Stream B (now the Whillans Ice Stream) in West Antarctica, for example, indicated that a metres-thick, saturated, dilatant sediment layer was deforming pervasively beneath the ice stream, accounting for the ice stream's fast velocity under extremely low driving stress (Alley *et al*., 1986; Blankenship *et al.*, 1986). Models assuming pervasive deformation based on linear or mildly non-linear viscous flow offered some promise for explaining fast ice-flow as well as the high sediment flux rates suggested from the mass of fine-grained glacial sediment deposited beneath the southern margin of the Laurentide Ice Sheet (LIS) (Alley, 1991; Jenson *et al.*, 1995). However, field studies in boreholes and laboratory testing of modern and Pleistocene till suggested that subglacial till is too weak to balance basal shear stress (Kamb, 1991; Humphrey *et al.*, 1993; Fischer and Clarke, 1994; Iverson *et al.*, 1994, 1998; Engelhardt and Kamb, 1998), and that ice movement must therefore occur primarily through basal sliding, with some as yet unidentified mechanism required to stabilize ice movement (Iverson *et al.*, 1994; Hooke *et al.*, 1997; Engelhardt and Kamb, 1998).

Studies of the sediment record provide valuable observations and insights by which to constrain inferences, assumptions, and hypotheses regarding basal conditions and processes (Clayton *et al.*, 1989; Alley, 1991; Hicock, 1992; Hicock and Dreimanis, 1992; Johnson and Hansel, 1999; Boulton *et al.*, 2001; Hooyer and Iverson, 2000b, 2002; Piotrowski *et al.*, 2001, 2004; Larsen *et al.*, 2004). Nevertheless, attempts to discern mechanisms of ice movement from the sediment record are complicated by the fact that processes beneath modern ice sheets are, to a first order, not directly observable, thus obviating a process-based approach to understanding sedimentation. Accordingly, interpretations of the sediment record have largely been based on deductive reasoning, which has often led to conflicting

interpretations of even the same sedimentological features (Boulton *et al*., 2001; Piotrowski *et al*., 2001). Piotrowski *et al.* (2004) tried to reconcile these conflicting interpretations with observations from tills deposited by the Scandinavian Ice Sheet that suggested a mosaic of deforming and decoupled sliding spots. Conceptually, this is an attractive model, but in the absence of direct observations, unequivocal sedimentological evidence of subglacial processes has yet to be demonstrated.

Here we present sedimentological observations of the Tiskilwa Till deposited by the Lake Michigan Lobe along the southern LIS margin, and the Sky Pilot Till deposited near the centre of the LIS in the Hudson Bay Lowlands, Manitoba (Fig. 2.1). Because these two regionally significant tills are representative of many fine-grained tills deposited beneath the LIS, developing a better understanding of the processes responsible for their formation will provide important constraints on LIS behavior over soft-bedded regions.

2.3. The Till Units

The Tiskilwa Till was deposited by the south-to-southwest-flowing Lake Michigan Lobe during the Last Glacial Maximum, ~21.5 to 19 ^{14}C kyr BP (Hansel and Johnson, 1996). It is one of the most extensive till units in the midcontinent (Wickham and Johnson, 1981) and is characteristic of the fine-grained tills that underlie much of the southern LIS (Mickelson *et al.*, 1983).

Johnson and Hansel (1990) conducted a detailed sedimentological study of the Tiskilwa Till at its type locality (Wedron Quarry, Illinois). Basal heterogeneous Tiskilwa Till is separated from an overlying homogeneous facies of Tiskilwa Till by an abrupt contact. Both the homogeneous and heterogeneous till facies have strong macrofabrics. Additionally, both facies contain sand inclusions, but the inclusions in the heterogeneous facies are more deformed than those in the homogeneous facies. Johnson and Hansel (1990) suggested that the sand inclusions were either deformed remnants of a subglacial drainage system or proglacial material incorporated into the till during ice advance. They interpreted the heterogeneous till to be a product of

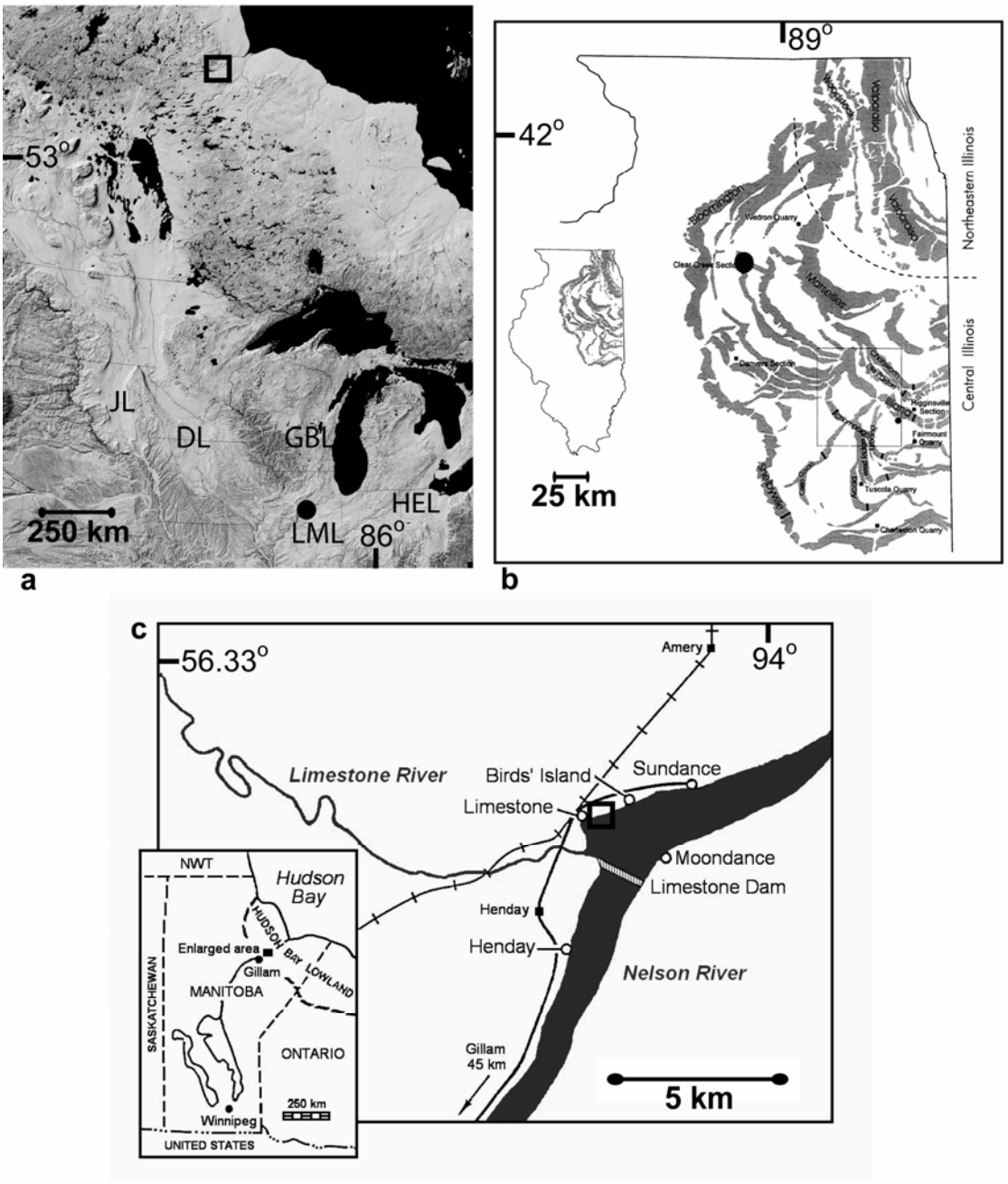

Figure 2.1. (**a**) Digital elevation shaded relief map of central North America. Solid circle is location of Tiskilwa Till exposures in Illinois, open square is location of Sky Pilot Till exposure in Manitoba. JL denotes the James Lobe, DL denotes the Des Moines Lobe, GBL denotes the Green Bay Lobe, LML denotes the Lake Michigan Lobe, HEL denotes the Huron-Erie Lobe. (**b**) North-central Illinois location map (modified from Johnson and Hansel, 1999). Solid circle shows the location of the Friday 3 and Clear Creek sections. (**c**) Northern Manitoba location map (modified from Roy, 1998). Open square shows the location of the Limestone section.

subglacial deformation whereas the overlying homogeneous till was deposited by lodgement with some subglacial deformation.

The Sky Pilot Till is part of a regionally extensive surface unit that was deposited across the Hudson Bay lowland sometime during the Late Wisconsin (after ~25 ^{14}C kyr BP and sometime before 8 ^{14}C kyr BP) (Dredge and Nielsen, 1985; Nielsen *et al.*, 1986; Dredge and Nixon, 1992; Thorleifson *et al.*, 1992; Dyke, 2004), and may be a representative substrate for a large area underlying the centre of the Laurentide Ice Sheet during the last glaciation. The till is fine-grained (Nielsen *et al.*, 1986) with a gravel fraction of ~4%, and contains a high proportion of carbonate content in both its matrix (39%) and clast component (76%), reflecting a bedrock source from the middle of Hudson Bay (Roy, 1998). Fabric strength is moderately strong in the Sky Pilot Till (Roy, 1998) showing some regional variability (Nielsen *et al.*, 1986; Roy, 1998).

2.4. Methods

We examined two exposures of the Tiskilwa Till in Putnam County, Illinois (the Friday Three and Clear Creek sections) and one exposure of the Sky Pilot Till along the Nelson River, approximately 55 km northwest of Gillam, Manitoba (the Limestone section) (Fig. 2.1, 2.2). Macrofabric was measured every metre by determining the long axis orientation on 25 elongate pebbles (2 to 10 cm in length, long to intermediate axis ratio of >2:1) over an area 20 cm high x 30 cm wide. Fabric data was plotted on lower-hemisphere Schmidt diagrams and fabric shape determined following Hicock *et al.* (1996). Eigenvalues (S1, S2, S3) and eigenvectors (V1, V2, V3) were determined following Mark (1973). It has been suggested that 50 pebble measurements are required to determine statistically significant fabric variability from between sample variability (Benn and Ringrose, 2001). However, Larsen and Piotrowski (2003) demonstrated that a smaller number of pebble measurements still produced significant fabric results. We thus use 25 measurements in accord with the previous work of Johnson and Hansel (1999) on the Tiskilwa Till. Thin section samples of Tiskilwa Till were taken from the same depth as macrofabric

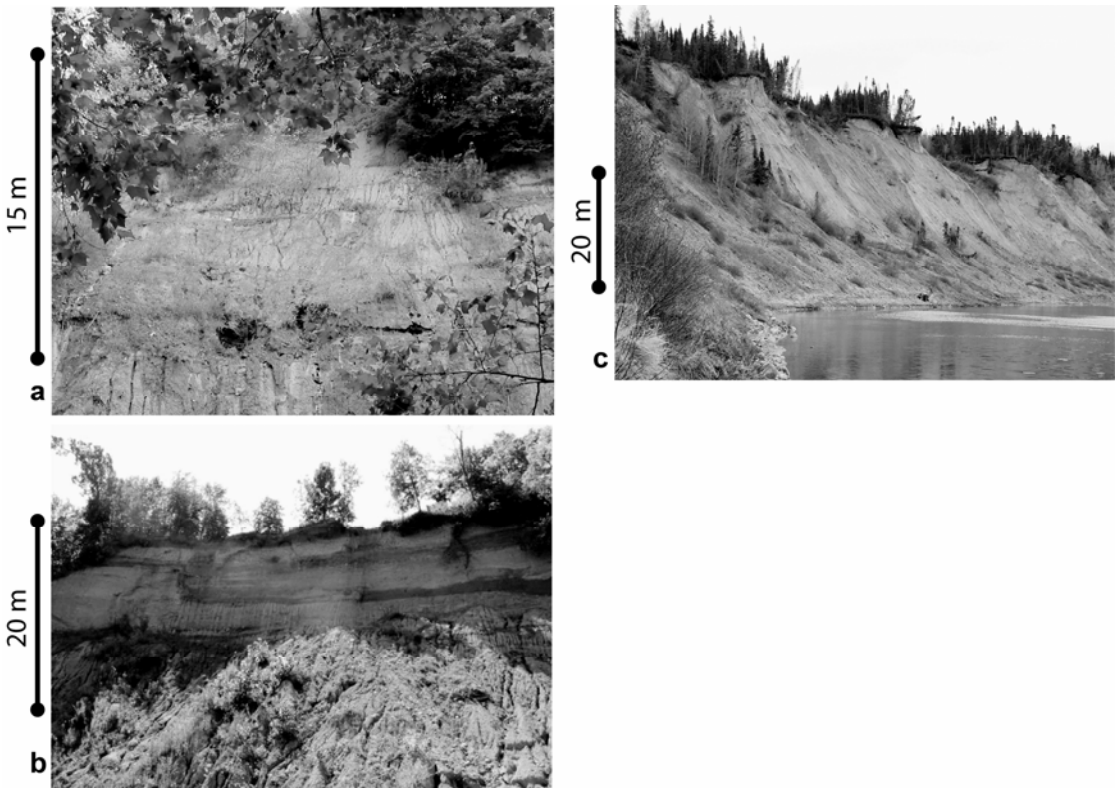

Figure 2.2. Bluff exposures. (**a**) Friday 3, IL; (**b**) Clear Creek, IL; (**c**) Limestone section, MB.

measurements. The high carbonate content of the Sky Pilot Till precluded its thin sectioning. Samples for grain size analysis by pipette method were collected every 0.5 m. Ten samples were analyzed from the Friday 3 section and 15 samples from the Limestone section. At the Clear Creek section, two samples of the Tiskilwa Till and three samples of the 1-m gradational basal contact were analyzed for grain size. The Friday Three section contained fragments of wood throughout the section. We noted the location, orientation and abundance of wood and dated six samples by radiocarbon.

2.5. Results

2.5.1. Tiskilwa Till

At the two Illinois sections, the Tiskilwa Till is a reddish-brown, massive, homogeneous, fine-grained diamicton 5 to 6 m thick (Figs. 2.3, 2.4). It overlies the grey, more heterogeneous Delavan Till with a ~1 m thick gradational contact. Thin sections of Tiskilwa Till from up to 2 m above the Tiskilwa-Delavan contact reveal small (<0.5 cm) inclusions of Delavan Till in the Tiskilwa Till matrix. At the Clear Creek section, the base of the Delavan Till is exposed and grades into underlying proglacial sediment over ~1 m thick interval (Fig. 2.3f). The Delavan and Tiskilwa Tills have a uniform grain size throughout the sections (Fig. 2.4a, b) (Table 2.1). At the Clear Creek section, however, the gradational contact between the Delavan Till and underlying sediment shows greater variability in grain size. Also at this section, sand inclusions in both till units are up to 1 m thick, have abrupt contacts with the surrounding till, and are deformed in the direction of ice-flow. Some inclusions contain balls of Tiskilwa Till within the sand and have diapirs of till rising into the sand (Fig. 2.3d). If the sand contained any original sedimentary structures, then they have been erased by deformation.

Till Unit	% Sand	stan. dev.	% Silt	stan. dev.	% Clay	stan. dev.
Sky Pilot	17	2	57	7	26	7
Long Spruce	21	6	54	7	25	2
Amery	30		40		30	
Tiskilwa	45	2	39	5	16	5
Delavan	45	1	42	1	13	1

Table 2.1. Grain size data for till units with standard deviation.

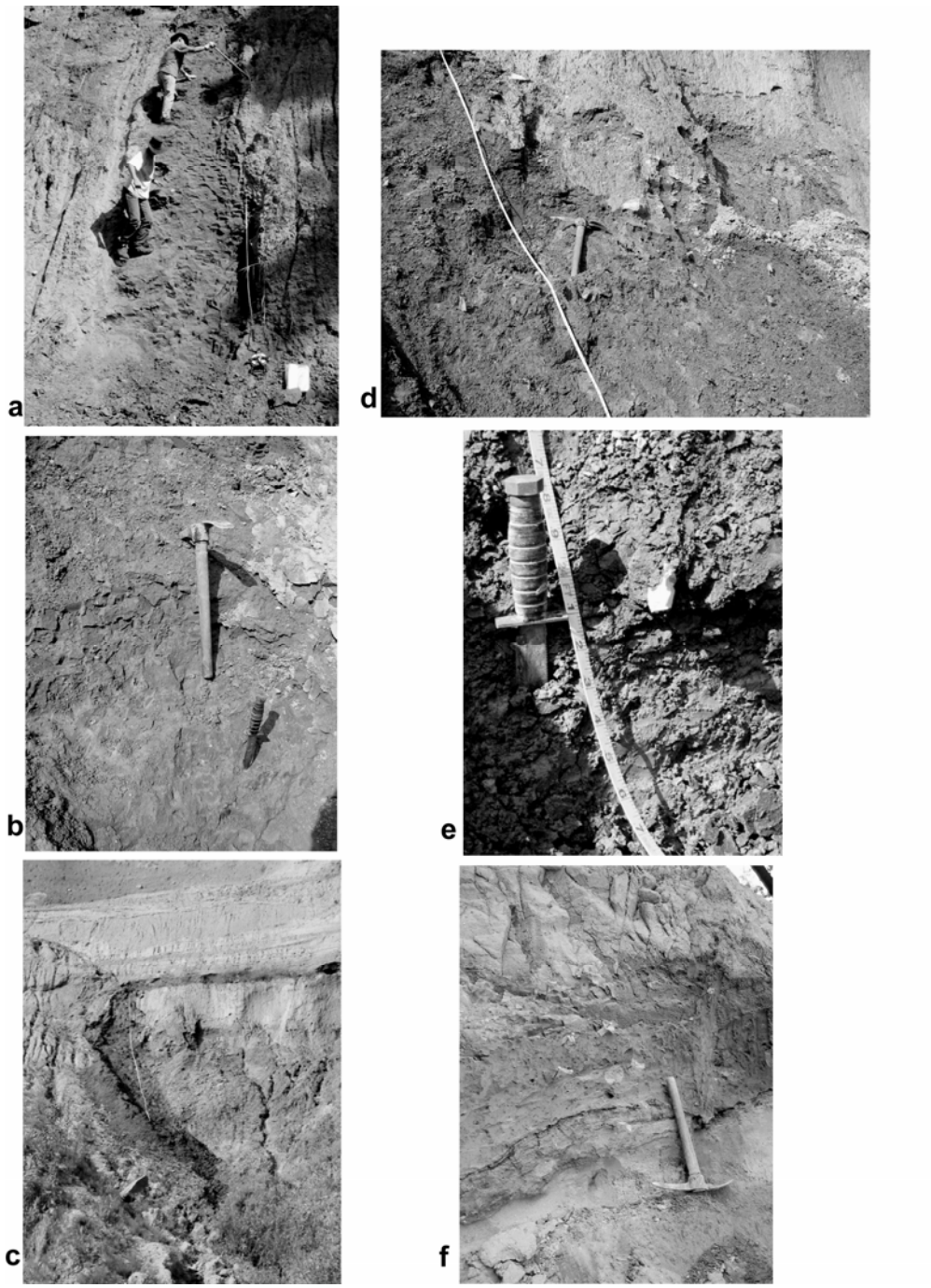

Figure 2.3. Tiskilwa Till sections. (**a**) Cleared exposure of Tiskilwa Till at Friday 3; (**b**) inset shows close up of uniform Tiskilwa Till from Friday 3. (**c**) Clear Creek exposure; (**d**) shows deformed sand inclusion with Tiskilwa Till within the sand at Clear Creek; (**e**) shows the basal contact between the Delavan Till and underlying sediment at Clear Creek. (**f**) Gradational contact between Delavan Till and underlying sediment at Clear Creek.

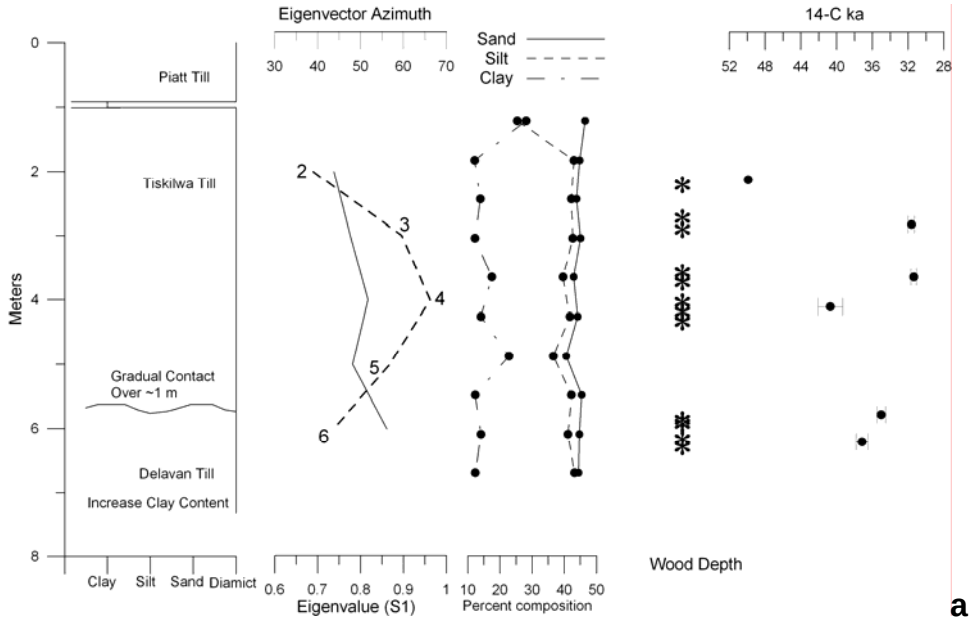
Eigenvector Azimuth
30 40 50 60 70
Sand
Silt
Clay
14-C ka
52 48 44 40 36 32 28
Meters
0
2
4
6
8
Piatt Till
Tiskilwa Till
Gradual Contact
Over ~1 m
Delavan Till
Increase Clay Content
2
3
4
5
6
Clay Silt Sand Diamict
0.6 0.7 0.8 0.9 1
Eigenvalue (S1)
10 20 30 40 50
Percent composition
Wood Depth

a

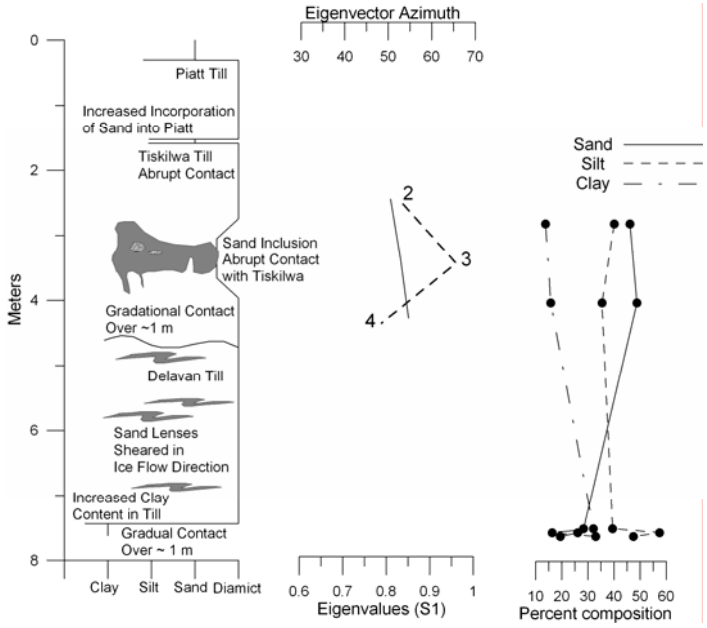
Eigenvector Azimuth
30 40 50 60 70
Meters
0
2
4
6
8
Piatt Till
Increased Incorporation
of Sand into Piatt
Tiskilwa Till
Abrupt Contact
Sand Inclusion
Abrupt Contact
with Tiskilwa
Gradational Contact
Over ~1 m
Delavan Till
Sand Lenses
Sheared in
Ice Flow Direction
Increased Clay
Content in Till
Gradual Contact
Over ~ 1 m
Clay Silt Sand Diamict
2
3
4
Sand
Silt
Clay
0.6 0.7 0.8 0.9 1
Eigenvalues (S1)
10 20 30 40 50 60
Percent composition

b

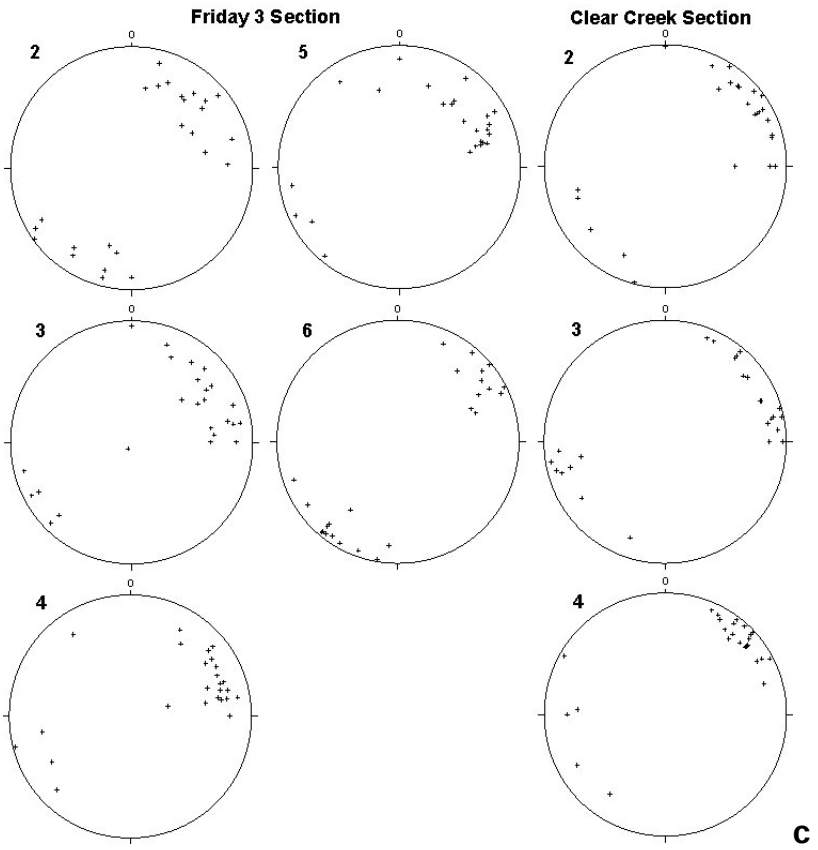

Figure 2.4. Tiskilwa Till section data. (**a**) Friday 3; (**b**) Clear Creek. The radiocarbon date at 2.1 m from Friday 3 is > 49.9 ^{14}C ka. (**c**) Fabric data from Friday 3 and Clear Creek. Numbers indicate the depth (m) in the section from which the data was collected.

The till contains glacially transported wood aligned with regional ice-flow, with greatest abundance near the base of the Friday 3 section (Fig. 2.4a) (Table 2.2). Radiocarbon dates on six pieces of wood range from 31.4 ^{14}C kyr BP to >49.9 ^{14}C kyr BP, with a general trend of decreasing age up-section followed by an increase in age at ~3 m.

Macrofabric is strong throughout the Tiskilwa Till, as indicated by principle eigenvalues (S1) between 0.74 and 0.85 (Fig. 2.4) with the fabric having a unimodal to spread unimodal shape (Hicock *et al.*, 1996). Thin sections also indicate strong alignment of particles in the Tiskilwa Till matrix. Macrofabric principle eigenvectors (V1) shift direction upward through the section from N40E to N60E, returning to N40E near the top of the Tiskilwa Till (Fig. 2.4).

Lab ID #	Sample	Material	Pretreatment	^{14}C Age	1 sigma
AA57002	F3-1	Wood	None	>49,900	
AA57003	F3-3	Wood	None	31,630	370
AA57004	F3-5	Wood	None	31,380	320
AA57005	F3-7	Wood	None	40,700	1400
AA57006	F3-9	Wood	None	35,010	500
AA57007	F3-12	Wood	None	37,160	660

Table 2.2. ^{14}C ages from Friday 3 section, IL.

2.5.2. Sky Pilot Till

In the study area, the Sky Pilot Till is a massive, homogeneous diamicton overlain by proglacial and lacustrine sediment. It is ~6 m thick, with a 1-m gradational contact into the underlying ~3 m thick Long Spruce Till (Figs. 2.5, 2.6). Long Spruce Till overlies the interglacial Nelson River Sediments (Dredge and Nielsen, 1985; Klassen, 1986; Nielsen *et al.*, 1986, Dredge and Nixon, 1992; Roy, 1998), which are deformed into the matrix of the Long Spruce Till (Fig. 2.5c). The Nelson River Sediments have an abrupt basal contact with the underlying Amery Till. Deformed sand lenses are present in all three till units. Grain size of the Sky Pilot and Long Spruce Tills is relatively uniform throughout the units (Fig. 2.6) (Table 2.1).

Eigenvalues are moderately strong (S1 between 0.50 and 0.81) in the three till units at the Limestone section. In the Sky Pilot Till, there is a general trend of increasing strength up-section in 2 to 3 m increments. The stronger fabrics have a unimodal to spread unimodal shape while the weaker fabrics are spread bimodal in shape (Hicock *et al.*, 1996) (Fig. 2.6). Eigenvectors change orientation up-section from north-northeast in the Amery Till to east-southeast in the Long Spruce to northeast in the Sky Pilot Till, identifying significant changes in ice-flow direction associated with deposition of each till (Dredge and Nielsen, 1985; Nielsen *et al.*, 1986; Dredge and Nixon, 1992; Thorleifson *et al.*, 1992; Roy, 1998). Within the Sky Pilot Till, eigenvectors rotate up-section from N45E to N75E (Fig. 2.6).

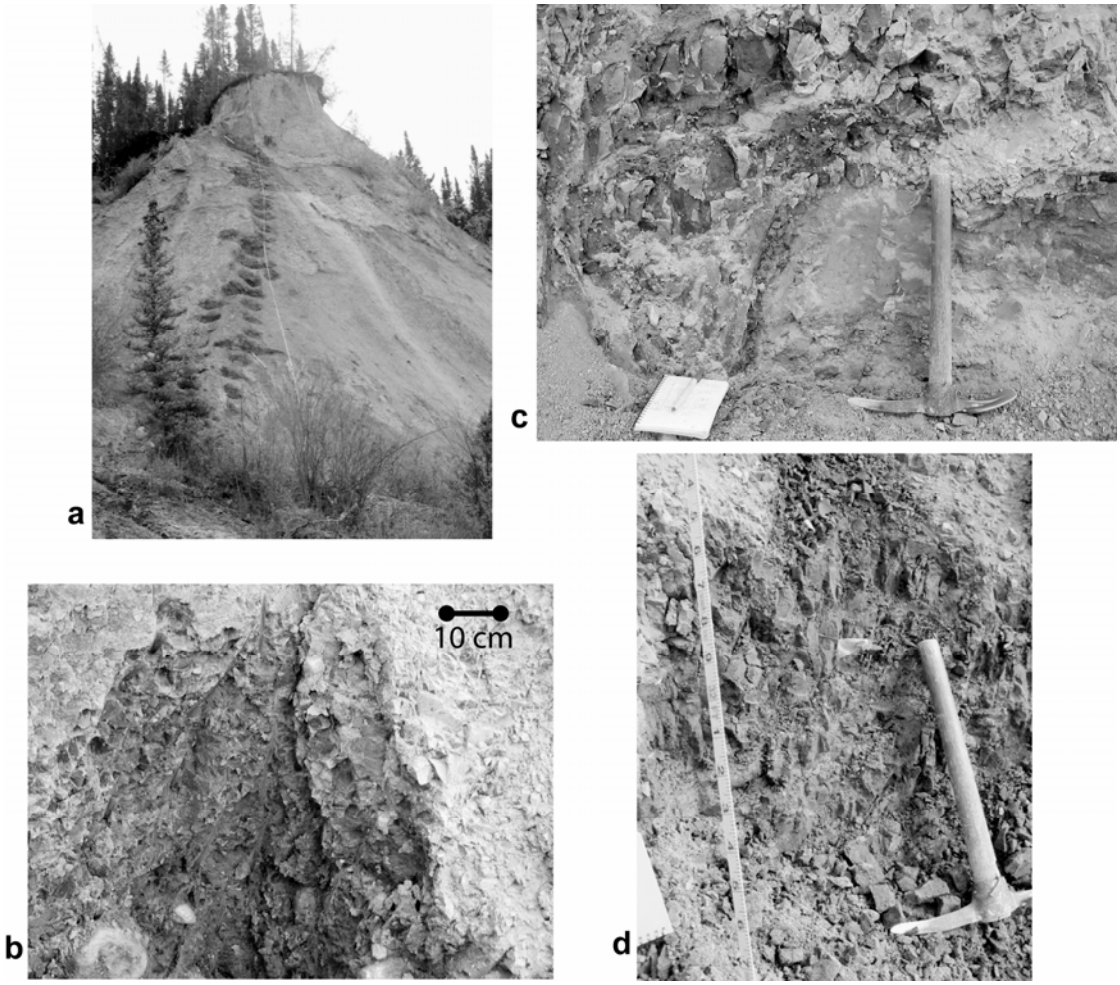

Figure 2.5. Limestone section of the Sky Pilot Till with a clean face (**a**); (**b**) is a close up of the Sky Pilot Till; (**c**) shows a deformed sand lens in the Sky Pilot Till; (**d**) shows deformed sediment into the Long Spruce Till.

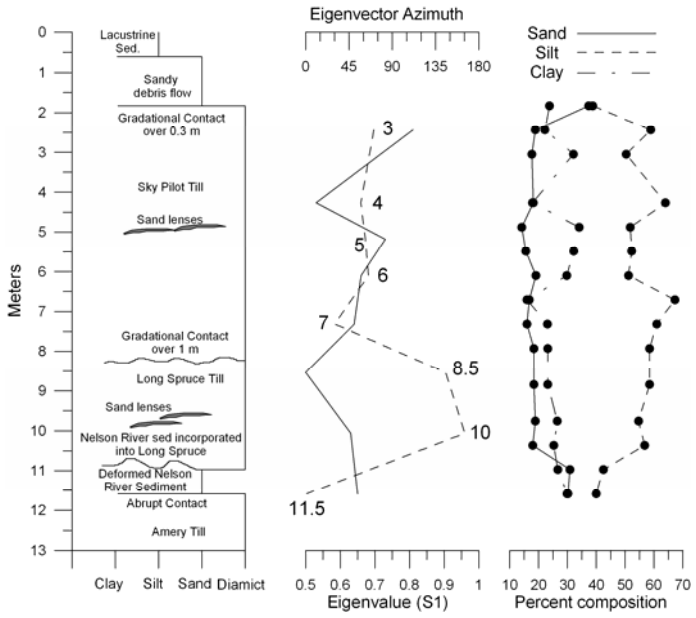

a

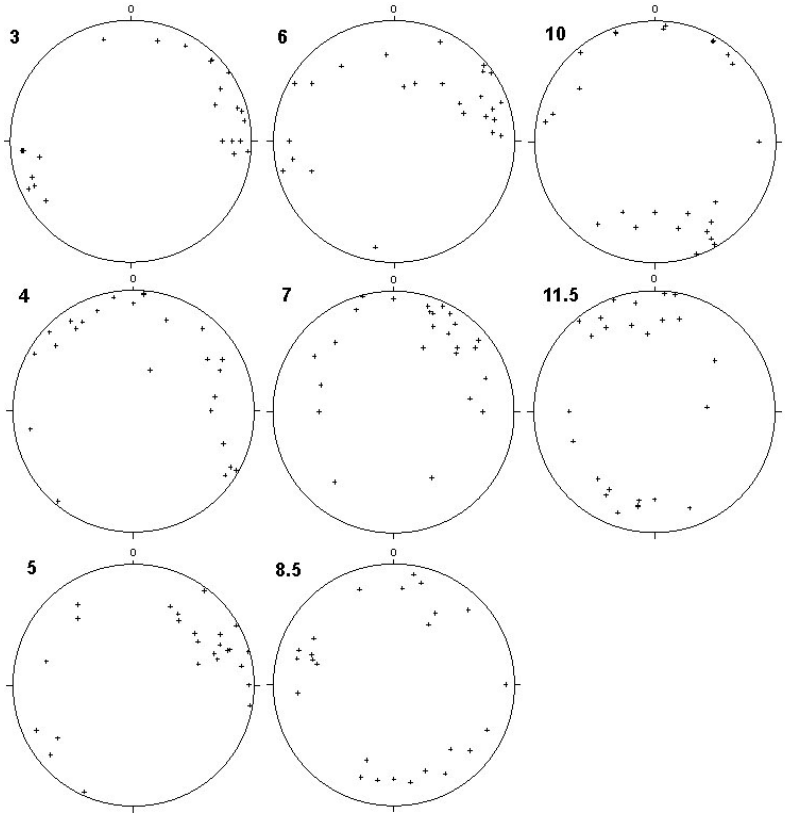

b

Figure 2.6. (**a**) Sky Pilot Till section data from the Limestone section. (**b**) Fabric data from the Limestone section. Numbers indicate depth (m) in the section from which the data was collected.

2.6. Discussion

We interpret the sedimentological features of the Tiskilwa Till to be most consistent with deposition from a subglacial deforming layer. The heterogeneous basal facies of the Tiskilwa Till indicates that the older Delavan Till was reworked and redeposited within a zone of mixing during the Tiskilwa ice readvance. The basal 1 m of the Delavan Till matrix also includes underlying sediments, suggesting a similar process of deformation and incorporation.

Further evidence of deformation is suggested by the sand inclusions. The sand may have been originally deposited in subglacial canals that were incised into the till at the base of the ice and subsequently deformed as they were entrained into the deforming subglacial sediment (Clark, 1997) (Fig. 2.3d). Tiskilwa Till balls in the sand may have originated as englacial sediment that melted off the roof of a canal into the underlying canal sediments. Alternatively, the till balls may represent till that was detached and incorporated into a sand body during deformation of the sediment mass. The inclusion of these till balls in the sand rules out the synchronous deposition of the sand and till by melt-out because the till must have existed prior to sand deposition to have the till included in the sand.

The fabric data of the Tiskilwa and Delavan Tills are strong throughout its thickness. Classical fabric interpretation (e.g. Dowdeswell and Sharp, 1986; Hicock *et al.*, 1996; Lian *et al.*, 2003) would suggest that till genesis can be inferred from fabric strength and shape. However, laboratory results using a ring-shear device suggest that fabric strength is not unique to a specific genesis (Hooyer and Iverson, 2000a). Fabric strength in these laboratory-deformed tills increased with increasing accumulated strain with highly strained tills having a strong fabric (similar to lodgement and melt-out tills). Similarly, these fabrics exhibited unimodal to spread unimodal shape similar to lodgement or melt-out tills suggesting that fabric shape is also not indicative of genesis. Based on the independent evidence for deformation (gradational basal contacts with reworked till and deformed sand inclusions), we interpret our fabric data from the Tiskilwa and Sky Pilot Tills as indicators of accumulated strain and local ice-

flow direction (Bennett *et al.*, 1999; Larsen *et al.*, 2004) but do not attempt to infer genesis from them.

The consistently strong fabric in the Tiskilwa Till suggests that the till underwent substantial strain throughout its thickness over time (Hooyer and Iverson, 2000; Larsen *et al.*, 2004), regardless of the depth of the deformation at any one location or time. Fabric data from Tiskilwa Till ~50 km to the northeast of our sites have shown similar strong fabrics (Johnson and Hansel, 1990; 1999) suggesting that the strong fabric of the Tiskilwa Till is regionally extensive. We interpret the up-section shift of the eigenvectors observed at two locations km's (check distance) apart to reflect changes in local ice-flow direction. These changes, however, are consistent with regional ice-flow changes associated with the advance and retreat of the Lake Michigan Lobe (Johnson and Hansel, 1999). Specifically, initial advance of the lobe over the site would have been from a more northeasterly direction, with flow shifting to a more westerly direction as the margin reached its limit and ice thickened over the site. A reverse flow-direction sequence would then occur as the lobe retreated and ice thinned over the site. The preservation of the shifting macrofabric orientation constrains the maximum depth of the deforming layer to ≤1 m thick. If the till was actively deforming to a greater depth, then earlier ice-flow directions recorded by the macrofabric would have been re-oriented by subsequent changes in ice-flow direction (e.g. MacClintock and Dreimanis, 1964).

The tills exposed along the Nelson River, Manitoba, display sedimentological features generally similar to the Tiskilwa Till, and we similarly attribute the formation of these features as a result of subglacial sediment deformation in accord with the interpretations of Roy (1998). The deformed sand inclusions may be remnant subglacial canals of a basal drainage system, as we suggested for the Tiskilwa Till, or they may represent interstadial events (Dredge and Nixon, 1992). Regardless of their origin, they are deformed into the till implying that the till was deformed with them. Gradational contacts between the Sky Pilot and the Long Spruce Tills, and between the Long Spruce Till and underlying interglacial sediment (Fig. 2.5, 2.6a), suggest a similar process of deformation and incorporation of preexisting sediments into an actively deforming sediment layer. Based on the gradational contacts, we suggest that

much of the till was transported in the deforming layer and originated from the mixing of the underlying sediment with till derived from up-ice. The till was then deposited when strain migrated upwards with the delivery of new till either released from the overlying ice or advected from up-ice.

In the case of the Sky Pilot Till, the up-section shift in eigenvector orientation indicates that local ice-flow migrated westward as the till was deposited, consistent with changes in regional ice-flow (Dyke, 2004). Fabric orientations of Roy (1998) from the Sky Pilot Till are consistent with our fabric data showing a shift in ice flow towards the west up-section. The Sky Pilot Till, however, may exhibit variability in fabric orientation based on four fabric measurements distributed over ~20 km (Nielsen et al., 1986). Our data, supported by that of Roy (1998), suggest that fabric orientation changed with depth in the till as ice-flow direction changed, indicating that observed regional fabric variability may be due to the varying depth at which the till fabric was measured. Multiple fabrics distributed throughout the till thickness are thus needed to distinguish local fabric variability from ice-flow variability.

Such changes in ice-flow direction recorded in till sections suggest that vertical examination of till fabric may delineate past changes in ice-flow during one advance and also the position of ice-flow divides in regions that otherwise lack surficial flow indicators (e.g. drumlins, flutes, lineations, striations). Unlike the Tiskilwa Till, however, the fabric strength of the Sky Pilot Till generally increases up-section in 2 to 3 m increments, suggesting an up-section increase in accumulation of strain, consistent with increasing sediment strength and decreasing strain with depth in the till. Similar to the Tiskilwa Till, the preservation of the migrating eigenvectors limits the depth of deformation in the Sky Pilot Till to ≤1 m. Till may have been deposited continuously at both locations in Illinois and Manitoba as indicated by the migration of eigenvector orientation up-section that reflect changes in ice-flow direction (Johnson and Hansel, 1999; Dyke, 2004).

It is interesting that the Tiskilwa and Sky Pilot Tills show similar features such as their deformed sand inclusions, basal contacts and migrating till fabrics, despite their differing depositional contexts with respect to the Laurentide Ice Sheet. While both tills were deposited by warm-based ice, the Tiskilwa Till was deposited under a

fast-moving lobe of the ice sheet, whereas the Sky Pilot Till was deposited near the centre of the ice sheet near or under an ice divide. The similarities between the two tills suggest that similar ice sheet motion and depositional processes were operating at both locations under the Laurentide Ice Sheet.

Hooyer and Iverson (2000b) used laboratory and field data to show that the contact between two tills in Minnesota contained a 40-cm thick mixed zone. They argued that the weak fabric strength (principle eigenvalues (S1) between 0.44 and 0.67) of the till deposited by the Des Moines Lobe in Iowa and Minnesota (Fig. 1) did not experience strain >2, and thus attributed much of the lobe motion to sliding (Hooyer and Iverson, 2002). This is in contrast to our data from the Lake Michigan Lobe (east of the Des Moines Lobe) that show mixing between the Delavan and Tiskilwa Tills in a zone up to 1 m thick and that the Tiskilwa Till experienced greater strain. Accordingly, we suggest that, to a first order, these sedimentological properties of tills (basal contacts, fabric strengths) provide some diagnostic information with respect to distinguishing between a large contribution to ice motion by sliding versus sediment deformation, as well as the depth of the deformation zone (e.g. Larsen et al., 2004). In particular, we would expect that where sliding makes a larger contribution to ice motion, strain in the underlying till would be smaller and hence the fabric of the underlying till to be weaker. Where conditions favor a larger contribution by deformation, fabrics would presumably be stronger. The central question then becomes what properties of the till and conditions of the subglacial environment determine the relative contribution of sliding or deformation.

2.7. Conclusions

Our observations of till sections from the Lake Michigan Lobe and Hudson Bay Lowlands suggest that sediment deformation may have occurred to depths up to 1 m in the Tiskilwa Till and Sky Pilot Till. The vertical uniformity of the strong fabric in the Tiskilwa Till suggests large accumulated strain in a deforming section up to 1 m thick that migrated upward over time. The upward-strengthening fabric in the Sky

Pilot Till, on the other hand, suggests an upward increase in strain through time. The relative contributions of sliding and sediment deformation cannot be discerned from the observations reported here. The uniformly strong fabric of the Tiskilwa Till and the strong fabric in the upper portion of the Sky Pilot Till, however, leave open the prospect that whatever deformation took place involved relatively high strain rates and sufficiently thick deforming layers to transport a significant mass of fine-grained sediment.

2.8. Acknowledgments

We thank Aubri Jenson for assistance in the field, Ardith Hansel for discussions relating to the Putnam County, IL, sites, and Martin Roy for discussions relating to the Limestone, MB, site. We also thank Chandrakant Desai, Dinshaw Contractor, and Shantanu Sane for particularly fruitful discussions. Reviews by S. Hicock and an anonymous reviewer improved this manuscript along with suggestions from A. Plouffe. This work was supported by NSF grants (EAR-0229513 and EAR-0229907) to Jenson and Clark.

2.9. References

Alley, R.B., 1991. Deforming-bed origin for southern Laurentide till sheets? Journal of Glaciology, 37: p. 67-76.

Alley, R.B., Blankenship, D.D., Bentley, C.R., and Rooney, S.T., 1986. Deformation of till beneath ice stream B, West Antarctica. Nature, 322: 57-59.

Benn, D.I., and Ringrose, T.J., 2001. Random variation of fabric eigenvalues: implications for the use of a-axis fabric data to differentiate till facies. Earth Surface Processes and Landforms, 26: 295-306.

Bennett, M.R., Waller, R.I., Glasser, N.F., Hambrey, M.J., and Huddart, D., 1999. Glacibenic clast fabrics: genetic fingerprint or wishful thinking. Journal of Quaternary Science, 14: 125-135.

Bentley, C.R., 1997. Rapid sea-level rise soon from West Antarctic Ice Sheet collapse? Science, 275: 1077-1078.

Blankenship, D.D., Bentley, C.R., Rooney, S.T., and Alley, R.B., 1986. Seismic measurements reveal a saturated porous layer beneath an active Antarctic ice stream. Nature, 322: 54-57.

Boulton, G.S., Dobbie, K.E., and Zatsepin, S., 2001. Sediment deformation beneath glaciers and its coupling to the subglacial hydraulic system. Quaternary International, 86: 3-28.

Clark, P.U., 1994. Unstable behavior of the Laurentide Ice Sheet over deforming sediment and its implication for climate change. Quaternary Research, 41: 19-25.

Clark, P.U., 1997. Sediment deformation beneath the Laurentide Ice Sheet, p. 81-97. *In* Martini, I.P., ed., Late Glacial and Postglacial Environmental Changes Quaternary, Carboniferous-Permian, and Proterozoic. Oxford University Press, London.

Clark, P.U., Alley, R.B., and Pollard, D., 1999. Northern Hemisphere ice-sheet influences on global climate change. Science, 286: 1104-1111.

Clayton, L., Mickelson, D.M., and Attig, J.W., 1989. Evidence against pervasively deformed bed material beneath rapidly moving lobes of the southern Laurentide ice sheet. Sedimentary Geology, 62: 203-208.

Dowdeswell, J.A. and Sharp, M.J., 1986. Characterization of pebble fabrics in modern terrestrial glacigenic sediments. Sedimentology, 33: 699-710.

Dredge, L.A. and Nielsen, E., 1985. Glacial and interglacial deposits in the Hudson Bay lowlands: a summary of sites in Manitoba, p. 247-257. *In* Current Research, Part A. Geological Survey of Canada, Paper 85-1A.

Dredge, L.A. and F.M., Nixon, 1992. Glacial and Environmental Geology of Northeastern Manitoba. Geological Survey of Canada Memoir 432: 80 p.

Dyke, A.S., 2004. An outline of North American Deglaciation with emphasis on central and northern Canada, p. 373-424. *In* Ehlers, J. and P.L. Gibbard, P.L., eds., Quaternary Glaciations-Extant and Chronology, Part II. Elsevier Sciences and Technology Books, Amsterdam.

Engelhardt, H., and Kamb, B., 1998. Basal sliding of Ice Stream B, West Antarctica. Journal of Glaciology, 44: 223-230.

Fischer, U.H., and Clarke, G.K.C., 1994. Ploughing of subglacial sediment. Journal of Glaciology, 40: 97-106.

Hansel, A.K., and Johnson, W.H., 1996. Wedron and Mason Groups: Lithostratigraphic reclassification of deposits of the Wisconsin Episode, Lake Michigan area. Illinois State Geological Survey Bulletin, 104 p.

Hicock, S.R., 1992. Lobe interactions and rheologic superposition in subglacial till near Bradtville, Ontario, Canada. Boreas, 21: 73-88.

Hicock, S.R. and Dreimanis, A., 1992. Deformation till in the Great Lakes region: implications for rapid flow along the south-central margin of the Laurentide Ice Sheet. Canadian Journal of Earth Sciences, 29: 1565-1579.

Hicock, S.R., Goff, J.R., Lian, O.B. and Little, E.C., 1996. On the interpretation of subglacial till fabric. Journal of Sedimentary Research, 66: 928-934.

Hooke, R.LeB., Hanson, B., Iverson, N.R., Jansson, P., and Fischer, U.H., 1997. Rheology of till beneath Storglaciären, Sweden. Journal of Glaciology, 43: 172-179.

Hooyer, T.S., and Iverson, N.R., 2000. Diffusive mixing between shearing granular layers: constraints on bed deformation from till contacts. Journal of Glaciology, 46: 641-651.

Hooyer, T.S., and Iverson, N.R., 2002. Flow mechanisms of the Des Moines lobe of the Laurentide ice sheet. Journal of Glaciology, 48: 575-586.

Humphrey, N., Kamb, B., Fahnestock, M., and Engelhardt, H., 1993. Characteristics of the bed of the lower Columbia Glacier, Alaska. Journal of Geophysical Research, 98: 837-846.

Iverson, N.R., Jansson, P., and Hooke, R.LeB., 1994. In-situ measurement of the strength of deforming subglacial till. Journal of Glaciology, 40: 497-503.

Iverson, N.R., Hooyer, T.S., and Baker, R.W., 1998. Ring-shear studies of till deformation: Coulomb-plastic behavior and distributed strain in glacier beds. Journal of Glaciology, 44: 634-642.

Jenson, J.W., Clark, P.U., MacAyeal, D.R., Ho, C., and Vela, J.C., 1995. Numerical modeling of advective transport of saturated deforming sediment beneath the Lake Michigan Lobe, Laurentide Ice Sheet. Geomorphology, 14: 157-166.

Johnson, W.H., and Hansel, A.K., 1990. Multiple Wisconsinan glacigenic sequences at Wedron, Illinois. Journal of Sedimentary Petrology, 60: 26-41.

Johnson, W.H., and Hansel, A.K., 1999. Wisconsin Episode glacial landscape of central Illinois: a product of subglacial deformation process? Geological Society of America Special Paper 337, 121-135.

Kamb, B., 1991. Rheological nonlinearity and flow instability in the deforming bed mechanism of ice stream motion. Journal of Geophysical Research, 96: 16,585-16,595.

Klassen, R.W., 1986. Surficial geology of the north-central Manitoba. Geological Survey of Canada Memoir 419, 57 p.

Larsen, N.K., and Piotrowski, J.A., 2003. Fabric in a basal till succession and its significance for reconstructing subglacial processes. Journal of Sedimentary Research, 73: 725-734.

Larsen, N.K., Piotrowski, J.A., and Kronborg, C., 2004. A multiproxy study of basal till: a time-transgressive accretion and deformation hypothesis. Journal of Quaternary Science, 19: 9-21.

Lian, O.B., Hicock, S.R. and Dreimanis, A., 2003. Laurentide and Cordilleran fast ice flow: some sedimentological evidence from Wisconsinan subglacial till and its substrate. Boreas, 32: 102-113.

MacAyeal, D.R., 1992. Irregular oscillations of the West Antarctic ice sheet. Nature, 359: 29-32.

MacAyeal, D.R., 1993. Binge/purge oscillations of the Laurentide Ice Sheet as a cause of the North Atlantic's Heinrich events. Paleoceanography, 8: 775-784.

MacClintock, P. and Dreimanis, A., 1964. Orientation of till fabric by overriding glacier in the Saint Lawrence Valley. American Journal of Science, 262: 133-142.

Mark, D.M., 1973. Analysis of axial orientation data, including till fabric. Geological Society of America Bulletin, 84: 1369-1373.

Marshall, S.J., and Clark, P.U., 2002. Basal temperature evolution of North American ice sheets and implications for the 100-kyr cycle. Geophysical Research Letters, 29: doi: 10.1029/2002GL015192.

Mickelson, D.M., Clayton, L., Fullerton, D.S., and Burns, H.W., Jr., 1983. The late Wisconsin glacial record of the Laurentide Ice Sheet in the U.S., p. 3-37. *In* Porter, S.C., ed., Late Quaternary environments of the United State. University of Minnesota Press, v. 1.

Nielsen, E., Morgan, A.V., Morgan, A., Mott, R.J., Rutter, N.W. and Causse, C., 1986. Stratigraphy, paleoecology, and glacial history of the Gillam area, Manitoba. Canadian Journal of Earth Sciences, 23, 1641-1661.

Piotrowski, J.A., Mickelson, D.M., Tulaczyk, S., Krzyszkowski, D., and Junge, F.W., 2001. Were deforming subglacial beds beneath past ice sheets really widespread? Quaternary International, 86: 139-150.

Piotrowski, J.A., Larsen, N.K., and Junge, F.W., 2004. Reflections on soft subglacial beds as a mosaic of deforming and stable spots. Quaternary Science Reviews, 23: 993-1000.

Roy, M., 1998. Pleistocene stratigraphy of the lower Nelson River area – implications for the evolution of the Hudson Bay lowland of Manitoba, Canada: M.S. Thesis, University of Quebec, Montreal, 220 p.

Thorliefson, L.H., 1989. Quaternary stratigraphy of the central Hudson Bay Lowland, northern Ontario: Ph.D. Thesis, University of Colorado, Boulder, 363 p.

Thorliefson, L.H., Wyatt, P.H., Shilts, W.W., and Nielsen, E., 1992. Hudson Bay Lowland Quaternary Stratigraphy: evidence for early Wisconsinan glaciation centered in Quebec, p. 207-220. In Clark, P.U., and Lea, P.D., eds., The Last Interglacial-Glacial Transition in North America. Geological Society of America, Special Paper 270.

Wickham, S.S., and Johnson, W.H., 1981. The Tiskilwa Till: A regional view of its origin and depositional processes. Annals of Glaciology, 2: 176-182.

CHAPTER 3

SUBGLACIAL HYDROLOGY OF THE JAMES LOBE OF THE LAURENTIDE ICE SHEET

Anders E. Carlson (1), John W. Jenson (2), Peter U. Clark (1), Roy Haggerty (1)

(1) Department of Geosciences, Oregon State University, Corvallis, OR 97331, USA

(2) WERI, University of Guam, Mangilao, GU 96923, USA

To be submitted to Quaternary Science Reviews

3.1. Abstract

To help constrain the plausible range of drainage conditions that might be expected to develop beneath soft-bedded ice sheets, we modeled the subglacial hydrology of the James Lobe of the Laurentide Ice Sheet from Hudson Bay to the Missouri River. Simulations suggest the JL had little effect on regional groundwater flow because the poorly conductive Upper-Cretaceous shale that occupies the upper layer of the bedrock would have functioned as a regional aquitard. This implies that general northward groundwater flow out of the Williston Basin has likely persisted throughout the Quaternary. Moreover, the simulations indicate that the regional aquifer system could not have drained even the minimum amount of basal meltwater that would have been produced from geothermal heat at the glacier bed. Therefore, drainage must have depended on the establishment of some sort of channelized drainage network at the ice-till interface. Using a theoretical karst aquifer analogue, we conducted simulations to bound the range of subglacial canal dimensions and spacing that would have been required at the ice-till interface to evacuate the minimum water flux. Results suggest a network of subglacial canals up to 50 cm wide, spaced about 40 to 70 meters apart, could have drained the ice sheet bed at basal water pressures below the ice overburden pressure.

3.2. Introduction

Rapid fluctuations of the lobes draining the southern margin of the Laurentide Ice Sheet (LIS) (Clayton and Moran, 1982; Mickelson et al., 1983) under driving stresses $\leq$10 kPa (Mathews, 1974; Clark, 1992; Hooyer and Iverson, 2002) require a significant component of ice motion by basal sliding and/or subglacial sediment deformation (Alley, 1991; Clark, 1994; Hooyer and Iverson, 2002). These processes of bed dynamics have broader implications for interpretations of global and abrupt climate change (see review in Clark et al., 1999). Their occurrence and importance require that basal water pressure be maintained near the ice load, which in turn depends on subglacial hydrological properties and processes. Of particular importance

are the ability of the regional aquifer to drain meltwater (Alley, 1989), and the properties of process that might develop to drain excess meltwater that cannot be accommodated by the regional aquifer.

The absence of modern analogues to the mid-latitude, terrestrial paleo-ice lobes and the limited access to the ice streams of the West Antarctic Ice Sheet, which are the most closely related modern phenomena have required the use of numerical model simulations to investigate the subglacial hydrology of ice sheets and lobes. Previous modeling studies have indicated that subglacial aquifers were unable to drain meltwater at the ice-till interface requiring the development of a basal drainage system such as a laminar film (Alley et al., 1989; Breemer et al., 2002), a canal system (Brown et al., 1987; Walder and Fowler, 1994), or periodic outburst floods (Piotrowski, 1997a; b) to maintain stable ice flow. However, films are unstable (Walder and Fowler, 1994; Engelhardt and Kamb, 1997), so such a film would at best be only the hypothetical, idealized hydrological equivalent of a channelized network such as the canal system of Walder and Fowler (1994). Adding a canal drainage system to a groundwater model is complicated by the assumption of laminar flow in the Laplace equation requiring the addition of a second model that includes turbulent flow making previous treatments of basal drainage at the lobe to ice sheet scale qualitative.

Here, we report the results of our simulation of the interaction between the James Lobe of the LIS (Fig. 3.1) and the regional aquifer system extending from the Hudson Bay Lowland south to the terminus of the James Lobe in South Dakota. Based on known characteristics of the regional aquifer and hypothetical subglacial meltwater production rates, we investigated whether a subglacial drainage network would have been necessary, and if so, what hydraulic properties and geometry would have been consistent with basal water pressures near the ice load. In doing so, we simulate for the first time a basal drainage system at the ice-till interface at the ice lobe scale.

3.3. Model Configuration

3.3.1. Groundwater model and parameterization

The James Lobe was the westernmost of the distinctive lobes that drained the southern margin of the LIS. Ice flow feeding the lobe originated in the Hudson Bay Lowland (Fig. 1), and the lobe, which reached its maximum extent in South Dakota ~14,000 ^{14}C years B.P. (Clayton and Moran, 1982), had a basal driving stress of ~1.0 kPa (Clark, 1992).

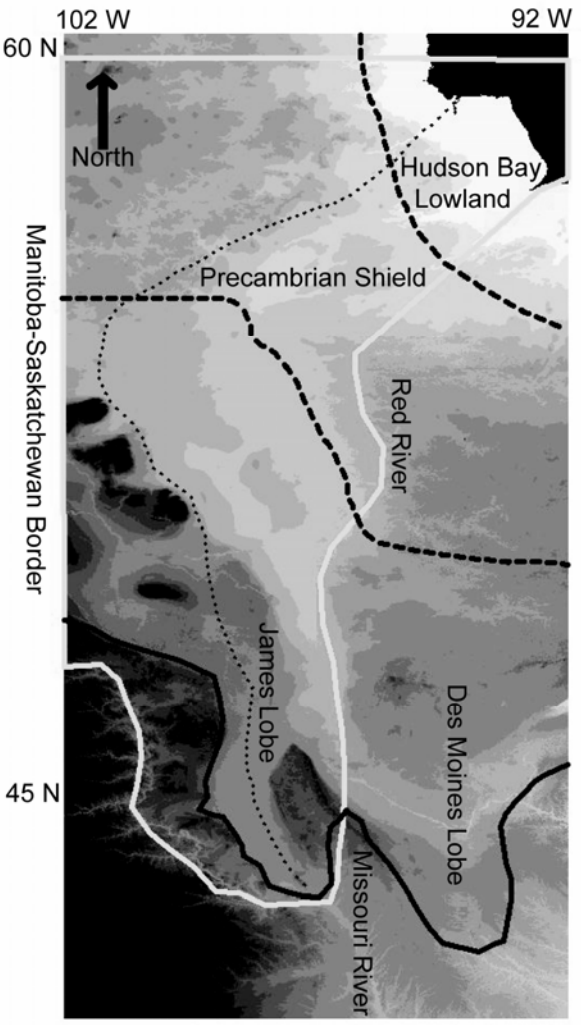

Figure 3.1. Map of the James Lobe (west) and neighboring Des Moines Lobe (east) margins (solid black line) and model domain (white line) overlain on a 50 m DEM. Thick dashed line denotes the Precambrian Shield boundary while the thin dashed line is the location of the cross section in Figure 3.2. Latitude north and longitude west are indicated.

To model the subglacial hydrology of the James Lobe, we use the three-dimensional, finite-difference groundwater modeling program MODFLOW (McDonald and Harbaugh, 1988) which solves the classic transient groundwater flow equation:

$$\nabla(Kb\nabla h) = S\frac{\partial h}{\partial t} - R(x,y,z,t) \qquad (3.1)$$

where h is hydraulic head [L] with respect to x, y, and z space [L]; S is the storage coefficient [L^{-1}]; K is hydraulic conductivity [$L\ T^{-1}$], b is layer thickness [L]; t is time [T], and R is recharge [$L\ T^{-1}$]. For steady state runs, $\frac{\partial h}{\partial t}$ is set equal to zero.

The model domain is from Hudson Bay to the Missouri River (Fig. 1). The eastern boundary is the Red River while the western boundary is the Manitoba-Saskatchewan Provincial border. The northern boundary corresponds with the ice divide at 14 ^{14}C ka reconstructed by Dyke and Prest (1987). The other boundaries are arbitrarily chosen at sufficient distance from the lobe that conditions can be assumed to reflect the ambient state of the regional aquifer, beyond the influence of the lobe. The model domain is underlain by Paleozoic sedimentary bedrock in the Hudson Bay Lowland, Precambrian crystalline bedrock of the Canadian Shield, and Paleozoic and Mesozoic bedrock of the North American plains (Fig. 3.2). The rock layers thicken and dip towards the north in the Hudson Bay Lowland and toward the southwest under the plains into the Williston Basin.

We group the rock layers into aquifers and aquitards following Downey (1986) and Downey and Dinwiddie (1988), and assign isotropic hydraulic conductivities (K) of Lennox (1993) (see Table 3.1). Because the local magnitude of K may vary substantially in this region (Lennox, 1993), we use order-of-magnitude regional averages for the major rock units. Two layers of till that thicken, from 1 to 15 m, towards the south are added atop these layers. We use the term *till* in the broad sense here to describe Quaternary sediment that is actually a combination of basal till, supraglacial debris flows, glaciofluvial sand and gravel, and glaciolacustrine sediment. These various glacial units have K values that range over 8 orders of magnitude (Stephenson et al., 1988). We account for this variability by assuming an average

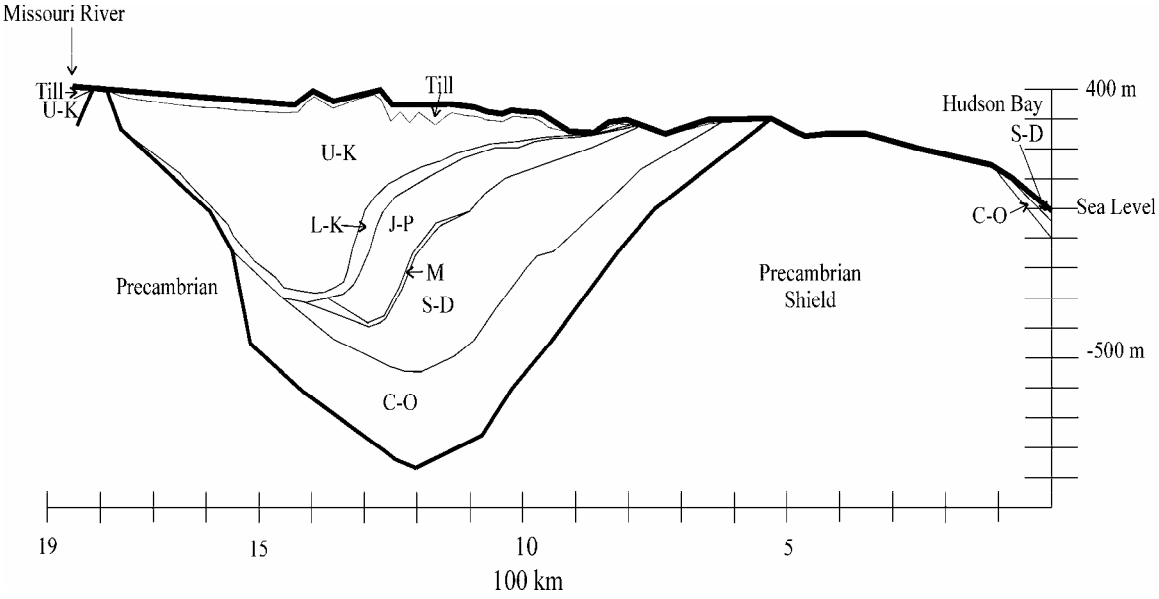

Figure 3.2. Simplified hydrostratigraphic bedrock cross-section used in the model. Location is indicated on Figure 3.1. See Table 3.1 for abbreviations and hydraulic conductivities.

Layer	Rock Units	k (m yr^{-1})	Unit Type
Till	Quaternary drift	10	aquifer
U-K	Upper K shale	0.01	aquitard
L-K	Lower K sandstone	1000	aquifer
J-P	Jurassic through Pennsylvanian units	0.0001	aquitard
M	Madison Limestone	10	aquifer
S-D	Silurian-Devonian limestone and shale	0.0001	aquitard
C-O	Cambrian-Ordovician sandstone	100	aquifer

Table 3.1. The grouping of rock units into hydrostratigraphic layers (Downey, 1986; Downey and Dinwiddie, 1988) and hydraulic conductivities (Stephenson et al., 1988; Lennox, 1993). Abbreviations used in Figure 2 and the text are in the left column.

value of 10 m yr^{-1} for this sediment package, which is at the upper end of unweathered basal till, the average of weathered basal till, and the lower end of glaciofluvial sediment (Stephenson et al., 1988), and then vary this value between 1 and 100 m yr^{-1} to test the sensitivity of this assumption. In the model, we treat the contact with the Precambrian igneous and metamorphic rocks as a no-flow boundary because the *K* values of these rocks are orders of magnitude lower than the *K* values of the aquifer units (Breemer et al., 2002).

Constant hydraulic head values are assigned to the boundary of each layer (Hitchon, 1969a; b; Downey, 1986; Downey and Dinwiddie, 1988). For the western boundary, these reflect recharge from the Rocky Mountains, where the aquifer rock layers are exposed at the surface. For the control run simulating modern conditions, the water table is held constant at the surface elevation (the top of the upper till layer). Recharge of 0.2 m yr^{-1} is applied to the upper till layer to simulate precipitation minus evapotranspiration (date from NOAA-CIRES Climate Diagnostics Center). In the full glacial simulations, constant hydraulic head values equivalent to the load inferred from the 14 ^{14}C ka maximum ice sheet of Licciardi et al. (1998) are imposed on the upper till layer. Recharge of 6 mm yr^{-1} is input to the lower till layer to simulate the basal geothermal melting of the ice sheet (Paterson, 1994). This provides a minimum value for basal meltwater productions; we excluded surface meltwater penetrating to the glacier bed and meltwater from frictional heating. Such sources of meltwater may play an important role in subglacial hydrology and ice sheet motion, but the objective of our simulations was to provide bounds for the type of basal hydraulic system that would be required to evacuate a plausible minimum volume of water that could be expected from the ice sheet. We also exclude the effect of permafrost at the boundary, which would presumably make for a tighter boundary, and thus less efficient drainage. The hypothetical system thus provides a basis for bounding the hydraulic conditions that would be associated with the least demanding basal water flux and the least restrictive discharge conditions at the southern boundary. In transient runs, a specific storage value of 4.6 x 10^{-6} m^{-1} is assigned to all layers (Breemer et al., 2002).

To validate the model, we simulated regional groundwater flow for modern boundary conditions and parameters (Fig. 3.3a) (for a list of simulations see Table

3.2). This was followed by a suite of simulations for glacial conditions (Fig. 3b & 4), including simulations of steady state. Steady state conditions were almost certainly never actually achieved in nature; the ideal steady state, however, provides a useful context for understanding and evaluating simulations of transient conditions. Two transient runs simulating evolution of conditions to 2,500 and 10,000 years duration were performed to evaluate the characteristic time of response of the aquifer system beneath the James Lobe.

Simulation	Description
Control	A control simulation with modern boundary conditions
Steady State Glacial	A full glacial simulation with ice sheet of Licciardi et al. (1998) run to steady state
Transient, 2,500 yrs	Similar to the steady state simulaiton but run for 2,500 years
Transient, 10,000 yrs	Similar to the steady state simulaiton but run for 10,000 years
Suglacial Drainage	20 simulations using an elevated *K* at the ice-till interface to simulate a subglacial drainage system

Table 3.2. List and description of the model simulations discussed in the text.

3.3.2. Subglacial drainage system models

To simulate a basal drainage system at the glacier bed, we ran a suite simulations with an elevated *K* (between 1 x 10^{9} and 2 x 10^{11} m yr^{-1}) at the ice-till interface (Table 3.2). We infer the canal width and spacing that would provide an equivalent hydraulic conductivity for a drainage system at the ice-till interface by applying the methodology of Vacher and Mylroie (2002), who evaluated the

relationship between equivalent bulk hydraulic conductivity and the diameter and density of a system of ideal parallel tubes in an evolving karst aquifer system. Thus:

$$K = \frac{n\rho g D^2}{32\mu\alpha} \tag{3.2}$$

where K is the equivalent hydraulic conductivity [L T^{-2}] of a porous medium with drainage canals, n is porosity [unitless], ρ is fluid density [M L^{-3}], g is gravity [L^2 T^{-1}], D is tube diameter [L], μ is fluid viscosity [M L^{-1} T^{-1}], and α is tube tortuosity [unitless] assumed to be 1. Tube diameter [D] is then related to tube density by:

$$\frac{N}{A} = \frac{4n}{\pi D^2} \tag{3.3}$$

where N is the number of tubes per unit area, A [L^2]. Canal dimensions are determined by calculating the area of an individual tube ($\pi(D/2)^2$) and equating this to an equal rectangular area with a depth of 10 cm (Walder and Fowler, 1994) to calculate area. Canal spacing is then determined from the tube density assuming a depth of 10 cm. We test the sensitivity of these results to the lower till layer K by varying this value from 1 to 100 m yr^{-1}. This equivalent porous medium method provides an estimation of the dimensions of a canal system where turbulent flow may occur. The finite difference model which we use, however, depends on the assumption of laminar flow in Darcy's Law. More accurate simulations would require the use of more complex, "hybrid" models that couple a continuum, laminar model and a turbulent, pipe network model (e.g., Liedl et al., 2003; Bakalowicz, 2005). However, comparisons between equivalent porous media models and coupled models that include both laminar and turbulent flow suggest that equivalency models can accurately simulate groundwater flow in karst regions (Scanlon et al., 2003). We are thus confident in our modeling approach but only attempt to approximate order of magnitude canal dimensions from our simulations.

Our model results for the subglacial canal system are back-checked using two independent tests. In the first test, we solve an equation for canal spacing (Carlson, 2004) using varied ice thicknesses (z_i [L]) and melt rates (m_r [L T^{-1}]):

$$x = \sqrt{\frac{\left(\left(\left(\frac{\gamma_i z_i}{\gamma_w} - x\right) m_r^{-1}\right) - 1\right)}{2}} \qquad (3.4)$$

where x [L] is the half the distance between canals, γ_i is the unit weight of ice, γ_w is the unit weight of water. This equation determines the maximum distance (twice x) that can exist between two canals with the pore water pressure remaining below ice flotation level in the till. We solve this equation for melt rates of 0.012 to 0.1 m yr^{-1} (Paterson, 1994) and ice thicknesses between 200 and 500 m (Clark, 1992).

For the second test, we set up a series of hypothetical ice sheet drainage configurations with canals represented by drains in MODFLOW. We increased the spacing between canals under two uniform 200- and 500-m thick ice sheets until pore water pressure exceeded ice overburden pressure to determine the maximum spacing between canals that can exist with the ice sheet remaining coupled to its bed. The canals are configured in square patterns with a maximum canal spacing being the diagonal across a given square. These canals are 1 m wide, with depths much less than width as theorized by Walder and Fowler (1994).

3.4. Results

3.4.1. Regional aquifer response

The control simulation of modern conditions is in agreement with other simulations and observations of hydraulic head and groundwater flow in the North American plains (Fig. 3.3a) (e.g. Hitchon, 1969a; b; Downey, 1986; Downey and Dinwiddie, 1988; Lennox, 1993). To quantitatively assess the skill of our model, we compare our control simulation against the observed hydraulic head in aquifers of the western North American Plains reported in Downey (1986) and Downey and Dinwiddie (1988). In the C-O aquifer, our simulated hydraulic head decreases from 950 m in the southwest to 400 m in the northeast whereas the observed hydraulic head decreases from 940 m to 395 m. In the M aquifer, hydraulic head is 700 m in the southwest decreasing to 400 m in the northeast, comparable to the observed hydraulic head of 730 m in the southwest to 450 m in the northeast. In the L-K aquifer, our

modeled hydraulic head decreases from 420 m in the southwest to 300 m in the northeast similar to the observed hydraulic head of 450 m in the southwest decreasing to 300 m in the northeast. In the control simulation, groundwater flow in the till is northeastward, toward Hudson Bay except in the extreme south of the model area, where flow is southward toward the Missouri River (Fig. 3.3a). Below the Quaternary sediment, groundwater flows out of the Williston Basin toward the Canadian Shield, where it is discharged into Quaternary sediment and continues northward toward the Hudson Bay lowland where it re-enters the Paleozoic layers.

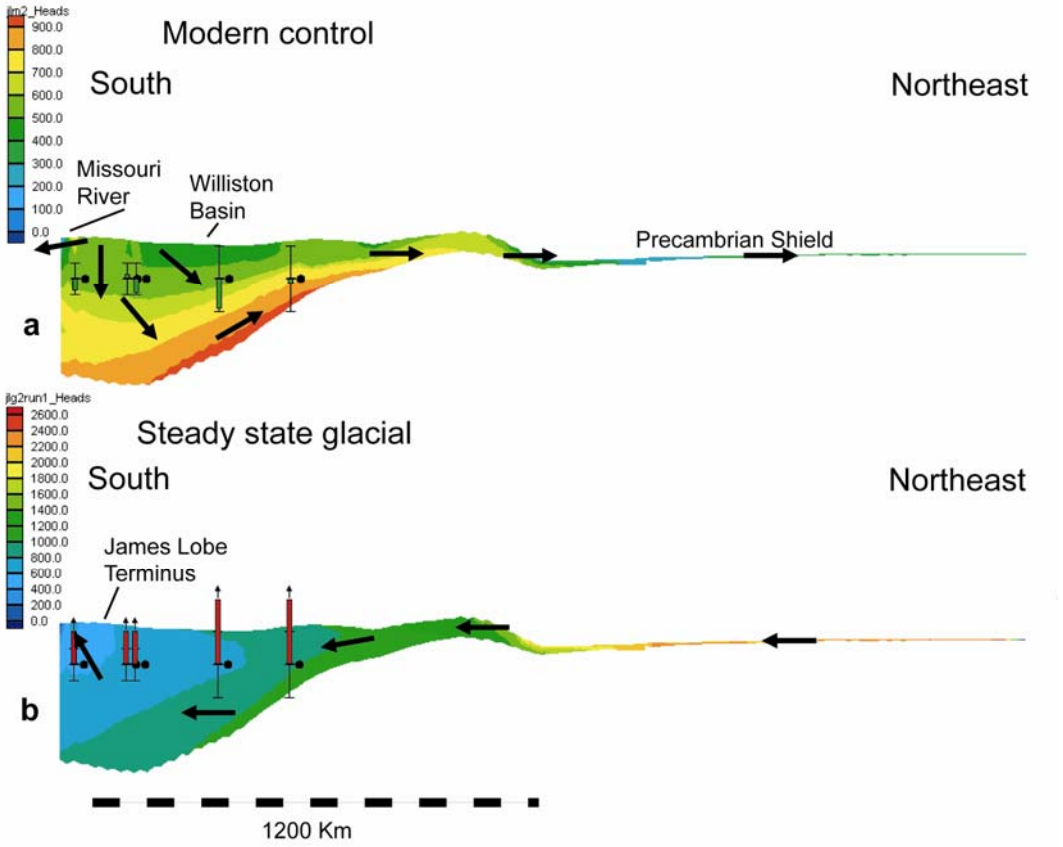

Figure 3.3. Flowline (northeast to south) cross-sections of groundwater hydraulic head in meters. Note color scale bars are different for modern and glacial simulations. Arrows show groundwater flow direction. Modern (**a**); steady state glacial (**b**). Black dots with error bars denote the location of modern measured hydraulic head. The error bars are of relative scale and denote the long-term variability of the well observation. The green bar indicates the simulated hydraulic head is within the error of the measured head for the modern simulation; red bars denote hydraulic head elevated above modern values as seen in the steady state glacial simulation.

Running the model to steady state with an ice sheet reverses flow in all model layers towards the south (Fig. 3.3b). Groundwater flows out of Hudson Bay onto the Canadian Shield at a velocity of ~4 m yr^{-1}. All layers have hydraulic heads that are elevated above the control run: 100 m in the Upper-Cretaceous shale (U-K) near the James Lobe terminus to 2300 m in the Cambrian-Ordovician sandstone (C-O) in Hudson Bay. Pore-water pressure at the ice-bed interface, as indicated by the pressure difference between the upper and lower till units, is in excess of ice-overburden pressure (90 % of the ice thickness), which would cause ice flotation. Varying till *K* between 1 and 100 m yr^{-1} does not affect these results.

In the transient simulations, groundwater flow in the till and U-K layer is southward but the Lower Mesozoic and Paleozoic layers in the Williston Basin maintain a component of northeastward flow (Fig. 3.4). The ice sheet only affects groundwater flow in these lower layers near where they are exposed at the surface between the edge of the U-K aquitard and the Canadian Shield (Fig. 3.2). In the southwestern area of the model, hydraulic head values in the Paleozoic layers remain near present values and groundwater flow direction is similar to the modern run. For both simulations pore water pressure at the ice-till interface is above ice-overburden pressure.

3.4.2. Subglacial drainage system simulations

Using the karst analogue, we increased *K* at the ice-till interface to a sufficiently high value to reduce basal pore water pressure below overburden pressure simulating a basal drainage system. Increasing the *K* to 10^9 m yr^{-1} (~3 x 10^6 m day^{-1}) reduced pore water pressure to slightly above ice-overburden pressure in the north and below ice-overburden pressure 400 km south of the Canadian Shield (Fig. 3.5). At 10^{10} m yr^{-1} (~3 x 10^7 m day^{-1}), basal pore water pressure across two thirds of the James Lobe is below ice flotation. There is an abrupt drop in till pore water pressure as *K* is increased to 10^{11} m yr^{-1} (~3 x 10^8 m day^{-1}) and the basal pore water pressure across the entire lobe is less than half of the ice-overburden pressure.

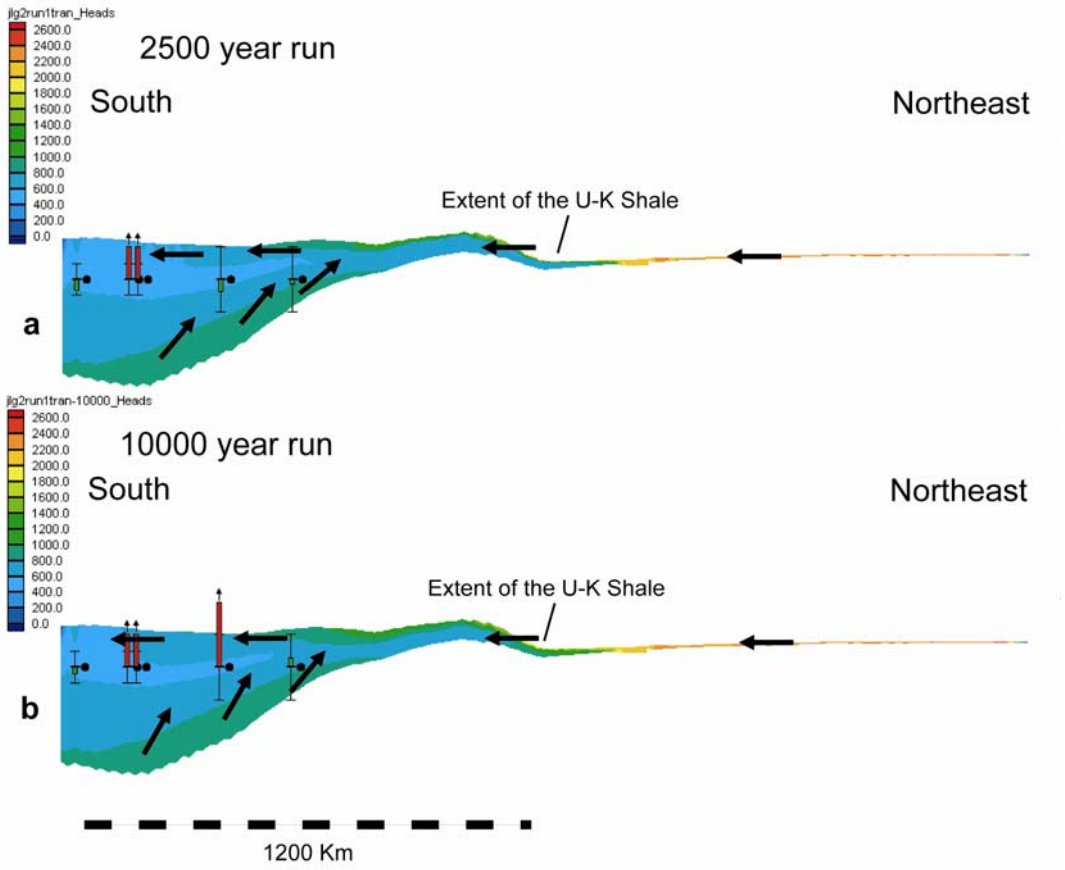

Figure 3.4. Flowline (northeast to south) cross-sections of groundwater hydraulic head in meters for transient simulations: 2,500 year duration (**a**); 10,000 year duration (**b**). Symbols are the same as in Figure 3.

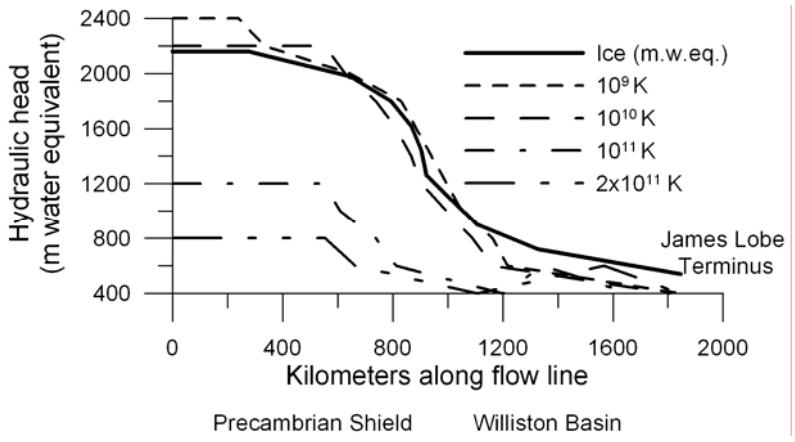

Figure 3.5. Selected simulations of hydraulic head along flow line (Fig. 3.1) due to varying *K* at the ice-till interface. In the legend, the *K* is the ice-till interface hydraulic conductivity. The thick black line is ice sheet overburden pressure in meters water equivalent (hydraulic head).

With these K values, we determine the rough dimensions of a canal drainage system (Vacher and Mylroie, 2002) that would exhibit an equivalent hydraulic conductivity for an assumed porosity of 0.4 for subglacial sediment (Tulaczyk et al., 2001) and a canal depth of 10 cm (Walder and Fowler, 1994). For 1 x 10^{11} m yr^{-1}, canals are 25 cm wide with spacing on the order of meters. At 2 x 10^{11} m yr^{-1}, the width increases to 50 cm with spacing on the order of tens of meters. Results are insensitive to the K used for the underlying till (i.e. 1 to 100 m yr^{-1}). The average water velocity in these canals is ~1 m s^{-1} and flow is turbulent. Given the uncertainty of estimating a turbulent system in a laminar model, we approximate that the canals have widths on the order of centimeters with spacing on the order of meters to tens of meters.

We further examine these finite difference model results using solutions to equation (4) (Carlson, 2004) (Fig. 3.6). In this equation, higher melt rates and thinner ice imply more closely spaced canals. For the range of melt rates (0.012 to 0.1 m yr^{-1}) and ice thicknesses (200 to 500 m) considered here (shaded boxes in Fig. 3.6), the pore water pressure at the ice sheet bed will remain below flotation with canals spaced every 50 to 240 m (x of 25 to 120 m, the open box in Fig. 3.6).

Our second test, the hypothetical ice sheet basal drainage model simulations, indicates that there is a rapid increase in pore water pressure to the ice flotation level when canal spacing is increased from 42 to 45 m (Fig. 3.7). This suggests a maximum canal spacing of ~42 m if the ice sheet is to remain coupled to its bed (Fig. 3.7a). These results are insensitive to the thickness of the ice sheet used.

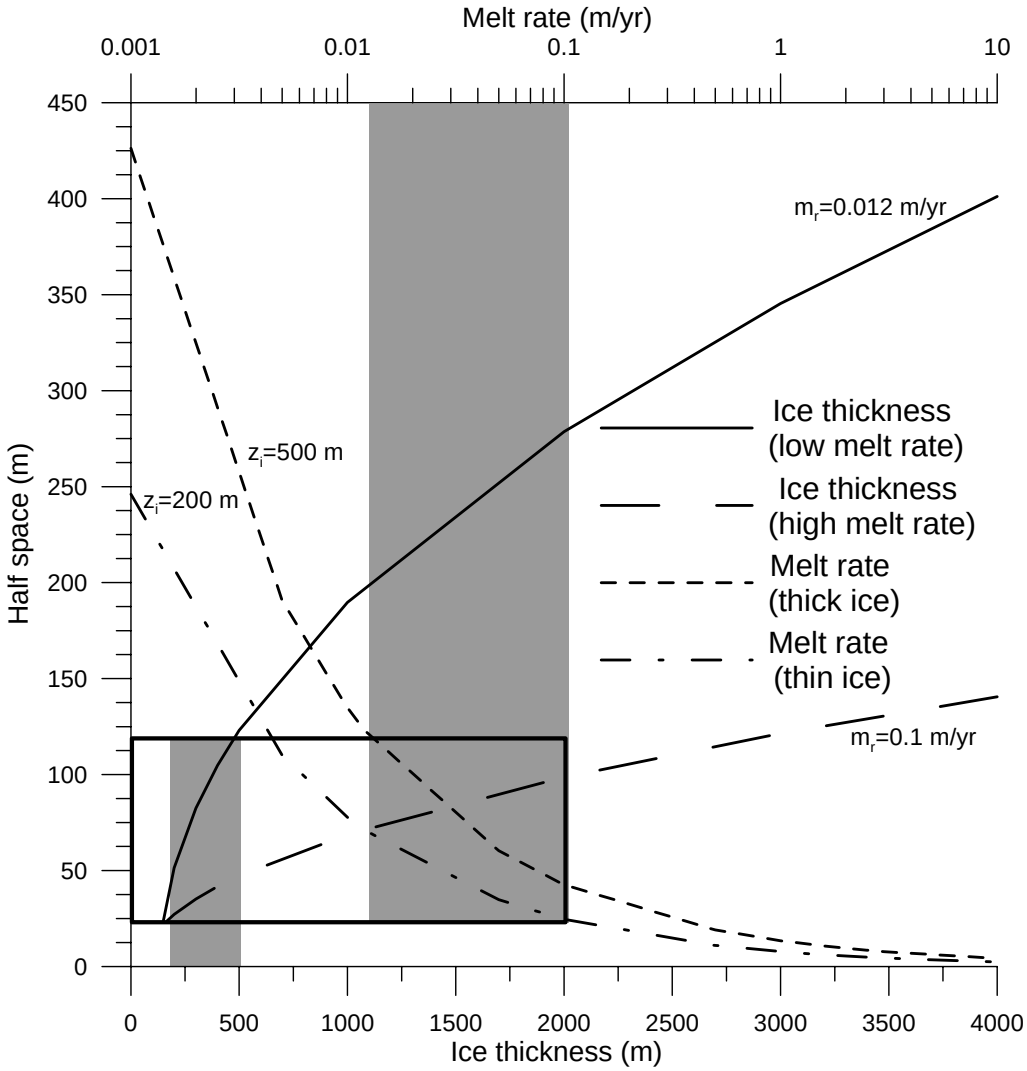

Figure 3.6. Graph of the solutions to the equation (3.4) from Carlson (2004) with varied melt rate and ice thickness. Shaded boxes denote the values for ice thickness and melt rate considered in the text and the open box shows the resulting half space (half the distance between channels) for these solutions.

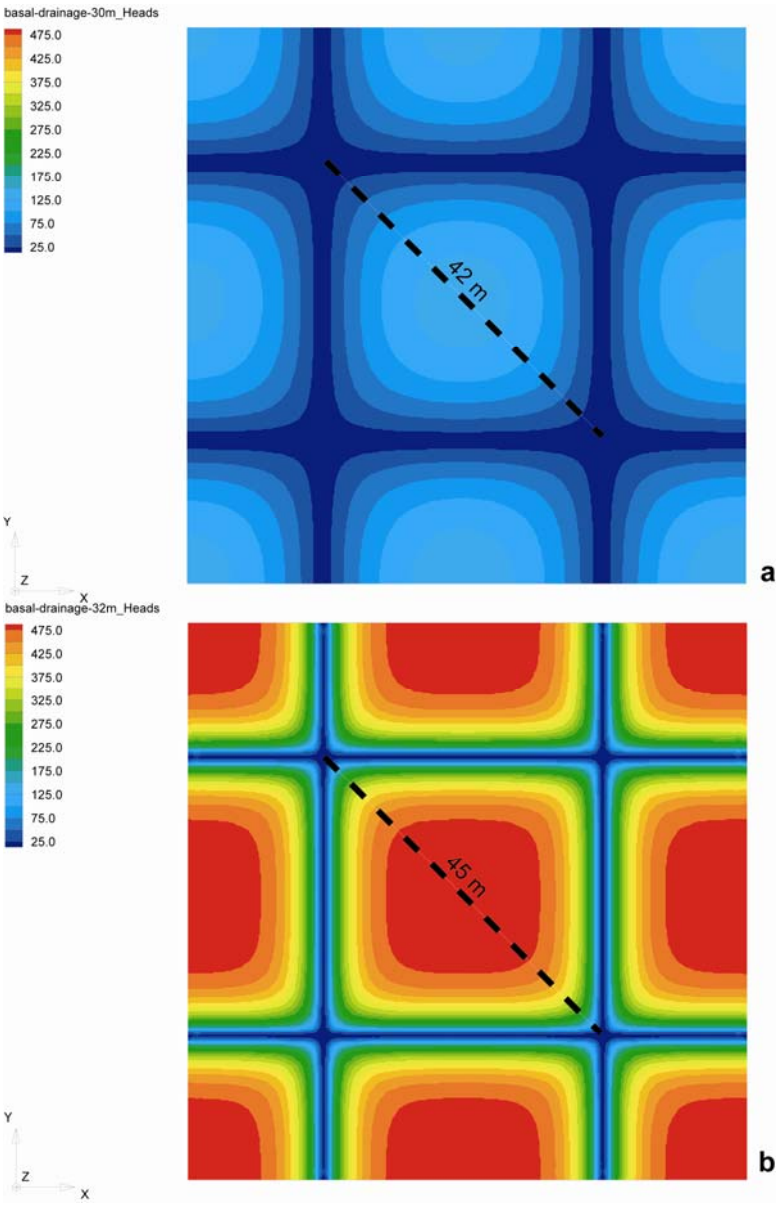

Figure 3.7. Idealized ice sheet drainage model results under 500 m of ice (200 m results not shown). Maximum canal spacing of 42 m (**a**); maximum canal spacing of 45 m (**b**). In the 42 m spacing simulation, pore water pressure is below ice overburden. In the 45 m spacing simulation, pore water pressure is at the ice overburden pressure and the ice sheet is floating.

3.5. Discussion

While the steady state glacial run predicts that groundwater flow in the western glaciated plains would be reversed were the ice sheet geometry to persist for longer than our most conservative transient run (10,000 years), the transient runs are more consistent with the history of the James Lobe, which occupied its maximum position for less than 1,000 years (Clayton and Moran, 1982). Prior to ~23 ^{14}C ka, the southwestern margin of the LIS was restricted to the Precambrian Canadian Shield (Dyke et al., 2002) not influencing groundwater flow in the North American plains. Ice advanced off the shield at ~22 ^{14}C ka (Dyke et al., 2002) and reached its maximum position ~14 ^{14}C ka, retreating shortly there after (Clayton and Moran, 1982). Thus our transient 10,000 year simulation provides a conservative assessment of the impact of the James Lobe on the groundwater flow of the North American plains. This simulation suggests that the James Lobe had little effect on regional groundwater flow below the Quaternary and U-K layers. Flow in the lower aquifers likely remained northeast due to the low *K* of the overlying U-K aquitard (Fig. 3.4). These results contradict the qualitative inferences by Downey (1986) and Downey and Dinwiddie (1988) that these aquifers would experience a reversal of flow direction during glaciations. However, our model results are in close agreement with the isotopic spring data of Grasby and Chen (2005), which indicate reversal of groundwater flow in the aquifers only near surface exposures that are in direct contact with the James Lobe. Thus, if advances of the James Lobe prior to the Last Glacial Maximum were similarly short lived, then northeastward groundwater flow under the North American plains is likely to have been unperturbed.

Similar modeling studies of other lobes of the LIS and the SIS have shown that results are sensitive to differences in regional hydrogeological conditions. Breemer et al. (2002) demonstrated a complete reversal of groundwater flow within 2,900 years under the Lake Michigan Lobe of the LIS. Similarly, transient and steady state modeling under the SIS show complete reorganization of groundwater flow in response to glaciation (Boulton et al., 1993; 1995; Piotrowski 1997a; b). These regions lack a regional aquitard such as the U-K shale, which hydrologically isolated

the lower layers. Accordingly, we conclude that groundwater flow in glaciated regions underlain by more permeable bedrock like the Great Lakes region of North America was likely greatly influenced by ice advance while regions underlain by less permeable substrates such as the North American plains were not.

Both the steady state and transient simulations suggest subglacial aquifers under the James Lobe could not have drained the base of the lobe rapidly enough to maintain basal pore water pressure below the ice flotation level. This requires meltwater drainage at the ice-till interface via a film (Alley, 1989) or a canal/channel system (Walder and Fowler, 1994) to prevent flotation. Our simulations show that a subglacial drainage system at the ice-till interface composed of canals with widths of 25 to 50 cm, spaced on the order of one to tens of meters apart could have drained the excess meltwater under the James Lobe efficiently enough to keep the lobe coupled to its bed (Fig. 3.5). Preconsolidation test results on tills in southern Saskatchewan which indicate subglacial effective pressures between ~160 and 190 m water-equivalent (Sauer et al., 1993) are consistent with our simulated effective pressure in southern Manitoba.

Our independent tests on canal spacing suggest maximum spacing between 42 and 240 m (Fig. 3.6 & 3.7). Thus, our canal simulation (the karst analogue) and two independent tests (equation (3.4) and hypothetical ice sheet drainage model) converge on spacing between 40 and 70 m, or on the order of tens of meters. These dimensions are at the lower end of those suggested for a canal system; that of width >> depth (10 cm) (Walder and Fowler, 1994) and spacing between 50 and 300 m (Engelhardt and Kamb, 1997). The theoretical upper limits for such a canal system, 0.1 m x 1 m, every 300 m, would imply a K of ~10^{12} m yr^{-1} (3 x 10^{9} m day^{-1}). Our model, however, neglects melting due to basal frictional heating and surface meltwater that penetrates to the glacier bed. If these additional meltwater sources are included, then an even higher equivalent K is needed to keep pore water pressure below flotation, which would require canal dimensions closer to the suggested upper limit (Walder and Fowler, 1994; Engelhardt and Kamb, 1997).

Interestingly, our simulations with an elevated K and using a hypothetical ice sheet both show an abrupt decrease in pore water pressure (Fig. 3.5 & 3.7) once a

threshold in canal spacing is crossed. We hypothesize that canal spacing can vary under an ice sheet with pore water pressure remaining below ice flotation until a critical spacing is reached. Increasing canal spacing beyond this point causes a rapid rise in pore water pressure because the till can no longer evacuate the meltwater produced to the canals and the ice sheet floats. This occurrence is similar to what has been observed under small valley glaciers where the diurnal melt cycle decreases the coupling of the glacier sole and the underlying sediment during periods of high pore water pressure (e.g., Iverson et al., 1995). The flotation of the ice sheet allows the formation of a new canal because effective pressure equals zero and sediment piping can occur reducing canal spacing. The reduced canal spacing would lower pore water pressure recoupling the ice sheet with its bed. This suggests that ice sheet basal drainage systems may be self-limiting systems.

These results suggest that the JL may have remained coupled to its bed with a drainage system similar to that proposed for the Whillans Ice Stream, West Antarctica (Engelhardt and Kamb, 1997) rather than experiencing the widespread bed decoupling as suggested for the neighboring Des Moines Lobe (Hooyer and Iverson, 2002) and the SIS (Piotrowski and Tulaczyk, 1999; Piotrowski et al., 2004).

3.6. Acknowledgments

We would like to thank J. LaNier and D. Wildenschild for assistance with of MODFLOW; and F. Anslow for discussion of ideas. J. Jenson wishes to thank his karst colleagues, L. Vacher and J. Mylroie, for the insight from their work that contributed to this paper. This research was supported by NSF grants to P.U.C. and J.W.J.

3.7. References

Alley, R.B., 1989, Water-pressure coupling of sliding and bed deformation: I. water system: Journal of Glaciology, v. 35, p. 108-118.

Alley, R.B., 1991, Deforming-bed origin for southern Laurentide till sheets?: Journal of Glaciology, v. 37, p. 67-76.

Alley, R.B., Blankenship, D.D., Rooney, S.T., and Bentley, C.R., 1989, Water-pressure coupling of sliding and bed deformation: III. Application to ice stream B, Antarctica: Journal of Glaciology, v. 35, p. 130–139.

Bakalowica, M., 2005. Karst groundwater: a challenge for new resources. Hydrogeology Journal, 13, 148-160.

Boulton, G.S., Slot, T., Blessing, K., Glasbergen, P., Leijnse, T., and van Gijssel, K., 1993, Deep circulation of groundwater in overpressured subglacial aquifers and its geological consequences: Quaternary Science Reviews, v. 12, p. 739-745.

Boulton, G.S., Caban, P.E., and VanGijssel, K., 1995, Groundwater flow beneath ice sheets: part I – large scale patterns: Quaternary Science Reviews, v. 14, p. 545-562.

Breemer, C.W., Clark, P.U., and Haggerty, R., 2002, Modeling subglacial hydrology of the late Pleistocene Lake Michigan Lobe, Laurentide Ice Sheet: Geological Society of America Bulletin, v. 114, p. 665-674.

Brown, N.E., Hallet, B., and Booth, D.B., 1987, Rapid soft bed sliding of the Puget Glacial Lobe: Journal of Geophysical Research, v. 92, p. 8985-8997.

Carlson, A.E., 2004, Genesis of dewatering structures and its implications for melt-out till identification: Journal of Glaciology, v. 50, p. 17-24.

Clark, P.U., 1992, Surface form of the southern Laurentide Ice Sheet and its implications to ice-sheet dynamics: Geological Society of America Bulletin, v. 104, p. 595-605.

Clark, P.U., 1994, Unstable behavior of the Laurentide Ice Sheet over deforming sediment and its implications for climate change: Quaternary Research, v. 41, p. 19-25.

Clark, P.U., Alley, R.B., and Pollard, D., 1999, Northern Hemisphere ice-sheet influences on global climate change: Science, v. 286, p. 1104-1111.

Clayton, L., and Moran, S.R., 1982, Chronology of late Wisconsinan glaciation in middle North America: Quaternary Science Reviews, v. 1, p. 55-82.

Downey, J.S., 1986, Geohydrology of bedrock aquifers in the northern Great Plains in parts of Montana, North Dakota, South Dakota, and Wyoming: U.S. Geological Survey Professional Paper 1402-E, 87p.

Downey, J.S., and Dinwiddie, G.A., 1988, The regional aquifer system underlying the northern Great Plains in parts of Montana, North Dakota, South Dakota, and Wyoming - Summary: U.S. Geological Survey Professional Paper 1402-A, 63 p.

Dyke, A.S., and Prest, V.K., 1987 Paleogeography of northern North America, 18,000 - 5,000 years ago: Geological Survey of Canada, Map 1703A, Scale 1:12,500,000.

Dyke, A.S., Andrews, J.T., Clark, P.U., England, J.H., Miller, G.H., Shaw, J., and Veillette, J.J., 2002: The Laurentide and Innuitian ice sheets during the Last Glacial Maximum: Quaternary Science Reviews, v. 21, p. 9-31.

Engelhardt, H., and Kamb, B., 1997, Basal hydraulic system of a West Antarctic ice stream: constraints from borehole observations: Journal of Glaciology, v. 43, p. 207-230.

Grasby, S.E., and Chen, Z., 2005, Subglacial recharge into the Western Canada Sedimentary Basin - Impact of Pleistocene glaciation on basin hydrodynamics: GSA Bulletin, v. 117, p. 500-514.

Hitchon, B., 1969a, Fluid flow in the Western Canadian sedimentary basin 1. Effect of topography: Water Resources Research, v. 5, p. 186-195.

Hitchon, B., 1969b, Fluid flow in the Western Canadian sedimentary basin 2. Effect of geology: Water Resources Research, v. 5, p. 460-469.

Hooyer, T.S., and Iverson, N.R., 2002, Flow mechanisms of the Des Moines lobe of the Laurentide ice sheet: Journal of Glaciology, v. 48, p. 575-586.

Iverson, N.R., Hanson, B., Hooke, R. LeB., Jansson, P, 1995. Flow mechanisms of glaciers on soft beds. Science, 267, 80-81.

Lennox, D.H., 1993, Groundwater in the interior plains region, *in* Stott, D.F., and Aitken, J.D., eds., Sedimentary Cover of the Craton in Canada: Geological Survey of Canada, Geology of Canada, n. 5, p 616-642.

Licciardi, J.M., Clark, P.U., Jenson, J.W., and MacAyeal, D.R., 1998, Deglaciation of a soft-bedded Laurentide Ice Sheet: Quaternary Science Reviews, v. 17, p. 427-448.

Liedl, R., Sauter, M., Hückinghaus, D., Clemens, T., Teutsch, G, 2003. Simulation of the development of karst aquifers using a coupled continuum pipe flow model. Water Resources Research, 39, doi: 10.1029/2001WR001206.

Lingle, C.S., and Brown, T.J., 1987, A subglacial aquifer bed model and water pressure dependent basal sliding relationship for a West Antarctic ice stream, *in* van der Veen, C.J., and Oerlemans, J., eds., Dynamics of the West Antarctic Ice Sheet: D. Reidel Publishing Company, p. 249-285.

Mathews, W.H., 1974, Surface profiles of the Laurentide Ice Sheet in its marginal areas: Journal of Glaciology, v. 13, p. 37-43.

Mickelson, D.M., Clayton, L., Fullerton, D.S., and Burns, H.W., Jr., 1983, The late Wisconsin glacial record of the Laurentide Ice Sheet in the U.S., *in* Porter, S.C., ed., Late Quaternary environments of the United State: University of Minnesota Press, v. 1, p. 3-37.

McDonald, M.G., and Harbaugh, A.W., 1988, MODFLOW: a modular three-dimensional finite-difference groundwater flow model: U.S. Geological Survey, Techniques of Water-Resources Investigation, Book 6, p. 1-1 to 13-29.

Paterson, W.S.B., 1994, The Physics of Glaciers, 3rd Edition: Butterworth Heinemann, Oxford, 480 p.

Piotrowski, J.A., 1997a, Subglacial groundwater flow during the last glaciation in northwestern Germany: Sedimentary Geology, v. 111, p. 217-224.

Piotrowski, J.A., 1997b, Subglacial hydrology in north-western Germany during the last glaciation: groundwater flow, tunnel valleys and hydrological cycles: Quaternary Science Reviews, v. 16, p. 169-185.

Piotrowski, J.A., Larsen, N.K., and Junge, F.W., 2004, Reflections on soft subglacial beds as a mosaic of deforming and stable spots: Quaternary Science Reviews, v. 23, p. 993-1000.

Piotrowski, J.A., and Tulaczyk, S., 1999, Subglacial conditions under the last ice sheet in northwest Germany: ice-bed separation and enhanced basal sliding?: Quaternary Science Reviews, v. 18, p. 737-751.

Sauer, E.K., Egeland, A.K., and Christiansen, E.A., 1993, Preconsolidation of tills and intertill clays by glacial loading in southern Saskatchewan, Canada: Canadian Journal of Earth Science, v. 30, p. 420-433.

Scanlon, B.R., Mace, R.E., Barrett, M.E., and Smith, B., 2003. Can we simulate regional groundwater flow in a karst system using equivalent porous media models? Case study, Barton Springs Edwards aquifer, USA. Journal of Hydrology, 276, 137-158.

Stephenson, D.A., Fleming, A.H., and Mickelson, D.M., 1988, Glacial deposits, *in* Back, W., Rosenshein, J.S., and Seaber, P.R., eds., Hydrology: Geological Society of America, The Geology of North America, v. O-2, p., 301-314.

Tulaczyk, S., Kamb, B., and Engelhardt, H.F., 2001, Estimates of effective stress beneath a modern West Antarctic ice stream from till preconsolidation and void ratio: Boreas, v. 30, p. 101-114.

Vacher, H.L., and Mylroie, J.E., 2002, Eogenetic karst from the perspective of an equivalent porous medium: Carbonates and Karst, v. 17, p. 182-196.

Walder, J.S., and Fowler, A., 1994, Channelized subglacial drainage over a deformable bed: Journal of Glaciology, v. 40, p. 3-15.

CHAPTER 4

FRESHWATER FORCING OF OCEAN AND CLIMATE VARIABILITY DURING THE YOUNGER DRYAS COLD INTERVAL

Anders E. Carlson (1), Peter U. Clark (1), Brian A. Haley (2),
Gary P. Klinkhammer (2), Edward J. Brook (1), Katrin Meissner (3)

(1) Department of Geosciences, Oregon State University, Corvallis, OR 97331, USA

(2) College of Oceanic and Atmospheric Sciences, Oregon State University, Corvallis, OR 97331, USA

(3) School of Earth and Ocean Sciences, University of Victoria, Victoria, BC, V8W 3P6, Canada

Carlson, A.E., Clark, P.U., Haley, B.A., Klinkhammer, G.P., Brook, E.J., and Meissner, K., in review, Freshwater forcing of ocean and climate variability during the Younger Dryas cold interval: Nature.

4.1. Abstract

Proxies of deepwater formation show that a large reduction in the Atlantic meridional overturning circulation (AMOC) occurred at the start of the Younger Dryas event[1,2], suggesting that the attendant loss of ocean heat transport caused Younger Dryas cooling in the North Atlantic region. The trigger of this ocean response remains unclear, however, with the leading mechanism, involving the routing of continental runoff to the St. Lawrence River[3,4], now questioned on the basis of marine[5-7] and terrestrial[8] evidence, and modeling[9]. Moreover, the rate of the AMOC varied during the Younger Dryas[1,2] which is not readily explained by the conventional routing argument. Here we capitalize on the well-known relation between river geochemistry and underlying bedrock lithology[10] to use changes in $^{87}Sr/^{86}Sr$, U/Ca, and Mg/Ca measured in planktonic foraminifera tests as tracers of routing of continental runoff derived from distinct geological terranes. These data, supported by changes in planktonic $\delta^{13}C$ and $\delta^{18}O$, confirm that routing of runoff from western Canada to the St. Lawrence River occurred at the start of the Younger Dryas. Changes in these tracers indicate that freshwater flux through the St. Lawrence River increased by 0.08 ± 0.03 Sv, which is sufficient to induce a large decrease in the meridional overturning circulation[11]. Additionally, our data identify a fluctuation in freshwater flux through the St. Lawrence River at ~12 kyr BP, thus explaining the variability in the overturning circulation and climate during the Younger Dryas.

4.2. Introduction

Opening of the eastern Lake Agassiz outlet and the Straits of Mackinaw ~12,900 cal yr BP by retreat of the southern Laurentide Ice Sheet margin more than doubled the size of the St. Lawrence River drainage basin, from 1.35 x 10^6 km^2 to 3.13 10^6 km^2 (ref. 4) (Fig. 4.1). Because the newly added drainage area included significantly different bedrock lithologies than those underlying the St. Lawrence drainage area prior to this event[12] (Fig. 4.1), the associated routing of surface water should be marked by changes in St. Lawrence water geochemistry[10].

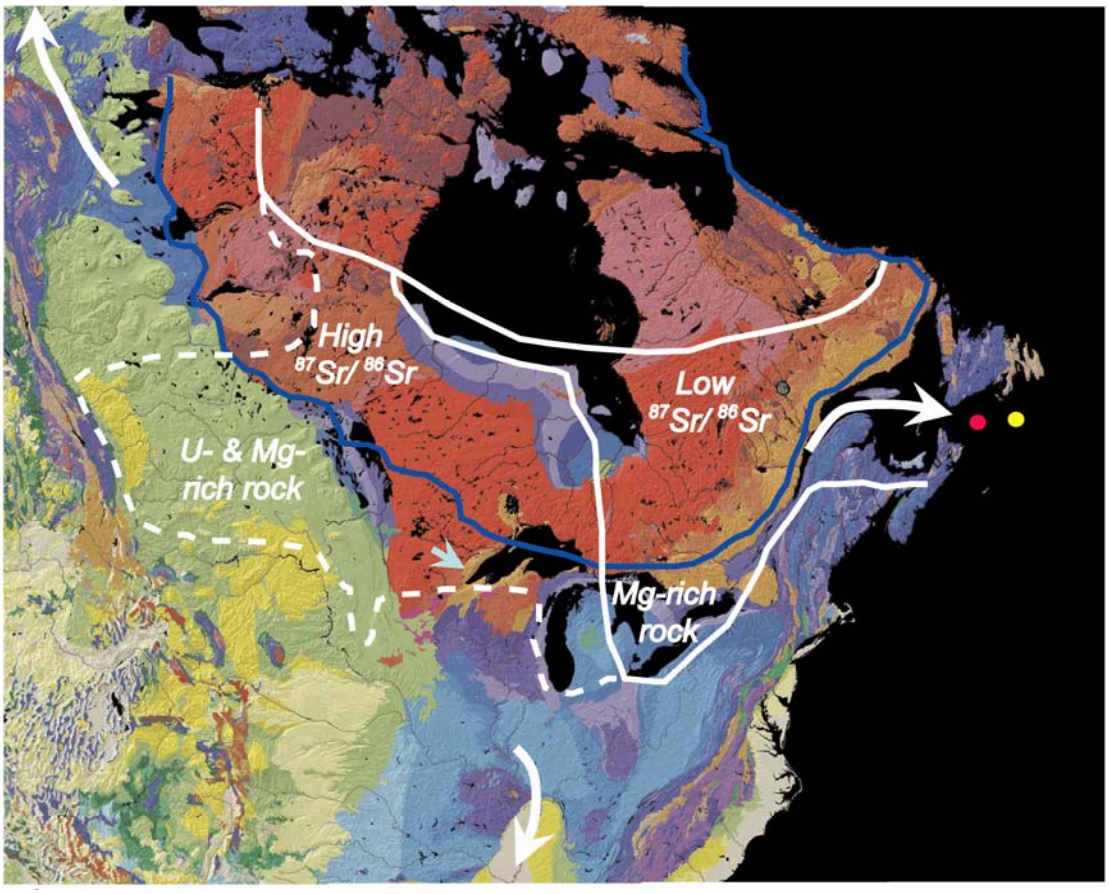

Figure 4.1. Bedrock map of central-eastern North America[12] showing major lithologies that influence river geochemistry. Colors are coded according to bedrock age: red shades are Precambrian, blue shades are Paleozoic, green shades are Mesozoic, and yellow is Cenozoic. We have identified those geochemical properties of bedrock types that produce distinctive signals in drainage basins. The western part of the Canadian Precambrian Shield has higher $^{87}Sr/^{86}Sr$ than the eastern Shield, Paleozoic bedrock underlying the eastern Great Lakes includes Mg-rich dolomite, and Mesozoic bedrock of the western Canadian Plains is enriched in U and Mg. Also shown is the outline (in blue) of the 12.7 cal. kyr BP ice margin[14] and the outlines of major drainage basins involved in routing around the time of the Younger Dryas[4]. The solid white line is the pre-Younger Dryas drainage area of the St. Lawrence with its northern margin controlled by the ice sheet divide[4]. The dashed white line represents the additional area routed to the St. Lawrence at the start of the Younger Dryas[4]. White arrows indicate the freshwater drainage routes to the Arctic, Gulf of Mexico and St. Lawrence River, and blue arrow indicates general location of eastern outlet for glacial Lake Agassiz. Core locations in outer St. Lawrence estuary also shown: core 90031-047 (red dot) and core 90031-044 (yellow dot).

In order to assess geochemical changes associated with these new sources of surface water, we picked planktonic foraminifera from two cores in the outer St. Lawrence estuary (Fig. 4.1) that span the Younger Dryas interval: *G. bulloides* and *N. pachyderma (s)* from core HU90031-047 (45°51.14'N, 57°37.56'W; 473 m depth), and *G. bulloides* from core HU90031-044 (44º39.41'N, 55º37.13'W; 1381 m depth). Samples were physically cleaned, prepared with a flow-through method[13] and analyzed by high-resolution ICP-MS for U/Ca and Mg/Ca. Sr-isotopes were analyzed by multi-collector ICP-MS. We constructed age models from previously published ^{14}C ages for core 044[7] and new ^{14}C dates from cores 044 and 047, giving us age control approximately every 430 years (Fig. 4.2). All ^{14}C ages are reservoir corrected[7,14] and calibrated[15]. The agreement between benthic mollusk shell ages and planktonic foraminifera ages[7] indicates that any changes in the freshwater flux to the estuary did not affect the reservoir age.

4.3. Results

Foraminiferal $^{87}Sr/^{86}Sr$ in our Younger Dryas samples is 7×10^{-5} higher than $^{87}Sr/^{86}Sr$ in samples that immediately predate the Younger Dryas (Fig. 4.2e). Because global seawater $^{87}Sr/^{86}Sr$ is invariant on this timescale, we attribute the higher $^{87}Sr/^{86}Sr$ in the St. Lawrence estuary during the Younger Dryas to the arrival of surface water derived from the western Canadian Shield associated with its routing following the opening of the eastern outlet of Lake Agassiz (Fig. 4.1). Specifically, rivers draining older bedrock of the western Canadian Precambrian Shield have an average $^{87}Sr/^{86}Sr$ of 0.724502, versus 0.71423 for rivers draining younger bedrock of the eastern Canadian Shield[16]. Assuming similar $^{87}Sr/^{86}Sr$ ratios in surface waters of Canada as today[16], we find that our measured increase in estuary $^{87}Sr/^{86}Sr$ would require discharge through the St. Lawrence River to increase by 0.10 ± 0.04 Sv ($1 \text{ Sv} = 10^6 \text{ m}^3 \text{ s}^{-1}$) (see Methods).

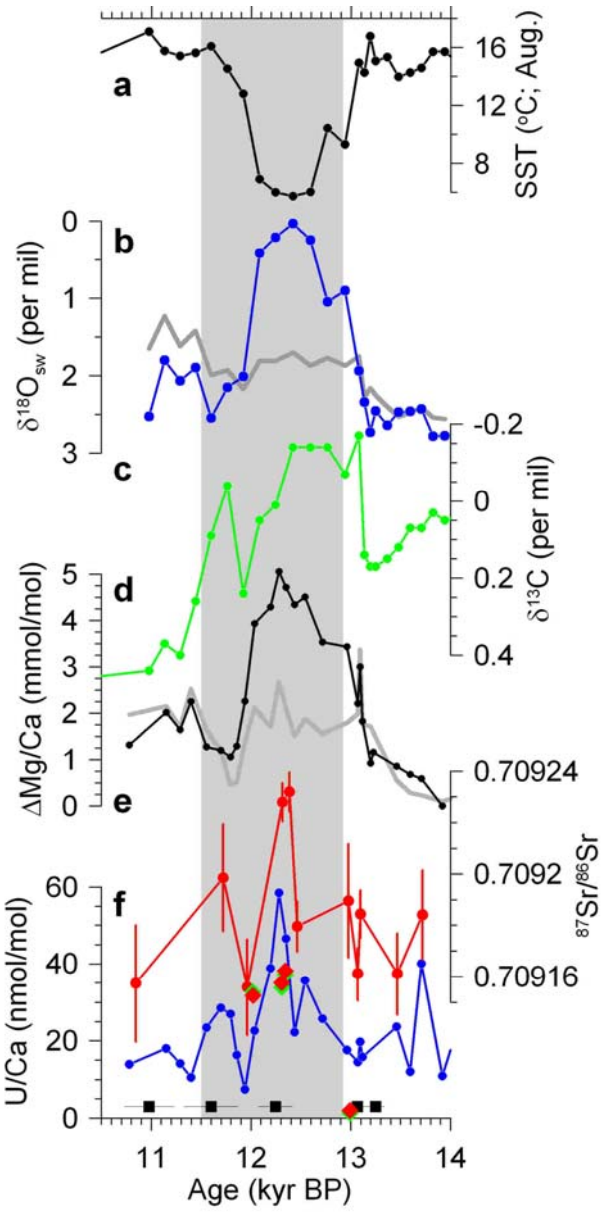

Figure 4.2. Geochemical time series for the Younger Dryas interval. Gray bars denote times of routing events inferred from terrestrial records[4]. (**a**) Dinoflagellate cyst sea surface temperature reconstruction (HU90031-044)[7]. (**b**) Planktonic (*N. pachyderma (s)*) $\delta^{18}O$ (gray)[7] and of seawater (blue) (HU90031-044). (**c**) Planktonic (*N. pachyderma (s)*) $\delta^{13}C$ record from the St. Lawrence (HU90031-044) (courtesy of C. Hillaire-Marcel). (**d**) Mg/Ca (gray) and ΔMg/Ca (black) of *G. bulloides* (HU90031-044). (**e**) Sr-isotopes of *G. bulloides* (HU90031-044). (**f**) U/Ca on *G. bulloides* (blue from HU90031-044, green from HU90031-047) and *N. pachyderma (s)* (red from HU90031-047). Black squares denote radiocarbon ages with 1 sigma error.

Changes in U and Mg concentrations further identify changes in the source and flux of surface waters reaching the St. Lawrence estuary. Foraminiferal U/Ca in *G. bulloides* and *N. pachyderma (s)* from core 047 and in *G. bulloides* from core 044 all reach peak values that are ~40 nmol/mol higher in Younger Dryas samples relative to older samples (Fig. 4.2f). The primary sources of seawater U are from rivers and by release from marine sediments in response to an increase in bottom-water oxygen, such as may be associated with an increased flux of oxygenated freshwater into the St. Lawrence estuary during a routing event. Assuming reasonable values for U concentration (25 ppm) in sediment with a 1-meter mixed-layer depth distributed over the area of the estuary, a change from anoxic to oxic conditions would release 24 x 10^6 moles of U to the estuary, corresponding to a foraminiferal U/Ca signal of ~0.7 nmol/mol[17], or significantly less than our measured values. On the other hand, rivers draining shale and carbonate bedrock of the western Canadian Plains (Fig. 4.1) have average U concentrations (20 nmol/kg) that are ~2 times the U concentrations relative to the average global river concentration[18], indicating that our measured increase in U/Ca is consistent with the routing of these U-rich surface waters following the opening of the eastern outlet of Lake Agassiz. Our mixing model of estuary geochemistry indicates that an increase in peak discharge through the St. Lawrence River of 0.08 ± 0.03 Sv would explain the 40 nmol/mol increase in foraminiferal U/Ca (see Methods).

Mean Mg/Ca values in *G. bulloides* from core 044 range from 1.1 to 3 mmol/mol (Fig. 4.2d). Changes in Mg/Ca in foraminifera reflect temperature- and salinity-dependent uptake of Mg as well as changes in the Mg concentration of the water. We used an existing sea surface temperature (SST) record from core 044, based on dinoflagellate-cyst assemblages[7] (Fig. 4.2a), to account for SST changes in our Mg/Ca record by applying the *G. bulloides* calibration (Mg/Ca (mmol/mol) = 0.474exp[0.107 x SST(^{o}C)])[19]. We then estimated salinity variations in the estuary on the basis of a $\delta^{18}O_{seawater}$ record from core 044 (Fig. 4.2b), and applied a salinity calibration (Mg/Ca (mmol/mol) = 0.311 x salinity)[19]. These combined corrections have a propagated error of ~30%[19]. Subtracting these temperature and salinity

components from our measured Mg/Ca values and normalizing to the lowest resulting value produces a ΔMg/Ca record that reflects changes in Mg/Ca of the estuary.

We attribute the 1 mmol/mol increase in ΔMg/Ca at ~13.8 kyr BP (Fig. 4.2d) to the first opening of the St. Lawrence River by ice retreat[4], with attendant routing of Mg-rich surface waters draining dolomite bedrock underlying the eastern Great Lakes region (Fig. 4.1). Foraminiferal ΔMg/Ca subsequently increases by ~4 mmol/mol during the Younger Dryas, a signal that had been masked in our Mg/Ca record by the corresponding decrease in SSTs and salinities (Fig. 4.2a, b). Rivers draining shale and carbonate bedrock in areas of western Canada that were routed to the St. Lawrence basin during the Younger Dryas (Fig. 4.1) have Mg concentrations that are up to 3.5 times higher than the average carbonate bedrock and 10 times that of the average shale bedrock[10]. Mixing model results indicate that a 0.07 $\pm$ 0.03 Sv increase in freshwater discharge to the St. Lawrence River derived from these source waters would explain the Younger Dryas ΔMg/Ca signal (see Methods). Our three geochemical tracers of source waters thus converge in indicating that freshwater discharge through the St. Lawrence River increased by 0.08 $\pm$ 0.03 Sv (average of our three estimates) during the Younger Dryas, with an attendant decrease in estuarine mixed layer salinity of 2.8 $\pm$ 0.9 p.s.u.

4.4. Discussion

The planktonic $\delta^{13}C$ record in core 044 provides additional support for substantial changes in freshwater flux to the St. Lawrence estuary. The $\delta^{13}C$ of dissolved inorganic carbon in freshwater primarily reflects some combination of the $\delta^{13}C$ of soil CO_2 derived from decay of organic matter (lighter values) and the $\delta^{13}C$ of any underlying carbonate bedrock (heavier values). A 0.14 per mil increase in $\delta^{13}C$ starting ~13.8 kyr BP (Fig. 4.2c) coincides with the increase in ΔMg/Ca, and we similarly attribute the $\delta^{13}C$ signal to ^{12}C-depleted source waters derived from carbonate bedrock in the eastern Great Lakes that also supplied Mg-rich waters upon the first opening of the St. Lawrence River. The subsequent abrupt 0.32 per mil decrease in $\delta^{13}C$ at the start of the Younger Dryas (Fig. 4.2c) indicates an increased

flux of ^{12}C-enriched surface runoff derived from the western Canadian Prairies, where the relatively small area of carbonate bedrock would have only slightly buffered the light $\delta^{13}C$ signal derived from soil CO_2 across the entire area affected.

These combined results appear contrary to the modest 0.5 per mil decrease in $\delta^{18}O_{calcite}$ measured in *N. pachyderma* from core 044 (Fig. 4.2b), which deVernal *et al.*[7] used to argue against any significant salinity decrease in the St. Lawrence estuary during the Younger Dryas. However, $\delta^{18}O_{calcite}$ reflects the combination of the offsetting effects of temperature and salinity, so that a 10°C decrease in SSTs during the Younger Dryas at this site[7] (Fig. 4.2a) would mask an additional 2.5 per mil salinity signal in $\delta^{18}O_{calcite}$, corresponding to a net 3 per mil decrease in $\delta^{18}O_{seawater}$ (Fig. 4.2b). Assuming simple mixing of river and estuary waters, we find that our estimated freshwater flux increase (0.08 ± 0.03 Sv) derived from western Canadian source waters with $\delta^{18}O$ of -25 per mil[20] would have decreased estuarine mixed-layer $\delta^{18}O$ by 2.0 ± 0.7 per mil (see Methods), thus explaining the $\delta^{18}O_{seawater}$ signal in core 044. The salinity decrease is contemporaneous with a 2 per mil increase in $\delta^{18}O_{seawater}$ from the Orca Basin, Gulf of Mexico[21], thus supporting Broecker's hypothesis[3] that routing of North American runoff from the Mississippi to the St. Lawrence River occurred at the start of the Younger Dryas.

According to the conventional routing hypothesis, surface waters from western Canada continued to drain through the eastern outlet of Lake Agassiz to the St. Lawrence River until ~11.5 kyr BP, when ice readvance across the outlet rerouted surface waters either to the south (Mississippi River)[3,4] or to the northwest (Mackenzie River)[22] (Fig. 4.1). In contrast, all proxies from core 044 indicate that freshwater flux, salinity and SST started to decrease ~12.3-12.4 kyr BP, and reached pre-YD values by ~12 kyr BP (Fig. 4.2), suggesting that rerouting occurred earlier. The terrestrial record of routing during this time is poorly constrained, but two lines of evidence suggest that this previously unrecognized intra-YD routing event occurred through the northwestern Clearwater outlet to the Arctic Ocean via the Mackenzie River (Fig. 4.1): a radiocarbon age of $10{,}310 \pm 290$ ^{14}C yr BP ($12{,}040 \pm 400$ cal yr BP) on a piece of wood obtained in flood deposits from the outlet[22], and a light $\delta^{18}O$ anomaly in a record from the Beaufort Sea that dates at 12 kyr BP[23].

Two proxies from core 004 (U/Ca and $\delta^{13}C$) indicate that freshwater flux to the St. Lawrence River subsequently increased for the remainder of the YD, whereas $\delta^{18}O_{seawater}$ and ΔMg/Ca show no change (Fig. 4.2). We attribute the increase in U/Ca and $\delta^{13}C$ to renewed routing of western Canadian runoff to the St. Lawrence, possibly due to isostatic uplift of the northwest outlet to the Arctic Ocean, causing Lake Agassiz waters to again start draining to the east. The absence of an equivalent ΔMg/Ca signal at this time may in part reflect source-rock changes in the eastern Great Lakes region, whereby the opening of more northerly outlets allowed westerly-derived waters from the Agassiz basin to bypass Lakes Erie and Ontario and flow directly from Lake Huron into the St. Lawrence River by way of the Ottawa River[14]. The attendant loss of Mg-rich waters due to bypassing the dolomites of the Erie and Ontario basins (Fig. 4.1) would thus have counteracted the gain of Mg-rich waters derived from the Agassiz basin. However, we should expect to see a ~4-5 mmol/mol gain in ΔMg/Ca relative to a loss of ~1 mmol/mol due to bypassing carbonate bedrock of the eastern Great Lakes. The absence of a ΔMg/Ca signal as well as a $\delta^{18}O_{seawater}$ signal during this late YD time is thus perplexing, but may result from the ~30% error in the temperature and salinity adjustments[19] that, combined with the ~20% error in the SST reconstructions during this interval[7], has obscured the rerouting signal in these temperature-dependent proxies.

Our source-water tracers provide the first direct oceanographic evidence of eastward routing of surface waters from western Canada to the St. Lawrence River during the Younger Dryas. According to climate models, our estimated increases in freshwater flux (0.08 ± 0.03 Sv) required to produce measured changes in $^{87}Sr/^{86}Sr$, U/Ca, and ΔMg/Ca would be sufficient to induce a significant reduction in the AMOC[11], such as occurred during the Younger Dryas[1,2]. Our results thus resolve the climate forcing mechanism for the Younger Dryas cold interval, and suggest new strategies for investigating whether similar mechanisms may have been responsible for other abrupt climate changes.

Additionally, our source-water tracers reveal the cause of ocean and climate variability that occurred during the Younger Dryas. All our routing proxies show that, rather than a constant flux of freshwater as generally implied by the conventional

routing mechanism[4], freshwater base discharge varied during the Younger Dryas with a decrease to pre-Younger Dryas values centered at ~12 kyr BP when freshwater was diverted to the Arctic Ocean. This intra-YD routing event is in excellent agreement with proxies that indicate an increase in the AMOC[1,2] (Fig. 4.3) and attendant warming of the ocean[24,25] (Fig. 4.4b,c) and atmosphere[26] (Fig. 4.4a) and increased southeast Asian monsoon intensity[27] (Fig. 4.4d) during the Younger Dryas. These same proxies then suggest that the AMOC subsequently decreased with attendant cooling at a time when our tracers suggest a rerouting of western Canadian freshwater back to the St. Lawrence River (Fig. 4.4). This tight coupling between changes in freshwater fluxes to the North Atlantic basin and changes in the AMOC further emphasizes the sensitivity of the Atlantic thermohaline circulation to relatively small changes in the hydrological cycle, and the rapid climatic response demonstrates the sensitivity of the climate system to changes in the AMOC.

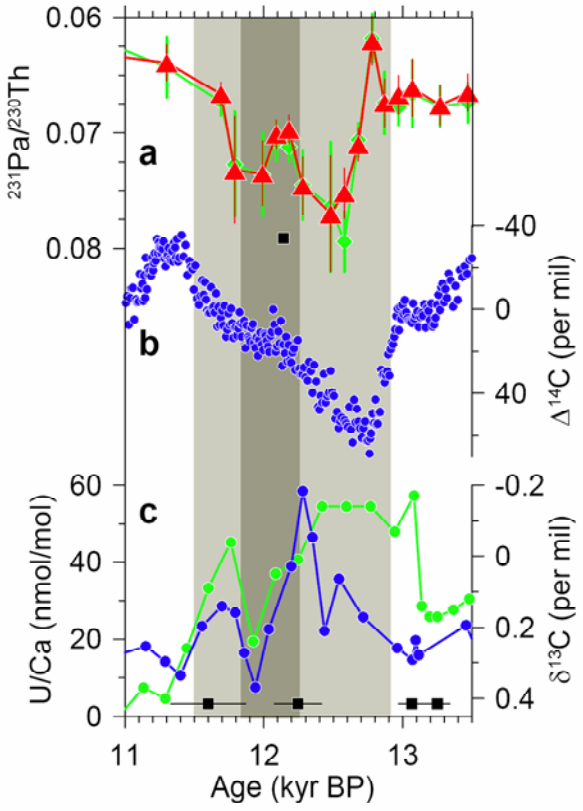

Figure 4.3. Proxies of Atlantic meridional overturning circulation and freshwater routing. Light gray bar denotes the Younger Dryas as defined in GISP2[26] and dark gray bar the Intra-Younger Dryas event. (**a**) $^{231}Pa/^{230}Th$ record from the subtropical North Atlantic[2]. (**b**) Detrended $\Delta^{14}C$ from Cariaco Basin[1]. (**c**) Planktonic U/Ca (blue) and $\delta^{13}C$ (green) from HU90031-044. Black squares denote radiocarbon ages with 1 sigma error.

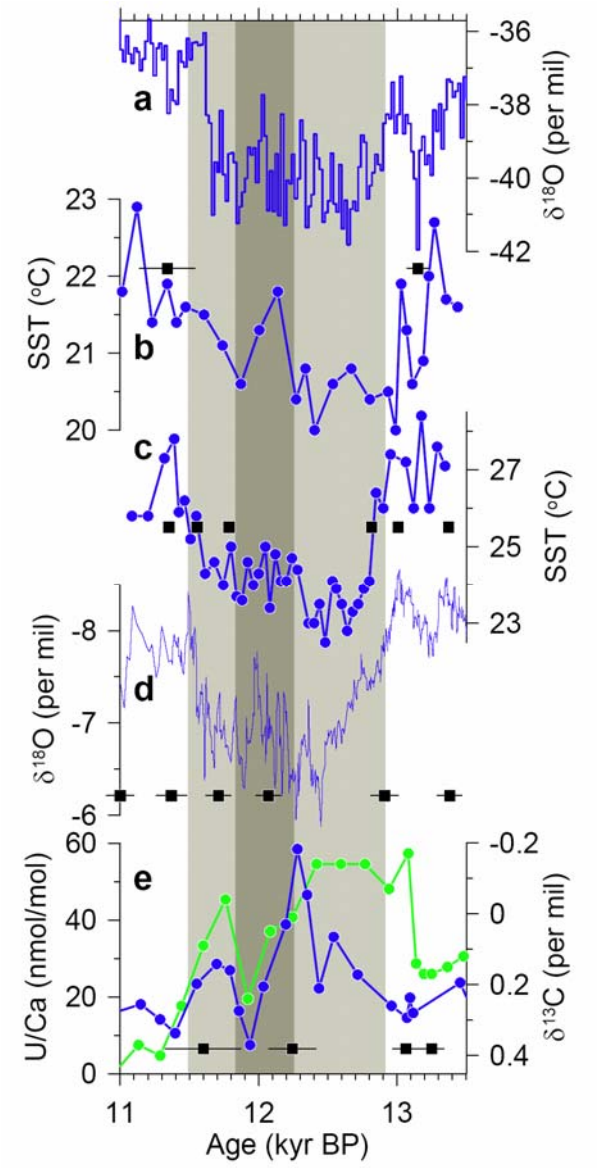

Figure 4.4. Proxies of Northern Hemisphere paleoclimate and freshwater routing. Gray bars are the same as in Figure 3. (**a**) Greenland $\delta^{18}O$ record[26]. (**b**) Sea surface temperature reconstruction from the coast of West Africa[24]. (**c**) Sea surface temperature reconstruction from Cariaco Basin[25]. (**d**) $\delta^{18}O$ from Hulu Cave, China[27]. (**e**) Planktonic U/Ca (blue) and $\delta^{13}C$ (green) from HU90031-044. Black squares denote ages with 1 sigma error.

4.5. Methods

We model changes in estuary geochemistry based on foraminifera O-isotopes and U- and Mg-concentrations using a simple flux-weighted mixing model. The model has five components: the isotopic ratio or concentration (mol m^{-3}) of the ocean end-member (I_o), the flux of the ocean water to the estuary (F_o, Sv), the isotopic ratio or concentration (mol m^{-3}) of the river end-member (I_r), the river flux (F_r, Sv), and the estuary isotopic ratio or concentration (mol m^{-3}) (I_e):

$$I_e = \frac{F_r I_r + F_o I_o}{F_r + F_o}. \qquad (4.1)$$

In the case of Sr-isotopes, we must also consider changes in the river concentration of Sr (Y_r, mol m^{-3}) and changes in the isotopic ratio (T_r) as well as the concentration (Y_o, mol m^{-3}) and isotopic ratio (T_o) of the ocean:

$$I_e = \frac{Y_r F_r T_r + Y_o F_o T_o}{Y_r F_r + Y_o F_o}. \qquad (4.2)$$

I_o, Y_o and F_o are considered constants. I_o and Y_o are calculated from the conservative behavior of U, Mg and Sr in the ocean. F_o comes from the net flux of ocean water into the St. Lawrence below 100 m depth (~0.74 Sv) (ref. 28). We assume all of this water exits in the upper 100 m mixed layer, the habitat of *G. bulloides* and *N. pachyderma (s)*[7]. This discharge depends on the bathymetry of the St. Lawrence estuary. To account for any changes in bathymetry, we correct for sea level lowering and isostatic depression as well as the marine incursion of the Champlain Sea[31]. These corrections, however, do not substantially change the geometry of the estuary from its modern shape. Also, our core locations are at the river distal end of the estuary and the chemistry there would likely not be influenced by a shift in the river-ocean mixing front due to an increase in river flux.

For Sr- and O-isotopes, we use previously determined ratios and concentrations for T_r and I_r. We use the modern Sr-isotope ratio for T_r[16] and the modern ocean ratio of 0.70917 for T_o. For O-isotopes, we use a $\delta^{18}O$ of -25 per mil for Lake Agassiz freshwater (I_r)[20] and $\delta^{18}O$ of 0 per mil for I_o.

To determine the river U, Mg (I_r) and Sr (Y_r) concentrations, we model basin-scale river geochemistry using a combination of previously measured modern river concentrations on known rock types[10,16,18] and river geochemistry data supplied by the Saskatchewan Watershed Authority. These concentrations are weighted by the exposure area of a given rock type relative to the basin area to determine the element concentration (X, mol m^{-3}) of river water leaving the basin:

$$X = \sum_{i}^{n} \frac{A_i}{A_b} R_i \qquad (4.3)$$

where A_i (m^2) is the exposed area of a specific rock type, A_b (m^2) is the area of the cryohydrological basins defined by Licciardi et al.[4], and R_i (mol m^{-3}) is the element river-water concentration for a given rock type. These basin concentrations are then weighted by their discharge and summed to calculate the concentration of U, Mg (I_r) and Sr (Y_r) in water discharged to the ocean through a given outlet:

$$I_r(Y_r) = \sum_{j}^{n} X_j W \qquad (4.4)$$

where W is a constant of proportionality that weights the chemistry of a basin by the discharge of the basin relative to the total discharge through an outlet (F_r). We initialize our value of W according to the discharges for each basin derived by Licciardi *et al.*[4]. We then assume that any change in total discharge through an outlet as needed to match our data will be accompanied by a proportional change in discharge from each basin so that W remains constant. Finally, to solve for F_r, we vary F_r until I_e matches our measured data.

To calculate discharge from our data, we convert foraminiferal U/Ca and ΔMg/Ca data to estuary concentrations following Russell et al.[17] and Delaney et al.[30], respectively. We solve our model for the change in the average estuary chemistry before and during the Younger Dryas to calculate our discharge estimate. We then calculate the standard deviation in our data from before and during the Younger Dryas at 1 sigma. Our estimate of error in the discharge is derived by solving the model for the maximum and minimum change in estuary chemistry at one standard deviation from the average before and during the Younger Dryas. In the case of Sr-isotopes, we determine our error by solving the model for the maximum and minimum changes

based on the measurement error before and during the Younger Dryas making this a conservative calculation of error. We do not calculate a standard deviation because of the low number of data points.

In using modern river data, we assume that chemical weathering rates during the Younger Dryas were analogous to modern weathering rates, which introduces some unknown error into our calculations. The error that we calculate for our base discharge estimates likely encompasses any climate induced changes in the weathering. The residence time of freshwater in Lake Agassiz may also have affected water chemistry. However, with a volume of 1,400 km^3 after the initial outbreak flood[31], the residence time of water in Lake Agassiz is 160 ± 40 days which is likely of short enough duration for limnologic processes to have had little effect on water chemistry.

Additionally, this model does not account for any consumption or production of Mg, Sr or U in the estuary. However, it is well established that Mg and Sr behave conservatively in estuarine environments. On the other hand, U can be both consumed by particulate rain at low salinities (psu < 10) and produced by colloid disintegration at high salinities (psu > 20)[32]. Based on our calculations of the effect of an anoxic to oxic switch in the sediments on the St. Lawrence estuary chemistry (discussed in the text), the exclusion of these particulate reactions in the water column likely has little effect on our modeling results.

4.6. Acknowledgments

We thank A. deVernal and C. Hillaire-Marcel for isotope data, the Bedford Institute of Oceanography for samples, the Saskatchewan Watershed Authority for river chemistry data, and D. Barber, G. Clarke, S. Hostetler and A. Mix for helpful comments and discussion. This research was funded by the NSF Earth System History Program (P.U.C.) and the NSF (G.P.K.).

4.7. References

1. Hughen, K.A., J.R. Southon, S.J. Lehman, & J.T. Overpeck, Synchronous radiocarbon and climate shifts during the last deglaciation. *Science* **290**, 1951-1954 (2000).
2. McManus, J.F. *et al.* Collapse and rapid resumption of Atlantic meridional circulation linked to deglacial climate changes. *Nature* **428***,* 834-837 (2004).
3. Broecker, W.S. *et al.* Routing of meltwater from the Laurentide Ice Sheet during the Younger Dryas cold episode. *Nature* **341**, 318-321 (1989).
4. Licciardi, J.M., J.T. Teller, & P.U. Clark, Freshwater routing by the Laurentide Ice Sheet during the last deglaciation, in *Mechanisms of Global Climate Change at Millennial Time Scales: Geophysical Monograph* **112***,* edited by P.U. Clark, R.S. Webb, & L.D. Keigwin, 177-201, AGU, Washington, D.C. (1999).
5. Rodrigues, C.G., & G. Vilks, The implications of glacial lake runoff on the Goldthwait and Champlain Seas: the relationship between glacial lake Agassiz runoff and the Younger Dryas. *Quaternary Science Reviews* **13,** 923-944 (1994).
6. Keigwin, L.D., & G.A. Jones, The marine record of deglaciation from the continental margin off Nova Scotia. *Paleoceanography,* **10,** 973-985 (1995).
7. deVernal, A., C. Hillaire-Marcel, & G. Bilodeau, Reduced meltwater outflow from the Laurentide ice margin during the Younger Dryas. *Nature* **381,** 774-777 (1996).
8. Teller, J.T., *et al.* Alternative routing of Lake Agassiz overflow during the Younger Dryas: new dates, paleotopography, and a re-evaluation. *Quaternary Science Reviews* (in press).
9. Tarasov, L., & W.R. Peltier, Arctic freshwater forcing of the Younger Dryas cold reversal. *Nature* **435**, 662-665 (2005).
10. Meybeck, M., Global chemical weathering of surficial rocks estimated from river dissolved loads. *American Journal of Science* **287,** 401-428 (1987).
11. Manabe, S., & R.J. Stouffer, Coupled ocean-atmosphere model response to freshwater input; comparison to Younger Dryas event. *Paleoceanography* **12,** 321-336 (1997).
12. Barton, K.E., D.G. Howell, & J.F. Vigil, The North America Tapestry of Time and Terrain. U.S. Geological Survey, *Geological Investigations Series* I-2781 (2003)
13. Haley, B.A., & G.P. Klinkhammer, Development of a flow-through system for cleaning and dissolving foraminiferal tests. *Chemical Geology* **185,** 51-69 (2002).
14. Dyke, A. S., in *Quaternary Glaciations-Extant and Chronology*, Part II, Vol. 2b (eds. Ehlers, J. & P.L. Gibbard) 373-424 (Elsevier Science and Technology Books, Amsterdam, 2004).
15. Stuiver, M. *et al.* INTCAL98 Radiocarbon Age Calibration, 24,000-0 cal BP. *Radiocarbon* **40,** 1041-1083 (1998).
16. Wadleigh, M.A., J. Veizer, & C. Brooks, Strontium and its isotopes in Canadian rivers: fluxes and global implications. *Geochimica et Cosmochimica Act.* **49,** 1727-1736 (1985).
17. Russell, A.D. *et al.* Uranium in foraminiferal calcite as a recorder of seawater uranium concentrations. *Geochimica et Cosmochimica Acta* **58,** 671-681 (1994).
18. Chabaux, F., J. Riotte, & O. Dequincey, U-Th-Ra fractionation during weathering and river transport, in *Uranium-Series Geochemistry: Reviews in Mineralogy &*

Geochemistry, 52, edited by B. Bourdon, G.M. Henderson, C.C. Lundstrom, & S.P. Turner, pp. 533-576 (2003).
19. Lea, D.W., T.A. Mashiotta, & H.J. Spero, Controls on magnesium and strontium uptake in planktonic foraminifera determined by live culturing. *Geochimica et Cosmochimica Acta* **63,** 2369-2379 (1999).
20. Remenda, V.H., J.A. Cherry, & T.W.D. Edwards, Isotopic composition of old ground water from Lake Agassiz: implications for Late Pleistocene climate. *Science* **266,** 1975-1978 (1994).
21. Flower, B.P., D.W. Hastings, H.W. Hill, & T.M. Quinn, Phasing of deglacial warming and Laurentide ice sheet meltwater in the Gulf of Mexico. *Geology* **32,** 597-600 (2004).
22. Smith, D.G., & T.G. Fisher, Glacial Lake Agassiz: the northwestern outlet and paleoflood. *Geology,* **21,** 9-12 (1993).
23. Andrews, J.T., & G. Dunhill, Early to mid-Holocene Atlantic water influx and deglacial meltwater events, Beaufort Sea slope, Arctic Ocean. *Quaternary Research* **61,** 14-21 (2004).
24. DeMenocal, P., J. Ortiz, T. Guilderson, & M. Sarnthein, Coherent high- and low-latitude climate variability during the Holocene Warm Period. *Science* **288,** 2198-2202 (2000).
25. Lea, D.W., D.K. Pak, L.C. Peterson, & K.A. Hughen, Synchroneity of tropical and high-latitude Atlantic temperatures over the Last Glacial Termination. *Science* **301,** 1361-1364 (2003).
26. Grootes, P.M. *et al.* Comparison of oxygen isotope records from the GISP2 and GRIP Greenland ice cores. *Nature* **369,** 552-554 (1993).
27. Wang, Y.J. *et al.* A high-resolution absolute-dated Late Pleistocene monsoon record from Hulu Cave, China. *Science* **294,** 2345-2348 (2001).
28. Dickie, L.M., & R.W. Trites, The Gulf of St. Lawrence, in *Ecosystems of the World 26, Estuaries and Enclosed Seas*, edited by B.W. Ketchum, pp. 403-425, Elsevier Scientific Publishing Company, New York (1983).
29. Shaw, J., P. Gereau, & R.C. Courtney, Palaeogeography of Atlantic Canada 13-0 kyr. *Quaternary Science Reviews* **21,** 1861-1878 (2002).
30. Delaney, M.L., A.W.H. Bé, & E.A. Boyle, Li, Sr, Mg, and Na in foraminiferal calcite shells from laboratory culture, sediment traps, and sediment cores. *Geochimica et Cosmochimica Acta* **49,** 1327-1341 (1985).
31. Teller, J.T., D.W. Leverington, & J.D. Mann, Freshwater outbursts to the oceans from glacial Lake Agassiz and their role in climate change during the last deglaciation. *Quaternary Science Reviews* **21,** 879-887 (2002).
32. Swarzenski, P.W., D. Porcelli, P.S. Anderson, & J.M. Smoak, The behavior of U- and The-series nuclides in the estuarine environment, in *Uranium-Series Geochemistry: Reviews in Mineralogy & Geochemistry, 52,* edited by B. Bourdon, G.M. Henderson, C.C. Lundstrom, & S.P. Turner, pp. 577-606 (2003).

CHAPTER 5

RAPID HOLOCENE DEGLACIATION OF THE LABRADOR SECTOR OF THE LAURENTIDE ICE SHEET

Anders E. Carlson (1), Peter U. Clark (1), Grant M. Raisbeck (2), Edward J. Brook (1)

(1) Department of Geosciences, Oregon State University, Corvallis, OR, 97331, USA

(2) Centre de Spectrométrie Nucléaire et de Spectrométrie de Masse, IN_2P_3/CNRS, Bât. 104 et 108, 91405 Orsay Campus, France

To be submitted to Science

5.1. Abstract

Cosmogenic ^{10}Be boulder ages from the Labrador Sector of the Laurentide Ice Sheet (LIS) indicate that following the deglaciation of the Hudson Bay coastline at 8.0±0.16 ka, this margin of the LIS rapidly retreated ~600 km by 6.80±0.20 ^{10}Be ka in ~620 years and contributed ~3 m of sea level rise to a postulated rapid rise in sea level 7.6 to 6.9 ka. The disappearance of the LIS ~6.8 ka and attendant reduction in freshwater runoff may have induced the formation of Labrador Deep Sea Water while the loss of the high albedo surface may have initiated the Holocene Thermal Maximum in eastern Canada and southern Greenland. The rapidity of retreat suggests that Northern Hemisphere ice sheets are more sensitive to climate warming than predicted by current ice sheet models.

5.2. Introduction

The Laurentide Ice Sheet (LIS) was the largest of the Northern Hemisphere ice sheets and had the greatest effect on climate and sea level during the Last Glacial Maximum (~21 ka) and deglaciation (*1*). Its Late Pleistocene retreat chronology is relatively well constrained by ^{14}C dates and moraine correlation. Following retreat onto the Canadian Shield ~10.2 ka (*2*), however, the Holocene retreat history is only poorly constrained because of the paucity of ^{14}C ages (*2*). In addition, these radiocarbon ages are from bulk sediment which may contain old carbon (*3*) reducing the accuracy of the date. Radiocarbon ages also do not date ice margin retreat but rather the arrival and accumulation of biomass and are thus not an accurate chronometer of ice margin retreat. This limited Holocene radiocarbon chronology indicates that the southern margin of the LIS retreated rapidly northward toward the Keewatin and Quebec/Labrador ice centers (*2*). The opening of Hudson Bay ~8.4 ka (*4*) caused the LIS to fragment into three ice caps; one over Keewatin, one over Baffin Island and Foxe Basin, and one over Quebec and Labrador (Fig. 5.1). Ice over Keewatin subsequently disappeared by ~7 ka (*2*) whereas ice over Baffin Island and Foxe Basin continued to retreat throughout the Holocene (*5*). In Quebec and

Labrador, ice retreated from the northeastern coast between 13 and 10.5 ka (*6*, *7*) and from the Hudson Strait coast between 8.9 and 8.4 ka (*8*, *9*). The western coast was likely deglaciated ~8.4 ka and the northwestern coast ~8 ka (*2*). Little is known, however, about the subsequent timing of retreat inland from the coast or of the final disappearance of the Labrador Sector of the LIS (*2*). While Dyke (*2*) presents 7 radiocarbon dates in western Quebec, only 2 of these dates actually constrain the ice margin position. These 2 dates suggest that the majority of the LIS deglaciated from Quebec/Labrador sometime before ~6 ka with ice persisting on the Ungava Peninsula until ~5.75 ka (*2*). The timing of retreat and disappearance of the LIS needs to be better constrained to interpret the causes of Holocene climate change, the partitioning of sea level rise between Northern and Southern Hemisphere ice sheets, and determine the sensitivity of land-based ice sheets to a warming climate.

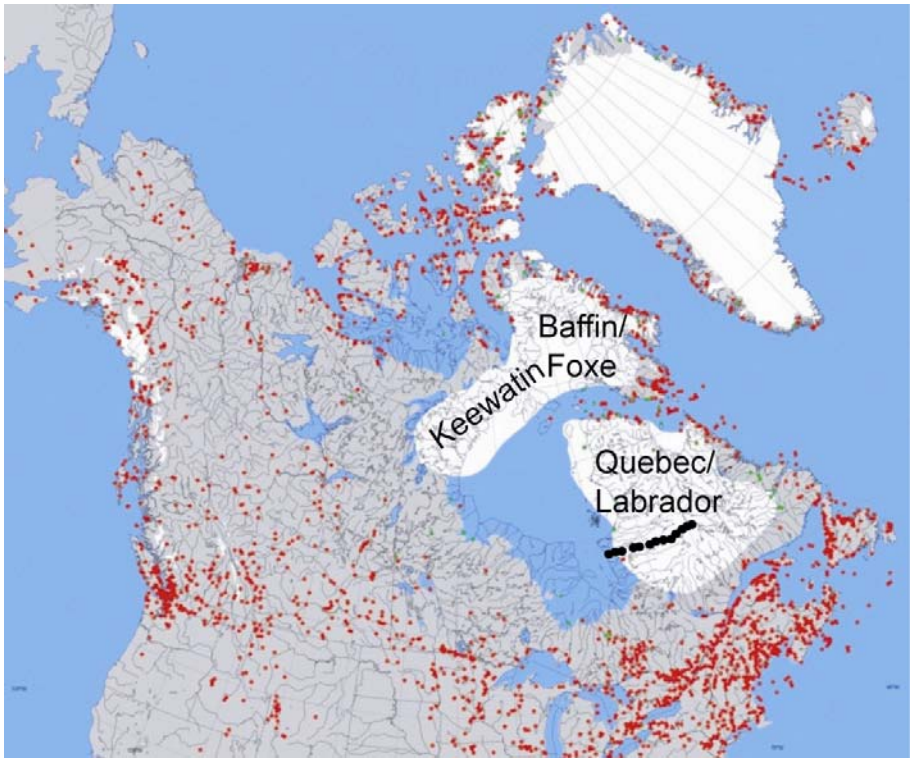

Figure 5.1. Sample locations (black dots) overlain on the 7.6 ^{14}C kyr BP (8.4 calendar kyr BP) map of Dyke (2004) with three remaining ice caps labeled. Red dots are minimum limiting radiocarbon dates; green dots are maximum limiting radiocarbon dates.

5.3. Results

Here we address these issues by using cosmogenic ^{10}Be ages from boulders sampled along an ~650 km long transect across north-central Quebec that is perpendicular to the general retreat direction of the western margin of the LIS to date the final retreat of the LIS (Fig. 5.1) (see supplementary Methods Section). Our ages range from 8,170±760 to 6,350±550 ^{10}Be yrs (Table 5.1). Based on relative sea level data (*10*), we divide our data into two geologically distinct groups; those that were covered by sea water and those that were not. The three western most samples (QC-2, 4 & 6, Table 5.1) were initially covered by sea water due to isostatic depression and should date the emergence of the coastline because of the rapid attenuation of cosmogenic ray penetration with depth in water (90% reduction in production at a depth of 5 m below sea level). These data, combined with the radiocarbon data of Hardy (*10*), indicate a marine limit of 8.0±0.16 ka (Fig. 5.2). Our remaining samples to the east are statistically indistinguishable from the mean at 1 sigma and thus we calculate an error-weighted mean age for those of 6,800±200 ^{10}Be yrs (Fig. 5.3). (Because the standard deviation between samples is less than the analytical uncertainty, we report here an error weighted mean age.) While some samples do not overlap with others at 1 sigma, we deem that the relatively close agreement between samples does not allow us to exclude any one sample from the population.

5.4. Discussion

Our ^{10}Be ages provide the first direct dating of the retreat of the Labrador Sector of the LIS. These data suggest that following retreat from the coast at ~8.0 ka (the marine limit) (Fig. 5.2), the LIS disintegrated rapidly just before ~6.8 ka (Fig. 5.3). The timing of the marine limit we calculate here (8.0±0.16 ka) based on 14 radiocarbon ages and three ^{10}Be ages is ~400 years younger than the ~8.4 ka retreat determined by Dyke (*2*). The latter value, however, is based on one radiocarbon age which may contain contamination of old carbon.

Sample	Altitude (m)	Latitude N (DD)	Longitude W (DD)	[10Be] atoms/g	Latitude & Altitude Scaling Factor	Time Average Scaling Factor	Age years	1 sigma error
QC-2	136	53.695	78.096	32886	1.16	1.06	6960	770
QC-4	167	53.384	77.527	39900	1.19	1.09	8170	760
QC-6	200	53.538	76.497	37719	1.23	1.13	7450	630
QC-10	299	53.528	74.871	44430	1.36	1.25	7920	920
QC-11	327	53.552	74.479	40943	1.40	1.31	6980	590
QC-13	467	53.834	73.5	44900	1.60	1.50	6700	580
QC-15	434	53.849	72.678	42500	1.55	1.45	6540	570
QC-27	460	53.984	72.057	44027	1.59	1.49	6600	590
QC-17	485	54.042	71.788	43369	1.63	1.53	6350	550
QC-19	519	54.195	71.479	45839	1.68	1.58	6490	670
QC-23	509	54.474	70.58	53131	1.66	1.56	7590	650
QC-24	606	54.688	70.273	49559	1.82	1.72	6460	550
QC-25	669	54.785	69.982	66441	1.92	1.82	8160	1080

Table 5.1. Sample characteristics, ^{10}Be concentration, scaling factors, age and error.

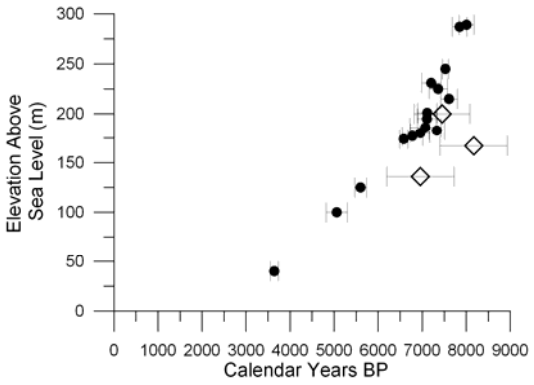

Figure 5.2. Relative sea level data for eastern James Bay and timing of the marine limit. Solid circles are ^{14}C ages from Hardy (*10*) calibrated using the reservoir correction of Barber *et al.* (*4*) and CALIB 5.01; open diamonds are ^{10}Be ages. 1 sigma error bars shown.

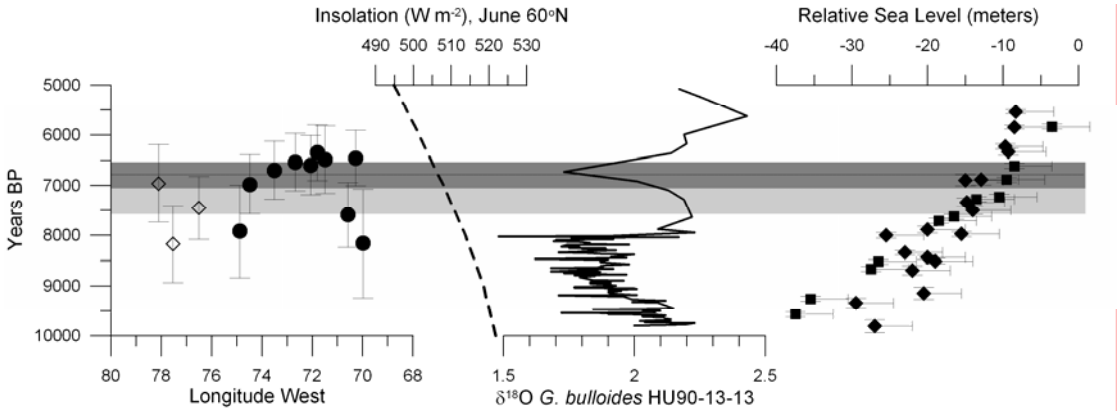

Figure 5.3. ^{10}Be chronology for the western margin of the Labrador Sector of the Laurentide Ice Sheet, deglaciation forcing, Labrador Sea δ^{18}O and relative sea level data. Dark gray bar denotes the error-weighted mean age of collapse of the Labrador Sector; the light gray bar indicates the postulated rapid sea level rise from 7.6 to 6.9 ka (*17*). From left to right: ^{10}Be ages with one sigma error bars (open diamonds date the emergence of the coast, filled circles date deglaciation) (see Fig. 5.1 for sample location); June insolation at 60 ºN (*31*) (dashed line); *G. bulloides* δ^{18}O record from the Labrador Sea (*22*) (solid line); and relative sea level data for the last 10,000 years: solid squares from Tahiti (*18*), and closed diamonds from the Caribbean (*20*). One sigma age error bars are shown along with the growth habitat of the corals.

We determine the ice margin retreat for our remaining ten samples distributed over 75 to 70 degrees west using Monte Carlo retreat simulations (see supplementary Methods Section). We calculate that the Labrador Sector of the LIS deglaciated in 620±760 years. This rapid retreat is in contrast with the existing radiocarbon chronology (*2*) where the 2 minimum limiting radiocarbon dates that actually constrain the LIS margin imply a more gradual eastward recession of the LIS margin from ~8.4 to 6.0 calendar kyr BP. However, these two ages date the arrival and accumulation of vegetation, not deglaciation as our cosmogenic dates do.

The cause of this rapid collapse of the LIS is not clear. The rapid gutting of the center of the LIS at ~8.4 ka (*4*) was likely induced by an extensive calving margin associated with the proglacial lakes and marine incursion into Hudson Bay. However, calving cannot explain the rapid 6.8 ka collapse because the LIS margin was land-based at that time. Instead, we attribute the rapid margin retreat to reflect the final stages of deglaciation following an interval of top-down melting induced by a large rise in the ELA. Such a rapid rise in the equilibrium line altitude may be in response to the collapse of Hudson Bay ice and the reorganization of regional atmospheric circulation combined with the increased thermal capacity of Hudson Bay sea water relative to ice. Using reasonable net mass balance values (b_n, m yr^{-1}) for an ice sheet without an accumulation zone (-5 to -15 m yr^{-1} at the terminus increasing to -0.1 m yr^{-1} at 2,320 m ice thickness) and our positive degree day model (see supplementary Methods Section), the Labrador Sector of the LIS melts within 860±170 years (Fig. 5.4), in good agreement with our Monte Carlo retreat scenarios considering that our positive degree day model does not include ice physics.

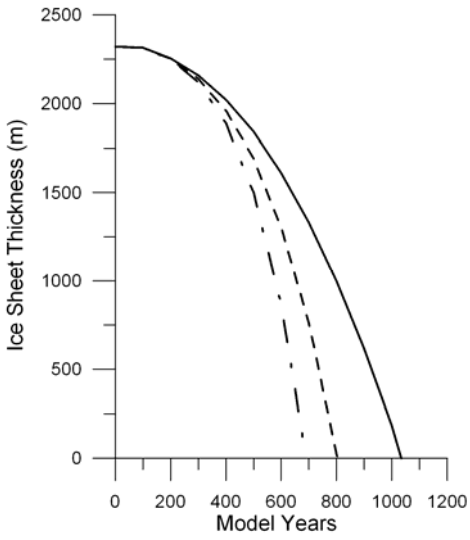

Figure 5.4. Positive degree day model results for the center of the ice sheet. The terminus b_n (net mass balance) rates for model simulations are as follows: the solid line is -5 m yr^{-1} b_n, the dashed line is -10 m yr^{-1} b_n, and the dashed-dotted line is -15 m yr^{-1} b_n.

Simulations with numerical climate models indicate that removal of the LIS would induce warming over eastern North America to northern Europe (*11-13*). Indeed, paleoclimate records show that the onset of the Holocene Thermal Maximum (HTM) occurred between 7 and 6 ka over central to northeastern North America and southern Greenland (*14*), indicating that the remnant LIS delayed the insolation-induced HTM by up to 4,000 years relative to the insolation maximum at ~11 ka (Fig. 5.3) through the attendant cooling associated with its high albedo. Thus, the remnant LIS had a climatic influence at least over eastern North America to southern Greenland.

Our results indicate that the Labrador Sector of the LIS contributed ~3 m sea level rise (*15*) between 8.0 and 6.8 ka in a period of lasting ~620 years. Any additional rise after this time must then be attributed to the continued deglaciation of Antarctica (*16*) and the ~1 m of sea level rise left in the Baffin Island/Foxe Basin Ice Cap and remnant ice on Ungava Peninsula (*15*). This rapid melting lasting ~620 years between 8.0 and 6.8 ka may be coincident with a postulated melt water pulse (mwp) ~7.6 to 6.9 ka (Fig. 5.3) (*17*), suggesting that much of this mwp originated from the LIS. Unfortunately, the timing and rate of this mwp is uncertain. Coral data from Tahiti indicate that the event occurred from ~7.6 to 6.9 ka (Fig. 5.3) but at a moderate rate of sea level rise of ~10 mm yr^{-1} (*18*, *19*). In contrast, coral data from the Caribbean (*20*) suggest the mwp occurred ~7 to 6.5 ka (Fig. 5.3) (recalibrated using

CALIB 5.01) with a rapid rate of sea level rise of >45 mm yr^{-1} (*17*). Despite these conflicts, it appears that sea level rose ~5 m during the period of rapid melting of the Labrador Sector of the LIS suggesting that the LIS is the major source for this mwp. The additional 2 m of sea level rise during this period may be sourced from the Keewatin and Foxe Basin Sectors of the LIS which disappeared ~7 ka (*2*). This mwp has previously been attributed to Antarctica (*17*), but, at least for the West Antarctic Ice Sheet, retreat did not accelerate until after 7 ka (*21*, *16*), indicating that this ice sheet did not play a substantial role in this mwp.

The disappearance of the majority of the Labrador Sector of the LIS at 6.8±0.20 ka is coincident within error with the initiation of Labrador Deep Seawater (LDSW) formation at ~7 ka (*22*). We postulate that melting of the Labrador Sector up to 6.8 ka may have freshened and stratified the Labrador Sea, thus preventing the formation of LDSW (*23*). This enhanced freshwater flux derived from the rapid melting of the LIS may be recorded by a light $\delta^{18}O$ surface water anomaly in the Labrador Sea (Fig. 5.3) (*22*). The subsequent disappearance of the majority of the LIS and reduction in freshwater runoff allowed the establishment of a more saline and stable surface water mass in the Labrador Sea ~7 ka (*24*), which would allow LDSW formation. Retreat of the Greenland Ice Sheet (GIS) may also have contributed to freshening of the Labrador Sea, but this is likely of a much smaller magnitude because the glacial-interglacial adjustment of the GIS was complete by the early Holocene (~9 to 8 ka) (*25*). The initiation of LDSW and attendant heat dissipation to the atmosphere may also have contributed to the warming associated with the HTM.

The rapid retreat of the Labrador Sector of the LIS provides a natural experiment to determine response of an ice sheet to a climate warmer than present permitting an assessment of model predictions for the future of the GIS. The Labrador Sector of the LIS was land-based as is the GIS and was of comparable size to the present GIS (~4 m of sea level equivalent for the LIS (*15*) relative to the modern ~7 m of sea level equivalent in the GIS). In addition, both ice sheets have similar latitudinal distribution with upwind sources of warm air and moisture (Hudson Bay for the LIS and the Labrador Sea for the GIS). The main sector of the remnant LIS retreated in ~620 years forced by summer surface temperatures between 1 and 3 °C warmer than

present (*26*, *27*, *14*) and likely contributed ~3 m of sea level rise (*16*) in that time span. Coupled ice sheet-climate model predictions for the future of the GIS suggest that with a 4 x pre-industrial CO_2 forcing (>5 °C annual mean surface warming over Greenland), the GIS would contribute ~3 m of sea level rise in ~700 years (*28*). We suggest that these model simulations under-predict the retreat rate of the GIS because our data show a comparable retreat rate and sea level contribution for the LIS under at least a 2 to 4 °C cooler climate than that used to force the GIS simulations. The GIS model simulations, however, do not include such physical feedbacks as surface meltwater penetrating to the ice sheet bed with attendant ice sheet acceleration (*29*) which would increase retreat rate. Thus, Northern Hemisphere ice sheets may be more sensitive to climate warming than current ice sheet models would suggest (*30*).

5.5. Supplementary Methods

We sampled boulders along a ~650 km long transect that is perpendicular to the general retreat direction of the western margin of the LIS from the coast of James Bay to near the Quebec-Labrador border (Fig. 5.1). Thirteen samples of granitic and gneissic Precambrian boulders were collected, giving us a spatial resolution of about one sample every 50 km. Only boulders greater than 1 m in diameter were sampled in order to reduce the possibility of snow cover. These boulders showed evidence of glacial abrasion, indicating absence of significant post-glacial erosion and removal of previously exposed surfaces. None of our boulders were shielded significantly by the surrounding topography. The top 1 to 2 cm from the center of horizontal surfaces on the highest part of each boulder was sampled to minimize attenuation of cosmogenic nuclide production with depth and limit any increased production due to cosmic ray penetration from the boulder side.

Samples were prepared for accelerator mass spectrometry (AMS) at Oregon State University following the procedures of Rinterknecht (*32*). Samples were crushed and sieved followed by magnetic separation, then boiled in phosphoric acid prior to sequential leaching in hydrofluoric and nitric acid to leave pure quartz. Purity of the samples was checked by ICP-AES before final dissolution in hydrofluoric acid,

together with 250 μg of ^{9}Be carrier. ^{10}Be was extracted using ion-exchange columns and selective precipitation techniques. ^{10}Be/^{9}Be ratios were determined at the AMS facility at Gif sur Yvette, France (*33*) relative to NIST standard 4325, using the certified ratio of 2.68 x10^{-11}.

Ages were calculated using the production rate of 5.1 atoms g^{-1} yr^{-1} at sea level and high latitude (*34*), (reduced by 14% because of the different standard used in these measurements compared to that used to make the production rate measurements) and scaling factors of Lal (*35*) modified by Stone (*34*). We corrected our data for isostatic uplift (*10*) following Rinterknecht *et al.* (*36*) which decreases our production scaling factor by 5 to 8%. We do not correct our production rate (determined at mid-latitudes) for secular variations in magnetic field intensity because secular variations have been shown to have little effect on mid-latitude production rates (*34, 37, 38*). No corrections were made for snow cover or erosion because of care taken in boulder selection. The samples may contain inheritance from previous exposure to cosmic rays which was not removed by glacial erosion due to cover by cold-based ice. However, we greatly reduce the likelihood of inheritance relative to bedrock samples by using boulders. The Quebec/Labrador region did experience periods of cold-based ice cover, but it also underwent extensive periods of erosive, wet-based ice cover during the last glacial period reflected in the numerous ice-flow indicators eroded into the bedrock surface (*39*). While this does not indicate the amount of erosion, it does reduce the likelihood of inheritance in our samples. Our three samples closest to James Bay experienced cover by sea water which we did not correct for assuming there was little production until the boulder was above sea water. We calculated 1 sigma error using counting statistics and a conservative 5% machine error (long-term error in the standards). We did not propagate any additional error involved in the production rate or scaling factors. We also did not consider any error involved in the migration of the magnetic pole because of the high latitude of our sample locations. In comparing ^{10}Be years to calendar years, we are aware of the additional uncertainty (~10%) involved in the production rate calibration, isostatic correction, and scaling factors (e.g. *7*).

While ^{10}Be dates are analytically less precise than radiocarbon dates, they are more accurate for determining ice margin retreat. Cosmogenic ages date the actual retreat of the ice margin whereas radiocarbon ages date the arrival of vegetation to a region. Furthermore, radiocarbon ages in northeastern Canada have an inherent problem of contamination by old carbon (*2, 3*) reducing their accuracy. To produce a robust determination of the timing of retreat, we use a Monte Carlo method that simulates numerous retreat possibilities allowed by the analytical error in the data. We generate 3,000 possible retreat scenarios by randomly choosing for each sample location from a normal distribution with mean and standard deviation given by the age and uncertainty at each site. Because we include the radiocarbon dated marine limit in these scenarios, we must consider any offset between calibrated radiocarbon ages and ^{10}Be ages. While the offset between these ages is likely small given the agreement between the coastal emergence ^{10}Be dates and radiocarbon dated beach sediments (Fig. 2), we increase the error in the marine limit age to 9% to account for any offset. From these scenarios, we can determine a robust estimate of the duration of retreat by calculating the mean and standard deviation.

To further examine the retreat of the LIS and its climatic implications, we model the inferred response of the LIS to a rise in the equilibrium line altitude (ELA) using a positive degree day model that calculates ice thickness (h in meters) as a function of the net mass balance (b_n in m yr^{-1}) which depends on the ice thickness (h) and time (t in years):

$$h(t) = h_0 - \int_0^t b_n(h,t)dt \,. \qquad (5.1)$$

We initialize the ice thickness to the same as that reconstructed for 8 ^{14}C ka by Licciardi *et al.* (*15*). Mass balance increases linearly with elevation and decreases linearly with time as more ice (lower albedo and rougher surface than snow) is exposed. The model does not include ice dynamics which would cause faster draw-down of the ice surface, making this model a conservative treatment of the ice sheet collapse.

5.6. Acknowledgments

We thank Allan Carlson for help in the field; Vincent Rinterknecht for discussing and demonstrating ^{10}Be sample processing; Brent Goehring for help with the isostatic uplift correction and laboratory preparation; Kelley Lake, Faron Anslow and Lica Ersek for help in the lab. Comments of two anonymous reviewers improved this manuscript. This research was supported by grants from NSF (BCS-0402325, A.E.C. and P.U.C.) and GSA (A.E.C.). Tandetron operation is supported by the IN_2P_3 and INSU divisions of the CNRS.

5.7. References

1. P.U. Clark, R.B. Alley, D. Pollard, *Science* **286**, 1104 (1999).
2. A.S. Dyke, *in* Quaternary Glaciations-Extant and Chronology, Part II, J. Ehlers, P.L. Gibbard, P.L., Eds., Elsevier Science and Technology Books, Amsterdam **2b**, 373 (2004).
3. S.K. Short, H. Nichols, *Arctic and Alpine Research* **9**, 265 (1977).
4. D.C. Barber, *et al.*, *Nature* **400**, 344 (1999)
5. G.H. Miller, A.P. Wolfe, J.P. Briner, P.E. Sauer, A. Nesje, *Quaternary Science Reviews* **24**, 1703 (2005).
6. P.U. Clark, W.W. Fitzhugh, *in* Paleoshorelines and prehistory: An investigation of method, Johnson, L.L., Ed., CRC Press, Boca Raton, Florida, 189 (1991).
7. P.U. Clark, E.J. Brook, G.M. Raisbeck, F. Yiou, J. Clark, *Geology* **31**, 617 (2003).
8. B. Lauriol, J.T. Gray, *Arctic and Alpine Research* **19**, 109 (1987).
9. P.U. Clark, W.W. Fitzhugh, *Quaternary Research* **34**, 296 (1990)
10. L. Hardy, thesis, McGill University-Montreal (1976).
11. J.F.B. Mitchell, N.S. Grahame, K.J. Needham, *Journal of Geophysical Research* **93**, 8283 (1988).
12. D. Pollard, J.C. Bergengren, L.M. Stillwell-Soller, B. Felzer, S.L. Thompson, *Paleoclimates; data and modeling* **2**, 183 (1998).
13. H. Renssen, *et al.*, *Climate Dynamics* **24**, 23 (2005).
14. D.S. Kaufman, *et al.*, *Quaternary Science Reviews* **23**, 529 (2004).
15. J.M. Licciardi, P.U. Clark, J.W. Jenson, D.R. MacAyeal, *Quaternary Science Reviews* **17**, 427 (1998).
16. J.O. Stone, *et al.*, *Science* **299**, 99 (2003).
17. P. Blanchon, J. Shaw, *Geology* **23**, 4 (1995).
18. E. Bard, *et al.*, *Nature* **382**, 241 (1996).
19. L. Montaggioni, L., *et al.*, *Geology* **25**, 555 (1997).
20. R.G. Lighty, I.G. Macintyre, R. Stuckenrath, *Coral Reefs* **1**, 125 (1982).
21. H. Conway, B.L. Hall, G.H. Denton, A.M. Gades, E.D. Waddington, *Science* **286**, 280 (1999).
22. C. Hillaire-Marcel, A. deVernal, G. Bilodeau, A.J. Weaver, *Nature* **410**, 1073 (2001).
23. M. Cottet-Puinel, *et al.*, *Quaternary Science Reviews* **23**, 449 (2004).
24. S. Solignac, A. deVernal, C. Hillaire-Marcel, *Quaternary Science Reviews* **23**, 319 (2004).
25. O. Bennike, S. Björck, *Journal of Quaternary Science* **17**, 211 (2002).
26. S.D. Muller, P.J.H. Richard, J. Guiot, J.-L. de Beaulieu, D. Fortin, *Palaeogeography, Palaeoclimatology, Palaeoecology* **193**, 51 (2003).
27. M. Sawada, A.E. Viau, G. Vettoretti, W.R. Peltier, K. Gajewski, *Quaternary Science Reviews* **23**, 225 (2004).
28. J.K. Ridley, P. Huybrechts, J.M. Gregory, J.A. Lowe, *Journal of Climate* **18**, 3409 (2005).
29. H.J. Zwally, *et al.*, *Science* **297**, 218 (2002).

30. R.B. Alley, P.U. Clark, P. Huybrechts, I. Joughin, *Science* **310**, 456 (2005).
31. A. Berger, M.F. Loutre, *Quaternary Science Reviews* **10**, 297 (1991).
32. V.R. Rinterknecht, thesis, Oregon State University-Corvallis.
33. G.M. Raisbeck, *et al.*, *Nuclear Instruments and Methods in Physics Research* **92**, 43 (1994).
34. J.O. Stone, *Journal of Geophysical Research* **105**, 23,753 (2000).
35. D. Lal, *Earth and Planetary Science Letters* **104**, 424 (1991).
36. V.R. Rinterknecht, *et al.*, *Quaternary Science Reviews* **23**, 2283 (2004).
37. F.M. Phillips, M.G. Zreda, M.R. Flinsch, D. Elmore, P. Sharma, *Geophysical Research Letters* **23**, 949 (1996).
38. J.M. Licciardi, M.D. Kurz, P.U. Clark, E.J. Brook, *Earth and Planetary Science Letters* **172**, 261 (1999).
39. J.J. Veillette, A.S. Dyke, M. Roy, *Quaternary Science Reviews* **18**, 993 (1999).

CHAPTER 6

CONCLUSIONS

6.1. Conclusions

The Laurentide Ice Sheet (LIS) affected climate during the last deglaciation through diminishment of its aerial extent and high albedo, and by the rapid advance and retreat of its southern margin, due in part to high pore water pressure and sediment deformation, with attendant routing of continental runoff to the North Atlantic and reduction in Atlantic meridional overturning circulation (AMOC).

6.2. Implications

The similarity of observations and thickness of the deforming layer in the Tiskilwa and Sky Pilot Tills from two glaciological different locations under the LIS suggest that sediment deformation contributes significantly to ice sheet motion not only for the southern margin of the LIS but also near the ice sheet center. This may have led to fast ice flow with attendant climatic impacts through the routing of freshwater to the North Atlantic (e.g., Clark et al., 2001) and increased flux of icebergs from Hudson Strait (MacAyeal, 1993). Furthermore, the similarity between the drainage systems simulated for the southern margin of the LIS and that proposed for the West Antarctic Ice Streams (Engelhardt and Kamb, 1997) suggests that similar subglacial processes contribute to and stabilize fast ice flow for both ice sheets. While the basal canal drainage system simulated here along with till deformation may stabilize the ice sheet, the canal drainage system shows threshold limits that, if crossed, could lead to collapse of the ice sheet. This implies that the ice margin instabilities observed during the last deglaciation of the LIS (Mickelson et al., 1983; Clark, 1994) may also occur in the West Antarctic Ice Sheet, and possibly in the Greenland Ice Sheet with global consequences (MacAyeal, 1992; Bentley, 1997; De Angelis and Skvarca, 2003; Alley et al., 2005).

The confirmation that the fluctuation of the southern margin of the LIS caused the Younger Dryas cold event (12.9 to 11.7 ka) through its attendant routing of 0.08±0.03 Sv (1 Sv = 10^6 m^3 s^{-1}) of freshwater to the North Atlantic that was sufficient to reduce AMOC (Manabe and Stouffer, 1997) demonstrates the sensitivity AMOC. The hemispheric climatic impact of the short-lived intra-Younger Dryas routing event at ~12 ka further verifies the sensitivity of AMOC and the climate system. This suggests that the conservative predictions of freshwater fluxes derived from the future retreat of the Greenland Ice Sheet of up to 0.12 Sv (Ridley et al., 2005) could slow AMOC as is currently being observed (Bryden et al., 2005). In addition, the enhanced hydrologic cycle of the circum-Arctic Ocean may also contribute enough freshwater to the North Atlantic to affect AMOC (Peterson et al., 2002). However, the current estimate of this flux is of insufficient magnitude according to the estimate that forced the Younger Dryas cold event.

The final rapid collapse of the majority of the LIS at ~6.8 ka also provides a sensitivity test of how ice sheets affect and respond to climate. This collapse contributed ~3 m of sea level rise and occurred in ~620 years under a climate 1 to 3 °C warmer than present. Model predictions for the response of the Greenland Ice Sheet (which has similar geographical setting to the remnant LIS) to a climate >5 °C warmer than present suggest a similar sea level contribution in ~700 years (Ridley et al., 2005). This indicates that current models underestimate the response of ice sheets to climate warming likely due to the omission of important ice dynamic positive feedbacks (Alley et al., 2005). If ice sheet responses to temperature are assumed to be linear (which they are not (e.g., Ridley et al., 2005)), then the retreat of the Greenland Ice Sheet under >5 °C forcing will be much more rapid than predicted with a great flux of freshwater to the North Atlantic. Furthermore, the disappearance of the LIS caused abrupt downwind warming at least to southern Greenland (Kaufmann et al., 2004). An analogous downwind warming pattern may occur with the retreat of the Greenland Ice Sheet offsetting cooling due to reduced AMOC.

6.3. References

Alley, R.B., Clark, P.U., Huybrechts, P., and Joughin, I., 2005, Ice-Sheet and Sea-Level Changes: Science, v. 310, p. 456-460.

Bentley, C.R., 1997, Rapid sea-level rise soon from West Antarctic Ice Sheet collapse?: Science, v. 275, p. 1077-1078.

Bryden, H.L., Longworth, H.R., and Cunningham, S.A., 2005, Slowing of the Atlantic meridional overturning circulation at 25°N: Nature, v. 438, p. 655-657.

Clark, P.U., 1994, Unstable behavior of the Laurentide Ice Sheet over deforming sediment and its implication for climate change, Quaternary Research: v. 41, p. 19-25.

Clark, P.U., Marshall, S.J., Clarke, G.K.C., Hostetler, S.W., Licciardi, J.M., and Teller, J.T., 2001, Freshwater forcing of abrupt climate change during the last glaciation: Science, v. 293, p. 283-287.

De Angelis, H., and Skvarca, P., 2003, Glacier surge after ice shelf collapse: Science, v. 299, p. 1560-1562.

Engelhardt, H., and Kamb, B., 1997, Basal hydraulic system of a West Antarctic ice stream: constraints from borehole observations: Journal of Glaciology, v. 43, p. 207-230.

Kaufman, D.S., et al., 2004, Holocene thermal maximum in the western Arctic (0-180°W): Quaternary Science Reviews, v. 23, p. 529-560.

MacAyeal, D.R., 1992, Irregular oscillations of the West Antarctic ice sheet: Nature, v. 359, p. 29-32.

MacAyeal, D.R., 1993, Binge/purge oscillations of the Laurentide Ice Sheet as a cause of the North Atlantic's Heinrich events: Paleoceanography, v. 8, p. 775-784.

Manabe, S., and Stouffer, R.J., Coupled ocean-atmosphere model response to freshwater input; comparison to Younger Dryas event: Paleoceanography, v. 12, p. 321-336.

Peterson, B.J., Holmes, R.M., McClelland, J.W., Vörösmarty, C.J., Lammers, R.B., Shiklomanov, A.I., Shiklomanov, I.A., and Rahmstorf, S., 2002, Increasing river discharge to the Arctic Ocean: Science, v. 298, p. 2171-2173.

Ridley, J.K., Huybrechts, P., Gregory, J.M., and Lowe, J.A., 2005, Elimination of the Greenland Ice Sheet in a high CO_2 climate: Journal of Climate: v. 18, p. 3409-3427.

BIBLIOGRAPHY

Alley, R.B., 1989, Water-pressure coupling of sliding and bed deformation: I. water system: Journal of Glaciology, v. 35, p. 108-118.

Alley, R.B., 1991, Deforming-bed origin for southern Laurentide till sheets?: Journal of Glaciology, v. 37, p. 67-76.

Alley, R.B., Blankenship, D.D., Bentley, C.R., and Rooney, S.T., 1986, Deformation of till beneath ice stream B, West Antarctica: Nature, v. 322 p. 57-59.

Alley, R.B., Blankenship, D.D., Rooney, S.T., and Bentley, C.R., 1989, Water-pressure coupling of sliding and bed deformation: III. Application to ice stream B, Antarctica: Journal of Glaciology, v. 35, p. 130–139.

Alley, R.B., and Clark, P.U., 1999, The deglaciation of the Northern Hemisphere: Annual Review of Earth and Planetary Science, v. 27, p. 149-182.

Alley, R.B., Clark, P.U., Huybrechts, P., and Joughin, I., 2005, Ice-Sheet and Sea-Level Changes: Science, v. 310, p. 456-460.

Andrews, J.T., 1998, Abrupt changes (Heinrich events) in late Quaternary North Atlantic marine environments: a history and review of data and concepts: Journal of Quaternary Science, v. 13, p. 3-16.

Andrews, J.T., and Dunhill, G., 2004, Early to mid-Holocene Atlantic water influx and deglacial meltwater events, Beaufort Sea slope, Arctic Ocean: Quaternary Research, v.61, p. 14-21.

Andrews, J.T., and Peltier, W.R., 1989, Quaternary geodynamics in Canada, *in* Fulton, R.J., ed., Quaternary Geology of Canada and Greenland, Geology of North America, v. K-1, p. 541-572.

Bakalowica, M., 2005, Karst groundwater: a challenge for new resources: Hydrogeology Journal: v. 13, p. 148-160.

Barber, D.C., Dyke, A., Hillaire-Marcel, C., Jennings, A.E., Andrews, J.T., Kerwin, M.W., Bilodeau, G., McNeely, R., Southon, J., Morehead, M.D., and Gagnon, J.M., 1999, Forcing of the cold event of 8,200 years ago by catastrophic drainage of Laurentide lakes: Nature, v. 400, p. 344-348.

Bard, E., Hamelin, B., Maurice, A., Montaggioni, L.F, Cabioch, G., Faure, G., and Rougerie, F., 1996, Deglacial sea-level record from Tahiti corals and the timing of global meltwater discharge: Nature, v. 382, p. 241-244.

Barton, K.E., Howell, D.G., and Vigil, J.F., 2003, The North America Tapestry of Time and Terrain: U.S. Geological Survey, Geological Investigations Series I-2781.

Benn, D.I., and Ringrose, T.J., 2001, Random variation of fabric eigenvalues: implications for the use of a-axis fabric data to differentiate till facies: Earth Surface Processes and Landforms, v. 26, p. 295-306.

Bennett, M.R., Waller, R.I., Glasser, N.F., Hambrey, M.J., and Huddart, D., 1999: Glacibenic clast fabrics: genetic fingerprint or wishful thinking: Journal of Quaternary Science, v. 14, p. 125-135.

Bennike, O., and Björck, S., 2002, Chronology of the last recession of the Greenland Ice Sheet: Journal of Quaternary Science: v. 17, p. 211-220.

Bentley, C.R., 1997, Rapid sea-level rise soon from West Antarctic Ice Sheet collapse?: Science, v. 275, p. 1077-1078.

Berger A. and Loutre M.F., 1991, Insolation values for the climate of the last 10 million years: Quaternary Sciences Review, v. 10, p. 297-317.

Bond, G., Showers, W., Cheseby, M., Lotti, R., Almasi, P., deMenocal, P., Priore, P., Cullen, H., Hajdas, I., and Bonani, G., 1997, A pervasive millennial-scale cycle in North Atlantic Holocene and glacial climates: Science, v. 278, p. 1257-1266.

Bond, G., Showers, W., Elliot, M., Evans, M., Lotti, R., Hajdas, I., Bonani, G., and Johnson, S., 1999, The North Atlantic's 1-2 kyr climate rhythm: relation to Heinrich events, Dansgaard/Oeschger cycles and the Little Ice Age, *in* Clark, P.U., Webb, R.S., and Keigwin, L.D., eds., Mechanisms of Global Climate Change at Millennial Time Scales: Geophysical Monograph 112, p. 35-58.

Blanchon, P., and Shaw, J., 1995, Reef drowning during the last deglaciation: evidence for catastrophic sea-level rise and ice-sheet collapse: Geology, v. 23, p. 4-8.

Blankenship, D.D., Bentley, C.R., Rooney, S.T., and Alley, R.B., 1986: Seismic measurements reveal a saturated porous layer beneath an active Antarctic ice stream: Nature, v. 322, p. 54-57.

Boulton, G.S., Caban, P.E., and VanGijssel, K., 1995, Groundwater flow beneath ice sheets: part I – large scale patterns: Quaternary Science Reviews, v. 14, p. 545-562.

Boulton, G.S., Dobbie, K.E., and Zatsepin, S., 2001, Sediment deformation beneath glaciers and its coupling to the subglacial hydraulic system:. Quaternary International, v. 86, p. 3-28.

Boulton, G.S., Slot, T., Blessing, K., Glasbergen, P., Leijnse, T., and van Gijssel, K., 1993, Deep circulation of groundwater in overpressured subglacial aquifers and its geological consequences: Quaternary Science Reviews, v. 12, p. 739-745.

Breemer, C.W., Clark, P.U., and Haggerty, R., 2002, Modeling subglacial hydrology of the late Pleistocene Lake Michigan Lobe, Laurentide Ice Sheet: Geological Society of America Bulletin, v. 114, p. 665-674.

Broecker, W.S., 1994, Massive iceberg discharges as triggers for global climate change: Nature, v. 372, p. 421-424.

Broecker, W.S., Kennett, J.P., Flower, B.P., Teller, J.T., Trumbore, S., Bonani, G., and Wolfli, W., 1989, Routing of meltwater from the Laurentide Ice Sheet during the Younger Dryas cold episode: Nature, v. 341, p. 318-321.

Brown, N.E., Hallet, B., and Booth, D.B., 1987, Rapid soft bed sliding of the Puget Glacial Lobe: Journal of Geophysical Research, v. 92, p. 8985-8997.

Bryden, H.L., Longworth, H.R., and Cunningham, S.A., 2005, Slowing of the Atlantic meridional overturning circulation at 25°N: Nature, v. 438, p. 655-657.

Cane, M. A., 1998, A role for the Tropical Pacific: Science, v. 282, p. 59-61.

Clement, A.C., and Cane, M., 1999, A role for the tropical Pacific coupled ocean-atmosphere system on Milankovitch and Millennial time scales. Part I: a modeling study of tropical Pacific variability, *in* Clark, P.U., Webb, R.S., and Keigwin, L.D. eds., Mechanisms of Global Climate Change at Millennial Time Scales: Geophysical Monograph 112, p. 363-371.

Carlson, A.E., 2004, Genesis of dewatering structures and its implications for melt-out till identification: Journal of Glaciology, v. 50, p. 17-24.
Chabaux, F., Riotte, J., and Dequincey, O., 2003, U-Th-Ra fractionation during weathering and river transport, *in* Bourdon, B., Henderson, G.M., Lundstrom, G.M., and Turner, S.P., eds., Uranium-Series Geochemistry: Reviews in Mineralogy & Geochemistry, v. 52, p. 533-576.
Clark, P.U., 1992, Surface form of the southern Laurentide Ice Sheet and its implications to ice-sheet dynamics: Geological Society of America Bulletin, v. 104, p. 595-605.
Clark, P.U., 1994, Unstable behavior of the Laurentide Ice Sheet over deforming sediment and its implication for climate change, Quaternary Research: v. 41, p. 19-25.
Clark, P.U., 1997, Sediment deformation beneath the Laurentide Ice Sheet, *in* Martini, I.P., ed., Late Glacial and Postglacial Environmental Changes Quaternary, Carboniferous-Permian, and Proterozoic: Oxford University Press, London, p. 81-97..
Clark, P.U., Alley, R.B., and Pollard, D., 1999, Northern Hemisphere ice-sheet influences on global climate change: Science, v. 286, p. 1104-1111.
Clark, P.U., Brook, E.J., Raisbeck, G.M., Yiou, F., and Clark, J., 2003, Cosmogenic ^{10}Be ages of the Saglek Moraines, Torngat Mountains, Labrador: Geology, v. 31, p. 617-620.
Clark, P.U., and Fitzhugh, W.W., 1990, Late deglaciation of the central Labrador coast and its implications for the age of glacial lakes Naskaupi and McLean and for prehistory: Quaternary Research, v. 34, p. 296-305.
Clark, P.U., and Fitzhugh, W.W., 1991, Postglacial relative sea level history of the Labrador coast and interpretation of the archaeological record, *in* Johnson, L.L., ed., Paleoshorelines and prehistory: An investigation of method: Boca Raton, Florida, CRC Press, p. 189-213.
Clark, P.U., Marshall, S.J., Clarke, G.K.C., Hostetler, S.W., Licciardi, J.M., and Teller, J.T., 2001, Freshwater forcing of abrupt climate change during the last glaciation: Science, v. 293, p. 283-287.
Clark, P.U., Pisias, N.G., Stocker, T.F., and Weaver, A.J., 2002, The role of the thermohaline circulation in abrupt climate change: Nature, v. 415, p. 863-869.
Clarke, G.K.C., 1987, Subglacial till: a physical framework for its properties and processes: Journal of Geophysical Research, v. 92, p. 9023-9036.
Clayton, L., Mickelson, D.M., and Attig, J.W., 1989, Evidence against pervasively deformed bed material beneath rapidly moving lobes of the southern Laurentide ice sheet: Sedimentary Geology, v. 62, p. 203-208.
Clayton, L., and Moran, S.R., 1982, Chronology of late Wisconsinan glaciation in middle North America: Quaternary Science Reviews, v. 1, p. 55-82.
Conway, H., Hall, B.L., Denton, G.H., Gades, A.M., and Waddington, E.D., 1999, Past and future grounding-line retreat of the West Antarctic Ice Sheet: Science, v. 286, p. 280-283.
Cottet-Puinel, M., Weaver, A.J., Hillaire-Marcel, C., de Vernal, A., Clark, P.U., and Eby, M., 2004, Variation of Labrador Sea Water formation over the Last

Glacial cycle in a climate model of intermediate complexity: Quaternary Science Reviews, v. 23, p. 449-465.
Dean, W.E., Forester, R.M., and Bradbury, J.P., 2002, Early Holocene change in atmospheric circulation in the Northern Great Plains: an upstream view of the 8.2 ka cold event: Quaternary Science Reviews, v. 21, p. 1763-1775.
De Angelis, H., and Skvarca, P., 2003, Glacier surge after ice shelf collapse: Science, v. 299, p. 1560-1562.
Delaney, M.L., Bé, A.W.H., and Boyle, E.A., 1985, Li, Sr, Mg, and Na in foraminiferal calcite shells from laboratory culture, sediment traps, and sediment cores: Geochimica et Cosmochimica Acta, v. 49, p. 1327-1341.
DeMenocal, P., Ortiz, J., Guilderson, T., and Sarnthein, M., 2000, Coherent high- and low-latitude climate variability during the Holocene Warm Period: Science, v.288, p. 2198-2202.
Dickie, L.M., and Trites, R.W., 1983, The Gulf of St. Lawrence, *in* Ketchum, B.W., eds., Ecosystems of the World 26, Estuaries and Enclosed Seas: Elsevier Scientific Publishing Company, New York, p. 403-425.
Dowdeswell, J.A. and Sharp, M.J., 1986, Characterization of pebble fabrics in modern terrestrial glacigenic sediments: Sedimentology, v. 33, p. 699-710.
Downey, J.S., 1986, Geohydrology of bedrock aquifers in the northern Great Plains in parts of Montana, North Dakota, South Dakota, and Wyoming: U.S. Geological Survey Professional Paper 1402-E, 87p.
Downey, J.S., and Dinwiddie, G.A., 1988, The regional aquifer system underlying the northern Great Plains in parts of Montana, North Dakota, South Dakota, and Wyoming - Summary: U.S. Geological Survey Professional Paper 1402-A, 63 p.
Dredge, L.A. and Nielsen, E., 1985, Glacial and interglacial deposits in the Hudson Bay lowlands: a summary of sites in Manitoba, *in* Current Research, Part A, Geological Survey of Canada, Paper 85-1A, p. 247-257..
Dredge, L.A. and F.M., Nixon, 1992, Glacial and Environmental Geology of Northeastern Manitoba: Geological Survey of Canada Memoir 432, 80 p.
Dyke, A. S., 2004, An outline of North American Deglaciation with emphasis on central and northern Canada, *in* Ehlers, J. and Gibbard, P.L., eds., Quaternary Glaciations-Extant and Chronology, Part II, Elsevier Science and Technology Books, Amsterdam, v. 2b p. 373-424.
Dyke, A.S., and Prest, V.K., 1987, Paleogeography of northern North America, 18,000 - 5,000 years ago: Geological Survey of Canada, Map 1703A, Scale 1:12,500,000.
Engelhardt, H., and Kamb, B., 1997, Basal hydraulic system of a West Antarctic ice stream: constraints from borehole observations: Journal of Glaciology, v. 43, p. 207-230.
Engelhardt, H., and Kamb, B., 1998, Basal sliding of Ice Stream B, West Antarctica: Journal of Glaciology, v. 44, p. 223-230.
Felzer, B., Oglesby, R.J., Webb III, T., and Hyman, D.E., 1996, Sensitivity of a general circulation model to changes in northern hemisphere ice sheets: Journal of Geophyscial Research, v. 101, p. 19,077-19,092.

Fichefet, T., Poncin, C., Goosse, H., Huybrechts, P., Janssens, I., and LeTreut, H., 2003, Implications of changes in freshwater flux from the Greenland ice sheet for the climate of the 21st century: Geophysical Research Letters, v. 30, doi: 10.1029/2003GL017826.

Fischer, U.H., and Clarke, G.K.C., 1994, Ploughing of subglacial sediment: Journal of Glaciology, v. 40, p. 97-106.

Fleming, K., Johnston, P., Zwartz, D., Yokoyama, Y., Lambeck, K., and Chappell, J., 1998, Refining the eustatic sea-level curve since the Last Glacial Maximum using far - and intermediate - field sites: Earth and Planetary Science Letters, v. 163, p. 327-342.

Flower, B.P., Hastings,D.W., Hill, H.W., and Quinn, T.M., 2004, Phasing of deglacial warming and Laurentide ice sheet meltwater in the Gulf of Mexico: Geology, v. 32, p. 597-600.

Grasby, S.E., and Chen, Z., 2005, Subglacial recharge into the Western Canada Sedimentary Basin - Impact of Pleistocene glaciation on basin hydrodynamics: GSA Bulletin, v. 117, p. 500-514.

Gray, J., Lauriol, B., Bruneau, D., and Ricard, J., 1993, Postglacial emergence of Ungava Peninsula, and its relationship to glacial history: Canadian Journal of Earth Science, v. 30, p. 1676-1696.

Grootes, P.M., et al., 1993, Comparison of oxygen isotope records from the GISP2 and GRIP Greenland ice cores: Nature, v. 369, p. 552-554.

Haley, B.A., and Klinkhammer, G.P., 2002, Development of a flow-through system for cleaning and dissolving foraminiferal tests: Chemical Geology, v. 185, p. 51-69.

Hansel, A.K., and Johnson, W.H., 1996, Wedron and Mason Groups: Lithostratigraphic reclassification of deposits of the Wisconsin Episode, Lake Michigan area: Illinois State Geological Survey Bulletin, 104 p.

Hardy, L., 1976, Contribution a l'etude geomorphologique de la portion Quebecoise de la Baie d James: Ph.D. Thesis, McGill University, Montreal.

Hicock, S.R., 1992, Lobe interactions and rheologic superposition in subglacial till near Bradtville, Ontario, Canada: Boreas, v. 21, p. 73-88.

Hicock, S.R. and Dreimanis, A., 1992, Deformation till in the Great Lakes region: implications for rapid flow along the south-central margin of the Laurentide Ice Sheet: Canadian Journal of Earth Sciences, v. 29, p. 1565-1579.

Hicock, S.R., Goff, J.R., Lian, O.B. and Little, E.C., 1996, On the interpretation of subglacial till fabric: Journal of Sedimentary Research, v. 66, p. 928-934.

Hillaire-Marcel, C., de Vernal, A., Bilodeau, G., and Weaver, A.J., 2001, Absence of deep-water formation in the Labrador Sea during the last interglacial period: Nature, v. 410, p. 1073-1077.

Hindmarsh, R., 1997, Deforming beds: viscous and plastic scales of deformation: Quaternary Science Reviews, v. 16, p. 1039-1056.

Hitchon, B., 1969a, Fluid flow in the Western Canadian sedimentary basin 1. Effect of topography: Water Resources Research, v. 5, p. 186-195.

Hitchon, B., 1969b, Fluid flow in the Western Canadian sedimentary basin 2. Effect of geology: Water Resources Research, v. 5, p. 460-469.

Hooke, R.LeB., Hanson, B., Iverson, N.R., Jansson, P., and Fischer, U.H., 1997, Rheology of till beneath Storglaciären, Sweden: Journal of Glaciology, v. 43: p. 172-179.

Hooyer, T.S., and Iverson, N.R., 2000, Diffusive mixing between shearing granular layers: constraints on bed deformation from till contacts: Journal of Glaciology, v. 46, p. 641-651.

Hooyer, T.S., and Iverson, N.R., 2002, Flow mechanisms of the Des Moines lobe of the Laurentide ice sheet: Journal of Glaciology, v. 48, p. 575-586.

Hostetler, S.W., and Bartlein, P.J., 1999, Simulation of the potential responses of regional climate and surface processes in Western North America to a canonical Heinrich event, *in* Clark, P.U., Webb, R.S., and Keigwin, L.S., eds., Mechanisms of Global Climate Change at Millennial Time Scales: Geophysical Monograph 112, p. 313-327.

Hostetler, S.W., Clark, P.U., Bartlein, P.J., Mix, A.C., and Pisias, N.J., 1999, Atmospheric transmission of North Atlantic Heinrich events: Journal of Geophysical Research, v. 104, p. 3947-3952.

Hughen, K.A., Southon, J.R., Lehman, S.J., and Overpeck, J.T., 2000, Synchronous radiocarbon and climate shifts during the last deglaciation: Science, v. 290, p. 1951-1954.

Humphrey, N., Kamb, B., Fahnestock, M., and Engelhardt, H., 1993, Characteristics of the bed of the lower Columbia Glacier, Alaska: Journal of Geophysical Research, v. 98, p. 837-846.

Iverson, N.R., Jansson, P., and Hooke, R.LeB., 1994, In-situ measurement of the strength of deforming subglacial till: Journal of Glaciology, v. 40, p. 497-503.

Iverson, N.R., Hanson, B., Hooke, R. LeB., and Jansson, P, 1995, Flow mechanisms of glaciers on soft beds: Science, v. 267, p. 80-81.

Iverson, N.R., Hooyer, T.S., and Baker, R.W., 1998, Ring-shear studies of till deformation: Coulomb-plastic behavior and distributed strain in glacier beds: Journal of Glaciology, v. 44, p. 634-642.

Jenson, J.W., Clark, P.U., MacAyeal, D.R., Ho, C., and Vela, J.C., 1995, Numerical modeling of advective transport of saturated deforming sediment beneath the Lake Michigan Lobe, Laurentide Ice Sheet: Geomorphology, v. 14, p. 157-166.

Kamb, B., 1991, Rheological nonlinearity and flow instability in the deforming bed mechanism of ice stream motion: Journal of Geophysical Research, v. 96, p. 16,585-16,595.

Kaufman, D.S., et al., 2004, Holocene thermal maximum in the western Arctic (0-180°W): Quaternary Science Reviews, v. 23, p. 529-560.

Keigwin, L.D., and Jones, G.A., 1995, The marine record of deglaciation from the continental margin off Nova Scotia: Paleoceanography, v. 10**,** p. 973-985.

Klassen, R.W., 1986, Surficial geology of the north-central Manitoba: Geological Survey of Canada Memoir 419, 57 p.

Koutavas, A., Lynch-Stieglitz, J., Marchitto, T.M., and Sachs, J.P., 2002, El Niño-like pattern in ice age Tropical Pacific sea surface temperature: Science, v. 297, p. 226-230.

Lal, D., 1991, Cosmic ray labeling of erosion surfaces: In situ nuclide production rates and erosion models: Earth and Planetary Science Letters, v. 104, p. 424–439.
Larsen, N.K., and Piotrowski, J.A., 2003, Fabric in a basal till succession and its significance for reconstructing subglacial processes: Journal of Sedimentary Research, v. 73, p. 725-734.
Larsen, N.K., Piotrowski, J.A., and Kronborg, C., 2004, A multiproxy study of basal till: a time-transgressive accretion and deformation hypothesis: Journal of Quaternary Science, v. 19, p. 9-21.
Lauriol, B., and Gray, J.T., 1987, The decay and disappearance of the late Wisconsin ice sheet in the Ungava Peninsula, Northern Quebec, Canada: Arctic and Alpine Research, v. 19, p. 109-126.
Lea, D.W., Mashiotta, T.A., and Spero, H.J., 1999, Controls on magnesium and strontium uptake in planktonic foraminifera determined by live culturing: Geochimica et Cosmochimica Acta v. 63, p. 2369-2379.
Lea, D.W., Pak, D.K., Peterson, L.C., and Hughen, K.A., 2003, Synchroneity of tropical and high-latitude Atlantic temperatures over the Last Glacial Termination: Science, v. 301, p. 1361-1364.
Lennox, D.H., 1993, Groundwater in the interior plains region, *in* Stott, D.F., and Aitken, J.D., eds., Sedimentary Cover of the Craton in Canada: Geological Survey of Canada, Geology of Canada, n. 5, p 616-642.
Lian, O.B., Hicock, S.R. and Dreimanis, A., 2003, Laurentide and Cordilleran fast ice flow: some sedimentological evidence from Wisconsinan subglacial till and its substrate: Boreas, v. 32, p. 102-113.
Licciardi, J.M., 2000, Alpine glacier and pluvial lake records of late Pleistocene climate variability in the western United States: Ph.D. Thesis, Oregon State University-Corvallis, 155 p.
Licciardi, J.M., Clark, P.U., Jenson, J.W., and MacAyeal, D.R., 1998, Deglaciation of a soft-bedded Laurentide Ice Sheet: Quaternary Science Reviews, v. 17, p. 427-448.
Licciardi, J.M., Teller, J.T., and Clark, P.U., 1999, Freshwater routing by the Laurentide Ice Sheet during the last deglaciation, *in* Clark, P.U., Webb, R.S., and Keigwin, L.D. eds., Mechanisms of Global Climate Change at Millennial Time Scales: Geophysical Monograph 112, p. 177-201.
Liedl, R., Sauter, M., Hückinghaus, D., Clemens, T., and Teutsch, G, 2003, Simulation of the development of karst aquifers using a coupled continuum pipe flow model: Water Resources Research, v. 39, doi: 10.1029/2001WR001206.
Lighty, R.G., Macintyre, I.G., and Stuckenrath, R., 1982, *Acropora palmata* reef framework: A reliable indicator of sea level in the Western Atlantic for the past 10,000 years: Coral Reefs, v. 1, p. 125-130.
Lingle, C.S., and Brown, T.J., 1987, A subglacial aquifer bed model and water pressure dependent basal sliding relationship for a West Antarctic ice stream, *in* van der Veen, C.J., and Oerlemans, J., eds., Dynamics of the West Antarctic Ice Sheet: D. Reidel Publishing Company, p. 249-285.
MacAyeal, D.R., 1992, Irregular oscillations of the West Antarctic ice sheet: Nature, v. 359, p. 29-32.

MacAyeal, D.R., 1993, Binge/purge oscillations of the Laurentide Ice Sheet as a cause of the North Atlantic's Heinrich events: Paleoceanography, v. 8, p. 775-784.
MacClintock, P. and Dreimanis, A., 1964, Orientation of till fabric by overriding glacier in the Saint Lawrence Valley: American Journal of Science, v. 262, p. 133-142.
Manabe, S., and Stouffer, R.J., Coupled ocean-atmosphere model response to freshwater input; comparison to Younger Dryas event: Paleoceanography, v. 12, p. 321-336.
Mark, D.M., 1973, Analysis of axial orientation data, including till fabric: Geological Society of America Bulletin, v. 84, p. 1369-1373.
Marshall, S.J., and Clark, P.U., 2002, Basal temperature evolution of North American ice sheets and implications for the 100-kyr cycle: Geophysical Research Letters, v. 29: doi: 10.1029/2002GL015192.
Mathews, W.H., 1974, Surface profiles of the Laurentide Ice Sheet in its marginal areas: Journal of Glaciology, v. 13, p. 37-43.
McDonald, M.G., and Harbaugh, A.W., 1988, MODFLOW: a modular three-dimensional finite-difference groundwater flow model: U.S. Geological Survey, Techniques of Water-Resources Investigation, Book 6, p. 1-1 to 13-29.
McManus, J.F., Francois, R., Gherardi, J.-M., Keigwin, L.D., and Brown-Leger, S., 2004, Collapse and rapid resumption of Atlantic meridional circulation linked to deglacial climate changes: Nature, v. 428, p. 834-837.
Meybeck, M., 1987, Global chemical weathering of surficial rocks estimated from river dissolved loads: American Journal of Science, v. 287, p. 401-428.
Mickelson, D.M., Clayton, L., Fullerton, D.S., and Burns, H.W., Jr., 1983, The late Wisconsin glacial record of the Laurentide Ice Sheet in the U.S., *in* Porter, S.C., ed., Late Quaternary environments of the United State. University of Minnesota Press, v. 1, p. 3-37.
Miller, G.H., Wolfe, A.P., Briner, J.P., Sauer, P.E., and Nesje, A., 2005, Holocene glaciation and climate evolution of Baffin Island, Arctic Canada: Quaternary Science Reviews, v. 24, p. 1703-1721.
Mitchell, J.F.B., Grahame, N.S., and Needham, K.J., 1988, Climate simulations for 9000 years before present: seasonal variations and effect of the Laurentide Ice Sheet: Journal of Geophysical Research, v. 93, p. 8283-8303.
Montaggioni, L., Cabioch, G., Camoin, G.,Bard, E., Ribaud-Laurenti, A., Faure, G., Déjardin, P., and Récy, J., 1997, Continuous record of reef growth over the past 14 ky on the mid-Pacific island of Tahiti: Geology, v. 25, p. 555-558.
Moore, P.L., and Iverson, N.R., 2002, Slow episodic shear of granular material regulated by dilatant strengthening: Geology, v. 30, p. 843-846.
Muller, S.D., Richard, P.J.H., Guiot, J., de Beaulieu, J.-L., and Fortin, D., 2003, Postglacial climate in the St. Lawrence lowlands, southern Québec: pollen and lake-level evidence: Palaeogeography, Palaeoclimatology, Palaeoecology: v. 193, p. 51-72.
Nielsen, E., Morgan, A.V., Morgan, A., Mott, R.J., Rutter, N.W. and Causse, C., 1986, Stratigraphy, paleoecology, and glacial history of the Gillam area, Manitoba: Canadian Journal of Earth Sciences, v. 23, p. 1641-1661.

Paterson, W.S.B., 1994, The Physics of Glaciers, 3rd Edition: Butterworth Heinemann, Oxford, 480 p.

Peterson, B.J., Holmes, R.M., McClelland, J.W., Vörösmarty, C.J., Lammers, R.B., Shiklomanov, A.I., Shiklomanov, I.A., and Rahmstorf, S., 2002, Increasing river discharge to the Arctic Ocean: Science, v. 298, p. 2171-2173.

Piotrowski, J.A., 1997a, Subglacial groundwater flow during the last glaciation in northwestern Germany: Sedimentary Geology, v. 111, p. 217-224.

Piotrowski, J.A., 1997b, Subglacial hydrology in north-western Germany during the last glaciation: groundwater flow, tunnel valleys and hydrological cycles: Quaternary Science Reviews, v. 16, p. 169-185.

Piotrowski, J.A., Larsen, N.K., and Junge, F.W., 2004, Reflections on soft subglacial beds as a mosaic of deforming and stable spots: Quaternary Science Reviews, v. 23, p. 993-1000.

Piotrowski, J.A., Mickelson, D.M., Tulaczyk, S., Krzyszkowski, D., and Junge, F.W., 2001, Were deforming subglacial beds beneath past ice sheets really widespread?: Quaternary International, v. 86, p. 139-150.

Piotrowski, J.A., and Tulaczyk, S., 1999, Subglacial conditions under the last ice sheet in northwest Germany: ice-bed separation and enhanced basal sliding?: Quaternary Science Reviews, v. 18, p. 737-751.

Pollard, D., Bergengren, J.C., Stillwell-Soller, L.M., Felzer, B., and Thompson, S.L., 1998, Climate simulations for 10,000 and 6,000 years BP: Paleoclimates; data and modeling, v. 2, p. 183-218.

Raisbeck, G.M., Yiou, F., Bourlès, D., Brown, E.T., Deboffle, D., Jouhanneau, P., Lestringuez, J., and Zhou, Z.Q., 1994, The AMS facility at Gif-sur-Yvette: progress, perturbations and projects: Nuclear Instruments and Methods in Physics Research, v. 92, p. 43-46.

Remenda, V.H., Cherry, J.A., and Edwards, T.W.D., 1994, Isotopic composition of old ground water from Lake Agassiz: implications for Late Pleistocene climate: Science, v. 266, p. 1975-1978.

Renssen, H., Goosse, H., Fichefet, T., Brovkin, V., Driesschaert, E., and Wolk, F., 2005, Simulating the Holocene climate evolution at northern high latitudes using a coupled atmosphere-sea ice-ocean-vegetation model: Climate Dynamics, v. 24, p. 23-43.

Ridley, J.K., Huybrechts, P., Gregory, J.M., and Lowe, J.A., 2005, Elimination of the Greenland Ice Sheet in a high CO_2 climate: Journal of Climate: v. 18, p. 3409-3427.

Rinterknecht, V.R., 2003, Cosmogenic ^{10}Be Chronology for the Last Deglaciation of the Southern Scandinavian Ice Sheet: Ph.D. Thesis, Oregon State University-Corvallis, 99 p.

Rinterknecht, V.R., Clark, P.U., Raisbeck G.M., Yiou, F., Brook, E.J., Tschudi, S., and Lunkka, J.P., 2004, Cosmogenic ^{10}Be dating of the Salpausselkä I Moraine in southwestern Finland: Quaternary Science Reviews, v. 23, p. 2283-2289.

Rodrigues, C.G., and Vilks G., 1994, The implications of glacial lake runoff on the Goldthwait and Champlain Seas: the relationship between glacial lake Agassiz runoff and the Younger Dryas: Quaternary Science Reviews, v. 13, p. 923-944.

Roy, M., 1998, Pleistocene stratigraphy of the lower Nelson River area – implications for the evolution of the Hudson Bay lowland of Manitoba, Canada: M.S. Thesis, University of Quebec, Montreal, 220 p.

Russell, A.D., et al., 1994, Uranium in foraminiferal calcite as a recorder of seawater uranium concentrations: Geochimica et Cosmochimica Acta, v. 58, p. 671-681.

Sauer, E.K., Egeland, A.K., and Christiansen, E.A., 1993, Preconsolidation of tills and intertill clays by glacial loading in southern Saskatchewan, Canada: Canadian Journal of Earth Science, v. 30, p. 420-433.

Scanlon, B.R., Mace, R.E., Barrett, M.E., and Smith, B., 2003, Can we simulate regional groundwater flow in a karst system using equivalent porous media models? Case study, Barton Springs Edwards aquifer, USA: Journal of Hydrology: v. 276, p. 137-158.

Sawada, M., Viau, A.E., Vettoretti, G., Peltier, W.R., and Gajewski, K., 2004, Comparison of North-American pollen-based temperature and global lake-status with CCCma AGCM2 output at 6 ka: Quaternary Science Reviews, v. 23, p. 225-244.

Shaw, J., Gereau, P., and Courtney, R.C., 2002, Palaeogeography of Atlantic Canada 13-0 kyr: Quaternary Science Reviews, v. 21, p. 1861-1878.

Short, S.K., and Nichols, H., 1977, Holocene pollen diagrams from subarctic Labrador-Ungava: vegetational history and climate change: Arctic and Alpine Research, v. 9, 265-290.

Shuman, B., Bartlein, P.J., and Webb, T., 2005, The magnitudes of millennial- and orbital-scale climatic change in eastern North American during the Late Quaternary: Quaternary Science Reviews, v. 24, p. 2194-2206.

Smith, D.G., and Fisher, T.G., 1993, Glacial Lake Agassiz: the northwestern outlet and paleoflood: Geology, v. 21, p. 9-12.

Solignac, S., de Vernal, A., and Hillaire-Marcel, C., 2004, Holocene sea-surface conditions in the North Atlantic – contrasted trends and regimes in the western and eastern sectors (Labrador Sea vs. Iceland Basin): Quaternary Science Reviews, v. 23, p. 319-334.

Stephenson, D.A., Fleming, A.H., and Mickelson, D.M., 1988, Glacial deposits, *in* Back, W., Rosenshein, J.S., and Seaber, P.R., eds., Hydrology: Geological Society of America, The Geology of North America, v. O-2, p., 301-314.

Stone, J.O., 2000, Air pressure and cosmogenic isotope production: Journal of Geophysical Research, v. 105, p. 23,753-23,759.

Stone, J.O., Balco, G.A., Sugden, D.E., Caffee, M.W., Sass III, L.C., Cowdery, S.G., and Siddoway, C., 2003, Holocene deglaciation of Marie Byrd Land, West Antarctica: Science, v. 299, p. 99-102.

Stott, L., Poulsen, C., Lund, S., and Thunell, R., 2002, Super ENSO and global climate oscillations at millennial time scales: Science, v. 297, p. 222-226.

Stuiver, M., et al., 1998, INTCAL98 Radiocarbon Age Calibration, 24,000-0 cal BP: Radiocarbon, v. 40, p. 1041-1083.

Swarzenski, P.W., Porcelli, D., Anderson, P.S., and Smoak, J.M., 2003, The behavior of U- and The-series nuclides in the estuarine environment, *in* Bourdon, B., Henderson, G.M., Lundstrom, C.C., and Turner, S.P., eds., Uranium-Series Geochemistry: Reviews in Mineralogy & Geochemistry, v. 52, p. 577-606.

Tarasov, L., and Peltier, W.R., 2005, Arctic freshwater forcing of the Younger Dryas cold reversal: Nature, v. 435, p. 662-665.
Teller, J.T., 1990, Volume and routing of late-glacial runoff from the Southern Laurentide Ice Sheet: Quaternary Research, v. 34, p. 12-23.
Teller, J.T., Leverington, D.W., and Mann, J.D., 2002, Freshwater outbursts to the oceans from glacial Lake Agassiz and their role in climate change during the last deglaciation: Quaternary Science Reviews, v. 21, p. 879-887.
Teller, J.T., et al., 2005, Alternative routing of Lake Agassiz overflow during the Younger Dryas: new dates, paleotopography, and a re-evaluation: Quaternary Science Reviews, v. 24, p. 1890-1905.
Thorliefson, L.H., 1989, Quaternary stratigraphy of the central Hudson Bay Lowland, northern Ontario: Ph.D. Thesis, University of Colorado, Boulder, 363 p.
Thorliefson, L.H., Wyatt, P.H., Shilts, W.W., and Nielsen, E., 1992, Hudson Bay Lowland Quaternary Stratigraphy: evidence for early Wisconsinan glaciation centered in Quebec, *in* Clark, P.U., and Lea, P.D., eds., The Last Interglacial-Glacial Transition in North America: Geological Society of America, Special Paper 270, p. 207-220.
Tulaczyk, S., Kamb, B., and Engelhardt, H.F., 2001, Estimates of effective stress beneath a modern West Antarctic ice stream from till preconsolidation and void ratio: Boreas, v. 30, p. 101-114.
Tudhope, A.W., Chilcott, C.P., McCulloh, M.T., Cook, E.R., Chappell, J., Ellam, R.M., Lea, D.W., Lough, J.M., and Shimmield, G.B., 2001, Variability in the El Niño-Southern Oscillation through a glacial-interglacial cycle: Science, v. 291, p. 1511-1517.
Turney, C.S.M., Kershaw, A.P., Clemens, S.C., Branch, N.B., Moss, P.T., and Fifield, L.K., 2004, Millennial and orbital variations in El Niño/Southern Oscillation and high-latitude climate in the last glacial period: Nature, v. 428, p. 306-310.
Vacher, H.L., and Mylroie, J.E., 2002, Eogenetic karst from the perspective of an equivalent porous medium: Carbonates and Karst, v. 17, p. 182-196.
Veillette, J.J., Dyke, A.S., and Roy, M., 1999, Ice-flow evolution of the Labrador Sector of the Laurentide Ice Sheet: a review, with new evidence from northern Quebec: Quaternary Science Reviews, v. 18, p. 993-1019.
Wadleigh, M.A., Veizer, J., and Brooks, C., 1985, Strontium and its isotopes in Canadian rivers: fluxes and global implications: Geochimica et Cosmochimica Act, v. 49, p. 1727-1736.
Walder, J.S., and Fowler, A., 1994, Channelized subglacial drainage over a deformable bed: Journal of Glaciology, v. 40, p. 3-15.
Wang, Y.J., et al., A high-resolution absolute-dated Late Pleistocene monsoon record from Hulu Cave, China: Science, v. 294, p. 2345-2348.
Wickham, S.S., and Johnson, W.H., 1981, The Tiskilwa Till: A regional view of its origin and depositional processes: Annals of Glaciology, v. 2, p. 176-182.
Wright, H.E., 1971, Retreat of the Laurentide ice sheet from 14,000 to 9,000 years ago: Quaternary Research, v. 1, p. 316-330.
Zwally, H.J., Abdalati, W., Herring, T., Larson, K., Saba, J., and Steffen, K., 2002, Surface melt-induced acceleration of Greenland Ice-Sheet flow: Science, v. 297, p. 218-222.